

Alma Mater Studiorum – Università di Bologna

**DOTTORATO DI RICERCA IN
INGEGNERIA CIVILE, CHIMICA,
AMBIENTALE E DEI MATERIALI**

Ciclo XIX

Settore Concorsuale di afferenza: 08/A4

Settore Scientifico disciplinare: ICAR/06

**INNOVATIVE USE AND INTEGRATION OF REMOTE
SENSED GEOSPATIAL DATA FOR 3D CITY MODELING
AND GIS URBAN APPLICATIONS**

Presentata da: Alessandro Lambertini

Coordinatore Dottorato:

Prof. Luca Vittuari

Relatore:

Prof. Gabriele Bitelli

Esame finale anno 2017

Creativity is just connecting things.

Steve Jobs (1955-2011)

Abstract

Modern remote sensing instruments, mounted on a modern aerial platform and assisted through the use of automated procedures are now capable of acquiring data over a vast area in a short timeframe. Thanks to innovative processing methods and algorithms it is then possible to rapidly deliver results with a high detail and accuracy. The discussed thesis provides a detailed overview, through different case studies and examples, on the evolving complete pipeline required to survey, process, store, integrate, analyze and deliver data in the form of a 3D city model and GIS in the urban environment. A comprehensive 3D city model is, in fact, the necessary multi-disciplinary backbone for the ubiquitous sensors of a Smart City.

Keywords

- Remote Sensing
- LIDAR
- Photogrammetry
- UAV
- Point cloud
- 3D city model
- Smart City
- GIS
- WebGIS
- Open Source
- Open Data

Table Of Contents

Abstract	4
Keywords	5
List Of Figures And Tables	9
Introduction	17
Outline	19
Chapter 1: Survey Platforms And Parameters	21
1.1 Resolutions Of Remote Sensing	22
1.1.1 Spatial Resolution.....	23
1.1.2 Spectral Resolution.....	24
1.1.3 Radiometric Resolution.....	24
1.1.4 Temporal Resolution	26
1.2 Spaceborne And Airborne Platforms	27
1.2.1 Satellite	27
1.2.2 Manned Aircraft Or Helicopter	28
1.2.3 Remotely Piloted Aircraft System	29
1.3 Other Platforms	31
1.4 Analysis Of The Proper Platform For Urban Applications.....	33
Chapter 2: Sensors, Data Acquisition And Integration	34
2.1 Sensors	34
2.2 Light Detection And Ranging Technology.....	35
2.2.1 Linear-Mode.....	36
2.2.2 Full Waveform.....	37
2.2.3 Single Photon	37
2.2.4 Geiger-Mode.....	38
2.2.5 Flash	39
2.2.6 Multispectral.....	40

2.3 Sensors For Remotely Piloted Aircraft System.....	41
2.3.1 Light Detection And Ranging Sensors	41
2.3.2 Digital Camera Sensors	43
2.4 Discussion	50
2.5 Data Fusion	51
2.5.1 Case Study	51
2.5.2 Integration Of Remote Sensed Data.....	52
2.6 Challenges And Perspectives.....	56
2.6.1 Growing Trend In Unmanned Aerial Vehicle Applications.....	56
2.6.2 Urban Geospatial Data And Self-Driving Vehicles	57
Chapter 3: Processing Algorithms And Storage	61
3.1 Software	61
3.2 Dense Point Cloud Processing.....	62
3.2.1 Case Study	62
3.2.2 Grass Gis Processing.....	65
3.2.3 Lastools Processing.....	66
3.2.4 Envi Lidar Processing.....	67
3.2.5 Results Comparison	68
3.3 Point Cloud Workflow	69
3.4 Point Cloud Storage	70
3.5 Voxel Models.....	71
3.6 Big Data Challenge.....	72
Chapter 4: Analysis At Different Urban Scales	74
4.1 Level Of Detail.....	74
4.2 Roof Planes From Point Cloud.....	75
4.2.1 Case Study	75
4.2.2 Data Analysis	77
4.3 Solar Radiation On Roof Planes.....	83

4.3.1 Case Study	84
4.3.2 Point Cloud Processing	85
4.3.3 Building Extraction	87
4.3.4 Solar Radiation Analysis	92
4.4 Point Cloud Density	94
4.5 Analysis At Building-Level.....	96
4.5.1 Voxel-Base Procedure	98
4.5.2 Pipeline From Point Cloud To Voxel Model.....	99
4.5.3 Slicing Method	102
4.5.4 Case Study	104
4.6 Rooftop Detailed Analysis.....	107
Chapter 5: Final Products	110
5.1 3D City Model For Decision Support Systems.....	110
5.2 Webgis For Solar Radiation Estimation.....	112
5.2.1 Case Study	114
5.2.2 Processing With Free And Open Source Software	115
5.3 Data Dissemination.....	117
5.3.1 Volunteered Geographic Information	117
5.3.2 Open Data Policies	119
Conclusions	122
References	124
Websites.....	124
Articles.....	125
Acknowledgements	135

List Of Figures And Tables

Figure 1: Boston, as the Eagle and the Wild Goose See It (James Wallace Black, 1860)	21
Figure 2: Platforms represented in logarithmic scale to their respective distance from the surveyed object	22
Figure 3: DN displayed in a digital image with resolution 10x10 (rows, columns) ...	22
Figure 4: Geometrical definition for image spatial parameters FOV and IFOV....	23
Figure 5: The same portion of urban environment captured from three different satellites (nasa.gov), from left to right with the respective sensor spatial resolution: Landsat ETM+ (28 m), ATLAS (10 m), QuickBird-2 (2 m)	24
Figure 6: Example of the spectral resolution of a multispectral sensor on a satellite platform (Landsat 8 Data Users Handbook, 2016)	24
Figure 7: Examples of different radiometric resolution.....	25
Figure 8: Different resolutions in a digital image	25
Figure 9: Venn diagram for resolutions of remote sensing.....	26
Figure 10: Pre and post-event images for earthquake in Algeria (Bitelli et al., 2004)	27
Figure 11: SENTINEL-2 satellite (ESA).....	28
Figure 12: Scheme for sensors and human operator inside a manned aircraft platform (RIEGL)	29
Figure 13: DJI Matrice 600 multi rotary-wing RPAS.....	30
Figure 14: Facade survey using TLS system	31
Figure 15: Segmentation of data acquired from a MLS platform (Yang et al., 2015)	32
Figure 16: Coverage of imagery acquired from balloon platform (Bitelli et al., 2004)	32
Table 17: Comparison between some parameters among the three different remote sensing platforms previously described	33
Figure 18: Example provided from laser scanner RIEGL VQ-1560i data sheet is possible to obtain a point density of 8 points per square meter with 2 sensors a 1M pulses/s with laser power level set at 100% from an altitude of 5600 feet and a speed of 170 knots.....	36
Figure 19: RIEGL VQ-1560i equipped with two laser scanner sensors	37

Figure 20: Leica SPL100 single photon LIDAR.....	38
Figure 21: Geiger-mode LIDAR scheme (HARRIS).....	39
Figure 22: ASC Peregrine 3D Flash LIDAR Vision System.....	39
Table 23: Main parameters for different airborne LIDAR technologies set to reach a point cloud density of 8 points per square meter (HARRIS)	40
Figure 24: Optech Titan Multispectral LIDAR system	40
Figure 25: Example of survey with Optech Titan Multispectral LIDAR with point clouds acquired at different wavelengths, from left to right: 532nm, 1064nm, 1550nm	41
Figure 26: RIEGL VUX-1 and RIEGL miniVUX-1	42
Figure 27: YellowScan Mapper	42
Figure 28: YellowScan Surveyor, KAARTA Stencil, Alpha AL3-16	43
Figure 29: DJI 3-axis gimbal functional diagram demonstrating angles for pan (-360°/+360°), tilt (-140°/+50°) and roll (-40°/+40°)	44
Figure 30: Example of DJI Matrice 600 equipped with Ronin-MX gimbal	45
Figure 31: Phase One iXU 1000	46
Figure 32: Hasselblad X1D	46
Figure 33: Sony A7.....	47
Figure 34: Sony A6300.....	47
Figure 35: DJI Zenmuse X4S.....	48
Figure 36: GoPro Hero 5 Black.....	48
Table 37: RPAS camera specifications comparison.....	49
Figure 38: Graph showing relative sizes of camera sensors	49
Figure 39: Two case studies represented over the DSM of the city.....	51
Figure 39: The two area studied in the Bologna case study	52
Figure 41: Very high-resolution multispectral satellite image, 3D point cloud acquired by aerial laser scanner, digital cartography used as reference data	52
Figure 42: Comparison between building elevation as recorded in digital cartography and elevation processed from LIDAR data	53
Figure 43: Classification of buildings.....	54

Figure 44: Geometric accuracy for the buildings processed and classified against the reference data from digital cartography	55
Figure 45: Classification of roof materials (Franci et al., 2014)	55
Figure 46: 'UAV' used as a keyword in scientific literature indexed in Elsevier's Scopus, the largest abstract and citation database of peer-reviewed literature...	56
Figure 47: UAV ecosystem (Drone Industry Insights, 2016)	57
Figure 48: Sensors today mounted on experimental self-driving vehicles: Velodyne HDL-32E (left) and HDL-64E (right)	58
Figure 49: Generated map from Velodyne HDL-64E in a test with SLAM techniques (Moosmann and Stiller, 2011)	59
Figure 50: Point cloud for the city of Vaihigen represented in shades proportional to relative elevation	63
Figure 51: Overview for the laser scanner strips acquired over the case study area in the city of Vaihigen, Germany (Rottensteiner et al., 2012).....	64
Figure 52: Details for each of the three area selected in the city of Vaihigen, from left to right: Area 1, Area 2, Area 3 (Rottensteiner et al., 2012).....	65
Figure 53: Comparison in GRASS GIS between two different parameters, highlighted in different colors, for object border definition in the point cloud.....	66
Figure 54: LAStools algorithm classification with points highlighted in different colors: buildings in orange, vegetation in green, ground in brown (Lambertini et al., 2016)	67
Figure 55: Tridimensional visualization of building extracted with ENVI LIDAR (Lambertini et al., 2016)	68
Table 56: Quantitative analysis for building modeled from the point cloud (Lambertini et al., 2016)	69
Figure 57: the concept of a voxel model (right) as a sequence of pixel images stacked one on top of the other (left)	72
Figure 58: Differences of the first five LOD as defined in CityGML.....	75
Figure 59: Aerial three-dimensional overview visualization for the Düsseldorf case study.....	76
Figure 60: Scheme provided by NRW with indications regarding point cloud classification and differentiation between first pulses (F), last pulses (L), and other ad-hoc categories	76
Figure 61: Hillshade for the point cloud subset	78

Figure 62: Data processed for the study area, from left to right: point cloud density, digital surface model, digital terrain model.....	78
Figure 63: The full pipeline of processing described in the sequence of workflow for a specific building.....	79
Figure 64: Cross Sections from the specific building	80
Figure 65: Reference building acquired from Google StreetView	81
Figure 66: DSM for a central area of the city	81
Figure 67: Building slopes processed from LIDAR data against reference data for buildings and aerial image in the background	82
Figure 68: LOD2 3D city model.....	82
Figure 69: CAD 3D models of roof slopes.....	83
Figure 70: Bologna Solar City web application	85
Figure 71: LIDAR data coverage with its density and Bologna district boundaries, highlighting the extension of the processing	86
Figure 72: Cross section in the analyzed point cloud.....	88
Figure 73: Manual adjustment performed by human operator	89
Figure 74: Vector roof models extracted from LIDAR data, displayed in a 3D visualization with the normal vectors applied to each separate slope.....	89
Figure 75: 3D extracted roofs along with buildings footprints from pre-existing digital cartography.....	90
Figure 76: Final LOD2 model for the study area	91
Figure 77: Aspect Map generated from LIDAR DSM masked with Municipality vector boundaries.....	91
Figure 78: 3D vector obtained from LIDAR data processing, TIN model, raster model, masked model, aspect analysis	92
Figure 79: Boxed building model with flat roof, sloped roof, south-facing slopes highlighted in red.....	93
Figure 80: Comparison of algorithm performance over different data density, from left to right: 30, 10, 2 points per square meter	94
Table 81: Results from ENVI LIDAR processing point clouds at different density ...	95
Table 82: Results from LAStools processing point clouds at different density	95

Figure 83: Point cloud and reconstructed model from data acquired both from terrestrial (white points) and airborne (orange points) platforms.....	97
Figure 84: Concept of CLOUD2FEM procedure	99
Figure 85: Workflow for the proposed method composed of completely automated procedures (green), semi-automated or manual procedures (orange) and the threshold detecting algorithm highlighted in red.....	101
Figure 86: Visualization of the concept of slices stacking	102
Figure 87: Visualization of the concept of slicing threshold	103
Figure 88: New displacement of slices after threshold application	104
Figure 89: A selection of 54 slices from the North Tower, two of them highlighted in order to explain the algorithm processing	105
Figure 90: Automatic change detection procedure applied at the slice sequence ...	105
Figure 91: Final voxel model composed stacking each raster, showing floors and vaults in a section cut.....	106
Figure 92: Different FE models with different voxel resolution (Castellazzi et al., 2016)	106
Figure 93: Examples of solar panels placement over complex roofs in the city of Bologna (comune.bologna.it)	107
Figure 94: Example of a building with a roof composed of complex slopes, obtained from Google Street View over the case study of Düsseldorf	108
Figure 95: Results carried out over a building with a roof composed of complex slopes highlight the necessity of high density and accurate point clouds (aerial image on the left, slopes reconstructed from the point cloud on the right).....	108
Figure 96: Explanation of building data acquired with different survey techniques..	109
Figure 97: Interference between existing structures and infrastructures of accessibility-connection (Bramerini and Castenetto, 2014).....	111
Figure 98: Workflow used to search for infrastructures of accessibility-connection .	111
Figure 99: Workflow used to search for structural aggregates interfering with emergency areas	111
Figure 100: Buildings interference with infrastructure as automatically computed with the proposed algorithm (green) and manually selected by human operators (yellow)	112

Figure 101: Buildings interference with infrastructure (left) and emergency area (right) shown in a 3D city model view	112
Figure 102: Localization of the study area	114
Figure 103: Validation of the results	115
Figure 104: Interface of the WebGIS service	116
Figure 105: Openstreetmap.org database statistics for number of ways and nodes added each day	118
Figure 106: OpenStreetMap Geography Awareness Week events held in 2016	119
Figure 107: Open access graph to scientific publication and research data in the wider context of dissemination and exploitation (European Commission Directorate-General for Research & Innovation, 2017).....	121

Acronyms List

- 3D: three-dimensional
- AGL: Above Ground Level
- ALS: Airborne Laser Scanner
- BIM: Building Information Modelling
- CAD: Computer-Aided Design
- COTS: Commercial Off-The-Shelf
- DEM: Digital Elevation Model
- DN: Digital Number
- DSLR: Digital Single-Lens Reflex (camera)
- DSM: Digital Surface Model
- DTM: Digital Terrain Model
- DXF: Drawing Exchange Format
- EPSG: European Petroleum Survey Group
- FE: Finite Element
- FOSS: Free and Open-Source Software
- FOV: Field Of View
- GCP: Ground Control Point
- GIS: Geographic Information System
- GML: Geography Markup Language
- GNSS: Global Navigation Satellite System
- GPS: Global Positioning System
- GRASS GIS: Geographic Resources Analysis Support System GIS
- IFOV: Instantaneous Field Of View
- IMU: Inertial Measurement Unit
- IT: Information Technology
- LIDAR: Light Detection and Ranging

- LOD: Level Of Detail
- MILC: Mirrorless Interchangeable Lens Camera
- MLS: Mobile Laser Scanner
- MMS: Mobile Mapping System
- NIR: Near Infrared
- OGC: Open Geospatial Consortium
- OSM: Open Street Map
- QGIS: Quantum GIS
- RADAR: Radio Detection And Ranging
- RPAS: Remotely Piloted Aircraft System
- RTK: Real Time Kinematic
- SAR: Synthetic Aperture Radar
- SFM: Structure From Motion
- SLAM: Simultaneous Localisation And Mapping
- SRTM: Shuttle Radar Topography Mission
- TIN: Triangulated Irregular Network
- TLS: Terrestrial Laser Scanner
- UAV: Unmanned Aerial Vehicle
- USGS: United States Geological Survey
- VGI: Volunteered Geographic Information

Introduction

Humanity is curious by nature, and thanks to new technological possibilities a large number of scientists, researchers, inventors, and creators have focused their efforts in acquiring information about the environment that surrounds us. In today society spatial information has a paramount importance at all scales and details. Before the invention of the modern airplane, one of the oldest platform to record geographical information over a large area were balloons, immediately followed by kites, rockets, and even pigeons.

Nowadays, modern remote sensing instruments, mounted on a modern platform and assisted with automated procedures are now capable of acquiring data over a vast area in a short timeframe and deliver results with a high detail providing even on-demand acquisition in case of necessity. Information acquired by these systems is processed with different kind of workflow that convert the initial raw data into meaningful products with further processing. This output can be further visualized, analyzed and delivered to other researchers, professionals or stakeholders in general. However, we must not forget the greatest importance of precision and accuracy at this moment when there is an overload of data but sometimes lack of reliable information and metadata.

Furthermore, a deep knowledge of the urban structure geometry is today essential for a significant number of applications such as urban planning, cadastre, environmental analysis, communication, and navigation.

In particular, Geographic Information System (GIS) are now more widespread than ever as they became mission critical tools in different industrial applications and are used by large numbers in various fields of scientific research. Therefore, precise, linked, detailed and updated geographic data is needed. This research focuses on some very promising techniques used to obtain geographic information.

In the last decades, in a standard surveying task, the main instrument used to be the total station. Nowadays new geographic data acquisition technologies brought different tools in the field of topographic mapping and the use of photogrammetry or laser scanning has become a viable choice.

The research has been focused on remote sensing in urban areas, paying particular attention to the analysis concerning the data acquired over buildings. The selection of the appropriate platform for such survey in urban areas is discussed among satellite data, airborne data, or data collected from an unmanned aerial platform. For each platform to use is studied based on the context and the objective of the analysis, adapting the choice at different scales

ranging from the whole urban area to the detail of individual buildings. Then the attention is focused on several sensors suitable for acquiring data in urban areas, fitted on different platforms, with a resolution and accuracy suitable for three-dimensional modeling of buildings. Several techniques are then studied for the acquisition of data in the form of point clouds, in particular, laser scanner and photogrammetric processing, considering the latest respective developments. Following the acquisition process, the performance and characteristics of different software and algorithms used to process the previously detected data are studied. Particular attention is paid to the possibility to increase the automatic processing of data identifying new workflows that may produce a result in an efficient and rigorous way. The innovative analysis made possible by the three-dimensional models constructed from point clouds are discussed and models that integrate data from different sensors, considering the relative accuracy, are studied with varying levels of detail depending on the context. Then different methods and storage formats of geographic data with high resolution and a wide geographical extension are evaluated. Finally, the analysis moves on the best methodologies to structure the data collected and processed within tested Geographic Information System (GIS), even in their 3D-GIS declinations for a complete representation of the building. WebGIS are instead useful to allow sharing of products resulting from the previously described methods, within a platform accessible by the entire scientific community and also understandable for stakeholders. In fact, geospatial analysis can help institutions and local municipalities in urban planning to give better and more efficient results to their citizens.

Many validation tests were performed during the whole three years of PhD research to assess the proposed methodology. This process started immediately after the results achieved in the Master's Thesis (Lambertini, 2011).

The research project aim is to study a reliable workflow that begins from the raw 3D point cloud. It is possible to process a first automatic classification, distinguishing the points of the cloud surveyed over buildings from those acquired over vegetation or terrain, employing advanced algorithms. Further analysis by semi-automatic procedures is possible to recreate the surfaces accurately oriented in space creating a true representation for each slope of the roof of each building. On this new data it is straightforward to perform further analysis such as a reliable estimate of solar radiation on each slope, depending on its orientation and area, and therefore an estimate of the potential use of a photovoltaic system installed on every building in a city.

Being able to produce a highly accurate and semantically complete 3D building model at urban scale is an essential support in managing the urban infrastructure

with a greater level of efficiency and better addressing any critical issues caused by the rapid pace of urbanization (Rottensteiner et al., 2014). A complete 3D city model is the necessary multi-disciplinary backbone for the ubiquitous sensors of a Smart City. In fact, the growing technological evolution will enable a great number of possibilities in sensing data in an urban environment for critical topics such as building and infrastructure monitoring, distribution and transport system (Hancke et al., 2013).

Remote sensed data are widely used in different applications and studies, some of them in urban areas, such as land use/cover mapping, updating of existing maps, detection of buildings and their characterization, urban growth, urban planning, emergency response and even web representations for citizens (Meixner and Leberl, 2011).

A great effort in research is devoted to the automatic reconstruction of building model from remotely sensed data. Therefore a multitude of case studies and procedures at different scales in an urban environment will be presented in the following chapters, trying to compose the big picture of remote sensing for 3D city modeling in the urban environment, with the latest innovation, some new algorithm proposals, and critical issues that are yet to be resolved.

Outline

Within the previously described context, the contents of this thesis will be structured into the following chapters:

- The first chapter discusses the choice of an appropriate aerial platform, based on the context and purpose of the survey, providing the necessary background information regarding the resolutions of remote sensing
- The second chapter is about the process of data acquisition, studying applications of different sensors in different scenarios and the new opportunities and challenges arising from the integration and fusion of such data.
- The third chapter compares performances and results carried out with different software and discusses the processing of the data previously acquired, with the possibilities to increase automation in the workflow in order to carry out a fast and efficient processing. Furthermore, it discusses new file formats and standards with different structures for storing point cloud data, considering the critical issues regarding processing and storage for huge volumes of data.
- The fourth chapter studies the workflow to produce different 3D models with required Level Of Detail (LOD) based on context, for the description of

buildings and features in urban areas, performing analysis at various scales and different LOD: from a complete urban scale to a single building detail.

- The final chapter discusses the end products for scientific community or stakeholders such as virtual 3D city models and WebGIS, and the policies for Open Data.

Chapter 1: Survey Platforms And Parameters

In the field of remote sensing, various platforms can be considered, based on user needs, as the best point of view defined to capture data with a particular sensor.

The French photographer Gaspard-Félix Tournachon, known as Nadar, flew his balloon over Paris in 1858 and captured what is seems to be the first aerial photography ever acquired. Unfortunately, that image is now lost.

Nowadays, what we can consider as the first surviving aerial photograph was captured on October 13, 1860 and is still today conserved at The Metropolitan Museum of Art in New York (Figure 1). It was acquired by James Wallace Black, an American photographer, who titled it “Boston, as the Eagle and the Wild Goose See It”. In agreement with the description contained in the title, the photo shows a portion of the city of Boston and was acquired from a relative height above ground level slightly over 600 meters (Graham and Read, 1987).

The disappearance of the photo acquired by Nadar, the first aerial photo in the world, emphasizes the importance of conservation and sharing of data, an issue that will be addressed in later chapters of the thesis.



Figure 1: Boston, as the Eagle and the Wild Goose See It (James Wallace Black, 1860)

In general terms, remote sensing defines the use of techniques to measure objects from a sensor mounted on a distant platform from the object itself, without any contact between the sensor and the surveyed object (Richards, 2013).

To better understand the consequences of acquiring data from a particular platform, the concept of resolution must be first introduced.

In the specific case of aerial platforms, the distance from the surveyed subject is directly the altitude of the platform itself above the ground (Figure 2).

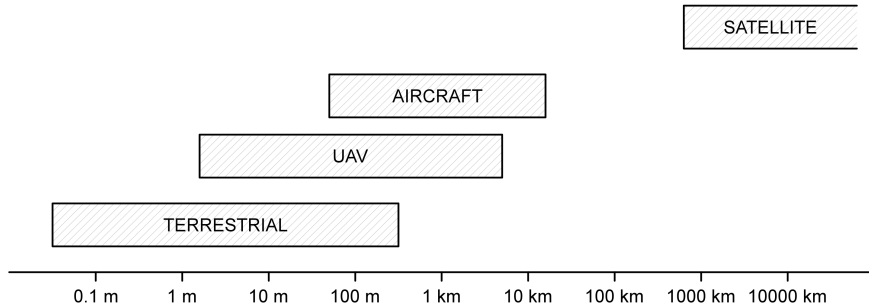


Figure 2: Platforms represented in logarithmic scale to their respective distance from the surveyed object

1.1 Resolutions Of Remote Sensing

In the field of remote sensing, in order to carry out a proper acquisition of data, is crucial to understand the parameters involved. The sensors usually measure the magnitude of reflected energy from the surveyed objects and transform physical phenomena in data. Digital sensors directly record the data acquired in digital formats such as digital images formed by a matrix of DN (Digital Numbers) commonly called raster image (Figure 3). DN in each digital image can represent different attributes such as color, brightness or energy. Each image is composed of a finite number of picture elements called pixel, arranged in rows and columns.

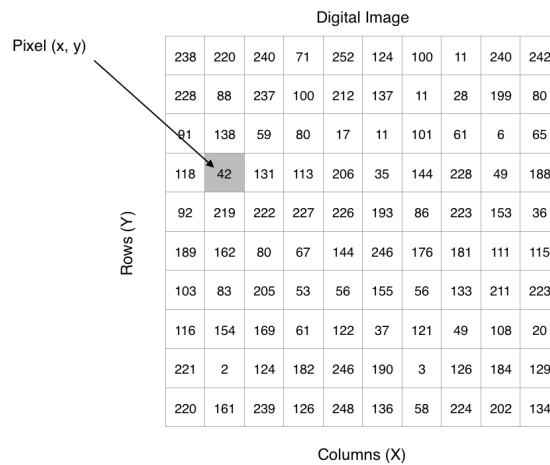


Figure 3: DN displayed in a digital image with resolution 10x10 (rows, columns)

Remote sensing instruments can measure variations defined within three different resolutions: spatial resolution, spectral resolution, and radiometric resolution. In the crucial planning phase, selecting a combination of remote sensing platform and sensor, it is essential to consider the ability to resolve spatial, spectral and radiometric differences in the survey area.

1.1.1 Spatial Resolution

The spatial resolution is determined by the pixel size on the chosen sensor and the distance between the sensor and the acquired object. It is directly represented by the dimension of the IFOV (Instantaneous Field Of View): the area on the ground observed by the sensor at a certain moment (Figure 4).

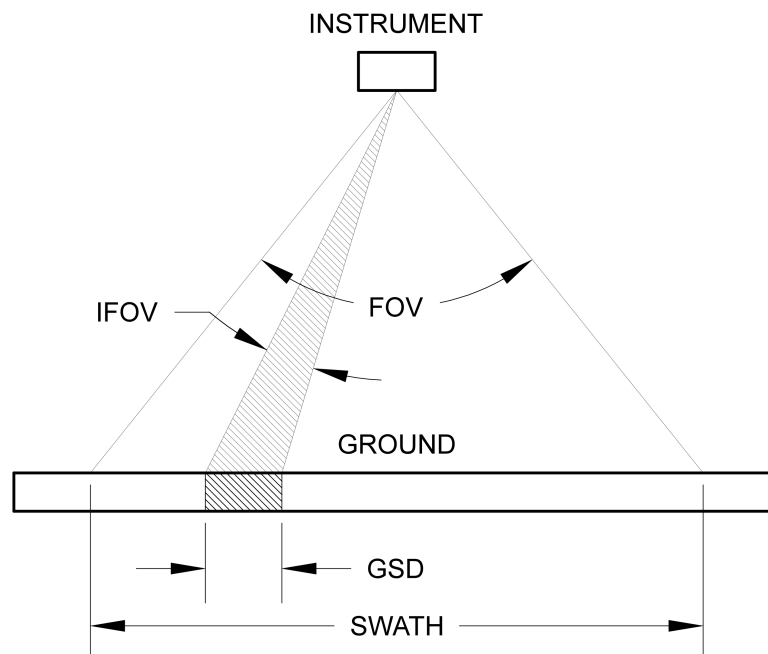


Figure 4: Geometrical definition for image spatial parameters FOV and IFOV

Therefore, is also considered as the area visible in each single pixel in the image acquired. It is also correlated to the GSD (Ground Sampling Distance): the distance between any two consecutive pixel centers, measured on the object. A proper choice for this parameter enables the possibility to observe even small details, important for the desired analysis (Figure 5).



Figure 5: The same portion of urban environment captured from three different satellites (nasa.gov), from left to right with the respective sensor spatial resolution: Landsat ETM+ (28 m), ATLAS (10 m), QuickBird-2 (2 m)

1.1.2 Spectral Resolution

The spectral resolution of an image is correlated with the number and width of the selected wavelength bands in the electromagnetic spectrum and enables the separation of spectral features into their different components. It is strictly connected to the physical properties of the sensor used within the selected platform (Figure 6).

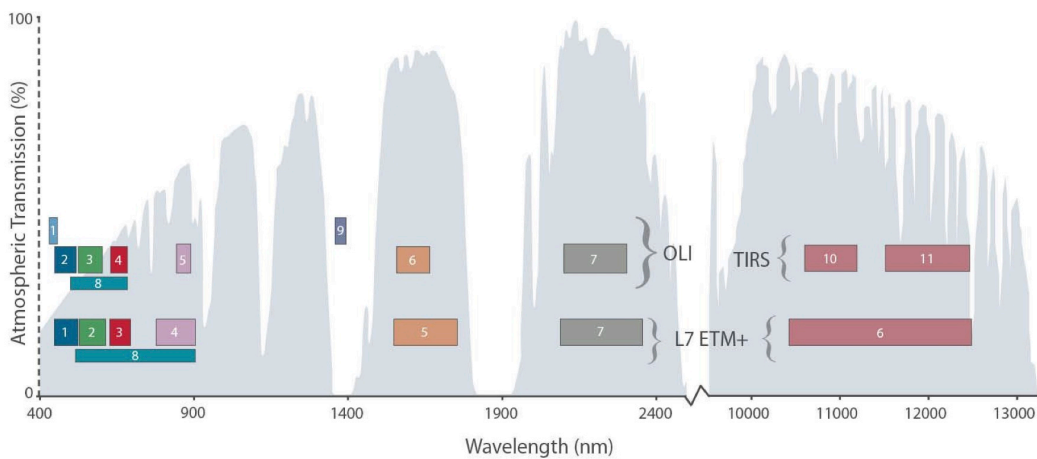


Figure 6: Example of the spectral resolution of a multispectral sensor on a satellite platform (Landsat 8 Data Users Handbook, 2016)

1.1.3 Radiometric Resolution

The radiometric resolution defines the capability of the sensor to measure very slight differences in energy. A very sensitive sensor in radiometric resolution is able to identify tiny differences in reflected or emitted energy from the surveyed objects. The representation of radiometric resolution in DN, it is usually indicated

in binary digits, called bit, needed to express the entire range of discrete available values. Each bit, in computing, as either a 0 or 1. The formula that connects available DN with bits is the following: $DN = 2^{\text{bit}}$. For example, data with a radiometric resolution of 8 bit has 256 different levels of available values (Figure 7), whereas a 16-bit image can represent 65536 values for each pixel.




BIT	DN	Radiometric resolution
1	$2^1=2$	
4	$2^4=16$	
8	$2^8=256$	

Figure 7: Examples of different radiometric resolution

Selecting the sensor and the appropriate platform for a survey, a compromise between the best spatial, spectral and radiometric resolution is inevitable (Figure 8).

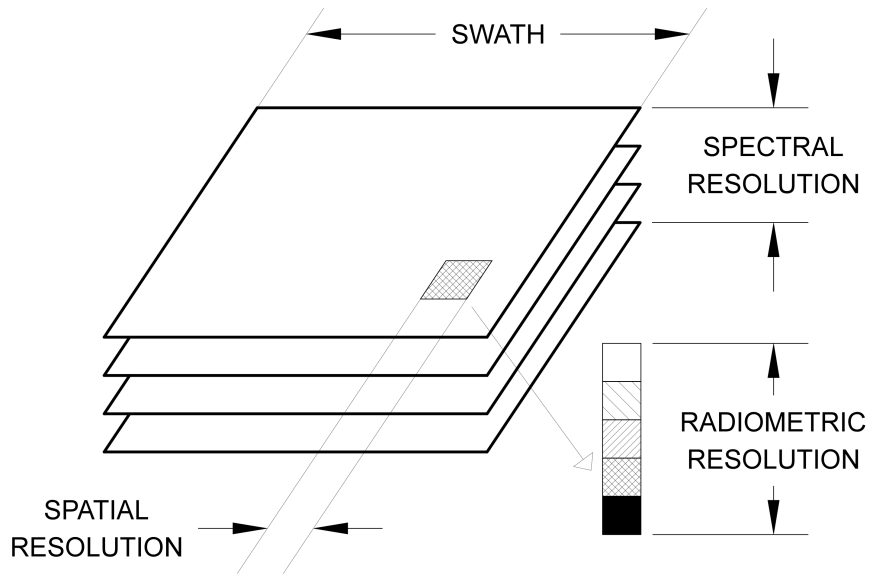


Figure 8: Different resolutions in a digital image

For example, to obtain a high spatial resolution, the sensor must necessarily have a small IFOV, effectively reducing the amount of energy that can be received by the sensor as the GSD becomes smaller obtaining, as a result, a reduction of radiometric resolution. Alternatively, in order to increase the

radiometric resolution without at the same time reducing the spatial resolution, we should broaden the spectrum of wavelengths detectable within the particular band, but this would reduce the spectral resolution of the sensor. On the contrary, a more coarse spatial resolution would allow better radiometric and spectral resolution (Figure).

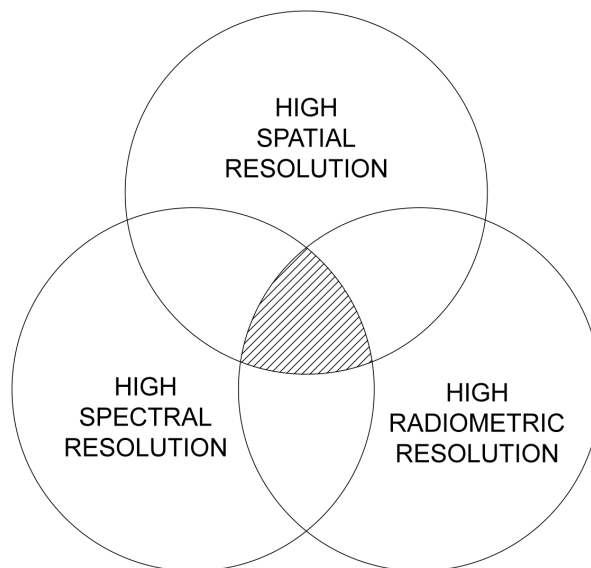


Figure 9: Venn diagram for resolutions of remote sensing

1.1.4 Temporal Resolution

Furthermore, there is a fourth crucial parameter in some applications of remote sensing, defined by temporal resolution. It is determined by the frequency at which a given area is surveyed and it is mainly dependent on the choice of the platform for the survey. In satellite platforms the temporal resolution is correlated with the orbital parameters and the FOV of the sensor. Temporal resolution is also directly correlated to the likelihood of a clear image acquisition, without cloud cover. In the dynamic world we live in, data with high temporal frequency gives the possibility to capture a time series of data in order to better understand different phenomena. In other terms, a high temporal resolution is fundamental when there are sudden and rapid changes. In the case of an emergency scenario, the possibility to immediately acquire post-event data is used to compare it with data previously acquired in order to give a rapid response (Figure 10).



Figure 10: Pre and post-event images for earthquake in Algeria (Bitelli et al., 2004)

A large number of researchers devoted their studies to the registration of pre and post-event data and the relative critical issues. In particular, for a post-event remote sensing survey, during or immediately after a catastrophic event, the strict deadline to deliver processed data to first responders, leaves no room for time-consuming processes, such as the displacement of a minimum number of Ground Control Points (GCP) over the surveyed area. In those scenarios, an automatic co-registration of multi-temporal data acquired over the interested area is precious and time-saving (Aicardi et al., 2016). These procedures can be efficiently used to monitor a specific area and process data with a change detection analysis after catastrophic events in order to address the changes in the topography of an area or in its structures.

1.2 Spaceborne And Airborne Platforms

1.2.1 Satellite

Satellites, as a spaceborne platform controlled by governments or commercial entities, have been used worldwide as remote sensing tool and gained always more importance over the years as a privileged platform for Earth observation. (Figure 11) Among the advantages of the satellite over other remote sensing platforms it is possible to cite its ability to cover large areas thanks to its high altitude and can be therefore considered very cost-effective when used to acquire data over large areas.

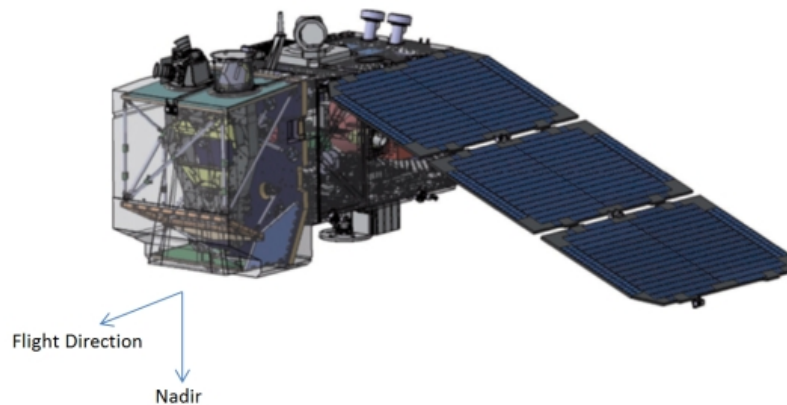


Figure 11: SENTINEL-2 satellite (ESA)

The Landsat programs have recently celebrated more than 40 years of data acquisition (Lulla et al., 2012), therefore it offers a high possibility for historical data evaluation and time series considerations thanks to the continuous data collection carried out over the years. Furthermore, the satellite platform can reach unavailable areas providing measurement and data otherwise inaccessible. Nevertheless, data collected from satellite sensors usually needs also ground-truth data collection to achieve a better accuracy. Moreover, due to the greatest distance between the sensor mounted on this platform and the surveyed object, it does not provide a very high spatial resolution and often it is not suitable for analysis at a local detail.

In February 2000 during the Shuttle Radar Topography Mission (SRTM) from NASA, a Synthetic Aperture Radar (SAR) was deployed on board of the Space Shuttle in order to obtain a new consistent and more accurate Digital Terrain Model (DTM) with almost global coverage. Data was acquired during the 11-day mission from all land surfaces between $+60^{\circ}$ and -56° in latitude (Werner, 2001) generating a DTM with a spatial resolution of one arcsecond (30 meters) providing a dataset of a great value for analysis at a certain scale. However, for analysis at a city scale, more spatially resulted models are needed.

1.2.2 Manned Aircraft Or Helicopter

The use of airborne platforms, such as a manned aircraft or helicopter, in order to carry a different kind of sensors such as laser scanners or digital cameras, can help to produce more accurate models and thematic maps for various applications covering even large areas with a minimum of ground control points. This platform has been the primary source of geospatial data for the developed part of the world until the most recent introduction of commercial remote sensing satellite. When government restriction on satellite imagery resolution was lifted and imagery with a high spatial resolution was finally sold, the difference between

airborne and satellite imagery has been reduced (Toth and Józków, 2016). However, it still maintains an order of magnitude advantage in spatial resolution over spaceborne platforms and therefore guarantees good performances when needed, such as in urban context. Moreover, it can carry different kind of sensors, not only passive but also active such as laser scanners or radar (Figure 12).

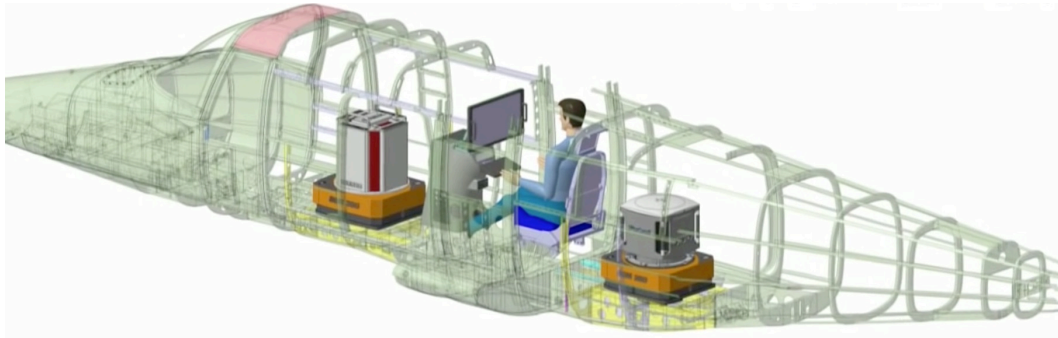


Figure 12: Scheme for sensors and human operator inside a manned aircraft platform (RIEGL)

In order to obtain results with an excellent spatial resolution and a better accuracy, the relative altitude to the average ground level must be kept to a minimum, if the aviation regulations of the area overflown permit it. An airborne survey productivity can be influenced by some constraints such as the weather, illumination of the scene and seasonality for vegetation cover. A low-speed flight aerial platform, such as the helicopter, is preferred over airplane when the survey requires an acquisition of a point cloud with high density. It is mandatory, for example, in surveys aiming to extract transmission lines (McLaughlin, 2006).

1.2.3 Remotely Piloted Aircraft System

The last aerial platform that will be examined in this thesis are the commonly called drones: aircraft without a human pilot onboard in which the control is remotely provided using a controller sending navigation command wirelessly. These platforms are worldwide known through different acronyms: Unmanned Aerial System (UAS), Unmanned Aerial Vehicle (UAV), Remotely Piloted Aircraft System (RPAS) or in general remotely piloted vehicle (RPV). In Italian the acronyms mainly used are Sistemi Aeromobili a Pilotaggio Remoto (SAPR), Aeromobili a Pilotaggio Remoto (APR), Mezzi Aerei a Pilotaggio Remoto (MAPR) or in general Sistemi a Pilotaggio Remoto (SPR).

Air traffic control and the regulatory environment for RPAS is still not harmonized and subject to various level of interaction. There are different interpretations from a global level to a national level and several entities work in a strict hierarchy:

International Civil Aviation Organization (ICAO), European Aviation Safety Agency (EASA), Ente Nazionale per l'Aviazione Civile (ENAC).

The rules for the deployment of a RPAS platform are still evolving, but regarding the structure of the airframe at least two different types can be easily distinguished: fixed-wing and rotary-wing, single or multi-rotor (Figure 13).



Figure 13: DJI Matrice 600 multi rotary-wing RPAS

An excellent review for RPAS in the context of remote sensing is provided by Colomina and Molina (2014).

In the latest years notable advancements have been made in terms of payload and autonomy, in order to increase flight productivity. Still, at the moment of writing this thesis, most operation Beyond Visual Line of Sight (BVLOS) are forbidden therefore limiting the potentiality of RPAS as a survey platform for data acquisition over large areas, such as an entire city.

Data acquired from UAV platform can be easily integrated with terrestrial surveys in order to have a complete survey at a local scale for specific buildings with great detail and good accuracy (Bolognesi et al., 2014).

It results in a productive platform in different fields and applications with a flexible flight planning processing, even for civil engineering surveys (Siebert and Teizer, 2014).

1.3 Other Platforms

There is a multitude of platforms for remote sensing that will not be discussed in detail in this thesis. Among them, mention must be made for terrestrial photogrammetry and terrestrial laser scanner (TLS) (Figure 14). In the urban context, at a local level, terrestrial surveys that can generate a dense point cloud are precious to create computational models for facades (Truong-Hong and Laefer, 2013).



Figure 14: Facade survey using TLS system

However, in order to obtain data for a wide area, such as at an entire city level, a more dynamic platform can deliver faster results with lower costs. In fact, the latter system, when employed on a mobile platform, is often called mobile laser scanner (MLS) or mobile mapping system (MMS) in general terms. MLS is a good platform from which is possible to acquire complete data on building facades from different angles. Using different procedures and methods it is then possible to extract buildings, vegetation, vehicles, poles and traffic signs in an urban environment (Yang et al., 2015) (Figure 15).

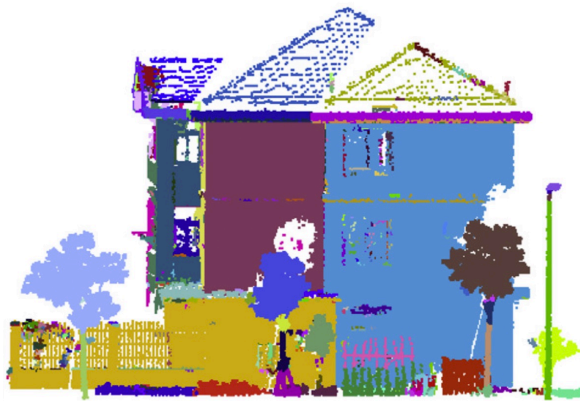


Figure 15: Segmentation of data acquired from a MLS platform (Yang et al., 2015)

There are also other less common aerial platforms, deployed in particular cases. Using ad-hoc developed systems, it is possible to operate sensors for specific needs within a platform lifted by tethered balloons or kites (Bitelli et al., 2004). However, using these unpowered platforms, only controlled by winds and ropes, it is harder to reach a regular image overlap (Figure 16), which is only possible operating with a navigation system controlled by waypoints and a pre-determined flight plan.

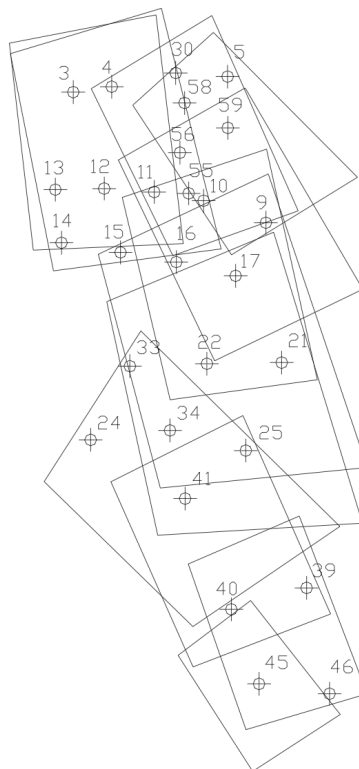


Figure 16: Coverage of imagery acquired from balloon platform (Bitelli et al., 2004)

1.4 Analysis Of The Proper Platform For Urban Applications

The choice of the correct platform for a survey in an urban area is not trivial. A unique answer does not exist and the choice should be based upon the specific requirements for the final products to obtain after the processing. As it was possible to understand, in this chapter all the main remote sensing platform were described with their characteristics, capabilities, efficiency and limitations, impacting mainly the spatial and temporal resolution for the survey (Table 17). Another clearly linked topic that will be discussed in the following chapter is about the sensors that could be installed on different platforms and some of them could also be structured as a multi-sensor system.

	Spaceborne	Airborne	UAV
Cost	High	Medium	Low
Operation	Global	Regional	Local
FOV	Narrow	Wide	Wide
Spatial Res.	Low	Medium	High
Temporal Res.	Days	Hours	Minutes

Table 17: Comparison between some parameters among the three different remote sensing platforms previously described

Chapter 2: Sensors, Data Acquisition And Integration

2.1 Sensors

Remote sensing is recently used as a term to indicate each acquisition of geospatial data completed without contact with the object to be detected. It is, therefore, becoming difficult to establish strict boundaries in remote sensing discipline. Remote sensing is undergoing a rapid technological progress with new developments in sensor technology and improved performance provided by the Information Technology (IT) infrastructure with more processing power and storage possibilities.

Still, remote sensing instruments can be at least divided into two main categories: passive and active sensors.

Passive sensors can record energy emanating from earth's surface, or the acquired object in general terms. This energy, such as natural solar reflected light or electromagnetic energy, is measured using different kinds of sensors mounted on an aerial platform and the measured energy is used to construct an image of the objects acquired from the platform (Richards, 2013).

On the other hand, active sensors emit a signal, in the form of an energy packet, addressed directly at the object of the survey. The same signal is reflected back at the instrument and detected by a sensor. Therefore they may be less dependent on environmental circumstances compared to passive sensors. Radar Among the active sensors that are widely used in remote sensing it is possible to cite Radio Detection And Ranging (RADAR) and Light Detection And Ranging (LIDAR) sensors.

The rapid developments in the fields of laser scanning, photogrammetry, and computer vision give the possibility to survey highly accurate three-dimensional data. Depending on the complexity of the objects various technologies can be applied, fused and integrated. For example, three-dimensional visualization for cultural heritage helps to preserve the memories of historic buildings and archaeological sites.

Nowadays point clouds are the primary source for three-dimensional information. LiDAR sensors have been the primary system to acquire point cloud data for many years, but recent advances in the field of computer vision have allowed a rapid generation of detailed point clouds processed from uncalibrated cameras

with Dense Image Matching (DIM) algorithms, used to generate point clouds from aerial images.

This chapter will provide a non-comprehensive list of accurate sensors that can be used to acquire data in an urban area and can be deployed on the previously described platforms.

2.2 Light Detection And Ranging Technology

LIDAR sensors typically emit near-infrared light to measure the distance from the sensor to acquired objects with a narrow laser-beam. Over the past few decades, the data obtained by airborne LIDAR sensors have become increasingly used in conjunction with data from aerial photogrammetry. Several techniques can be involved in the production of Digital Elevation Models (DEM) due to different filtering algorithm and sensors involved in the acquisition process. The importance of DEM in a vast number of GIS applications is well proven (Weibel and Heller, 1991). Among the main uses of LIDAR sensors it is, in fact, possible to mention the creation of Digital Surface Model (DSM) and the effective filtering and interpolation method for an automatic classification of the laser points into terrain and vegetation in order to create Digital Terrain Model (DTM) even in the presence of dense vegetation (Kraus and Pfeifer, 1998). Consequently, the main applications include the monitoring of forest areas, land mapping, disaster management, urban planning, hydrological modeling and corridor mapping.

Data acquired with a laser scanner is directly a three-dimensional point cloud. The accuracy of 3D coordinates of the points contained in the aforementioned cloud depends on various factors that can be grouped in three main categories: range, position and direction of the laser beam (Baltsavias, 1999) and since the results are georeferenced from the onboard GNSS receiver the final the final results is also dependent on the accuracy of the transformation between WGS84 and any local coordinate system.

The first LIDAR sensors recorded just the first return. Only at a later time, the ability to record also the last return was introduced in order to acquire terrain data which is in some scenarios located at the bottom of vegetation. In those areas coverage given by foliage usually is not completely impervious and while a part of the pulse is typically reflected from the leaves, another part may pass into the spaces left empty reaching the bare soil. With this method is possible to obtain different benefits. It becomes possible to generate a digital terrain model (DTM) also in the presence of vegetation with foliage, a practice not possible with photogrammetric techniques. In addition, calculating the difference between the first and last return it is possible to obtain a measure of the height of the

vegetation. Subsequently, with the progress of technology, it was made possible to record not only the first and last return but also an additional number of intermediate discrete return ensuring the acquisition of more valuable information.

One of the crucial parameters in the choice of an specific airborne laser scanner system for a particular survey is its resolution intended as the point cloud density that it can record at ground level. This is dependent on the technology used, speed of the aircraft, its flying height and the instrument properties such as FOV, the pulse frequency and the speed of rotation of the scanning mirror (Figure 18).

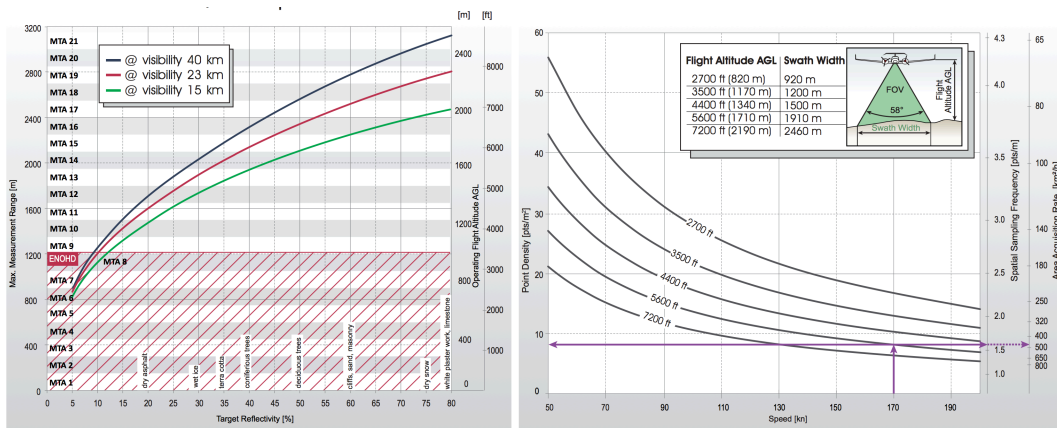


Figure 18: Example provided from laser scanner RIEGL VQ-1560i data sheet is possible to obtain a point density of 8 points per square meter with 2 sensors a 1M pulses/s with laser power level set at 100% from an altitude of 5600 feet and a speed of 170 knots

2.2.1 Linear-Mode

The most common and widely used LIDAR technology is the one defined as Linear-mode. A finite number of laser pulses using an high level of energy are emitted from the sensor with an high spatial precision. Each pulse reflected from the acquired surface is received back and recorded by the instrument and recent LIDAR systems can measure multiple returns for any pulse emitted. However, some physical limitations have to be taken into account, such as a limit on the maximum number of pulse rates. As a simple example, at a flight altitude of 1500 meters AGL, considering the time of flight of each pulse traveling at 300000 km/s, the pulse rate of the instrument must be lower than 100 kHz because each pulse have to be received before the emission of the subsequent pulse in order to avoid confusion between different returns. This directly limits the number of points per square meters at ground level that is directly correlated with the pulse rate of the instrument.

To overcome these intrinsic limitations of the first LIDAR systems, in order to increase the point cloud density at ground level, recent technologies allowed to

send multiple pulses in air. Furthermore, new high-end LIDAR systems often combine two sensors able to emit and receive different pulses at the same time, doubling the global frequency of the instrument (Figure 19).

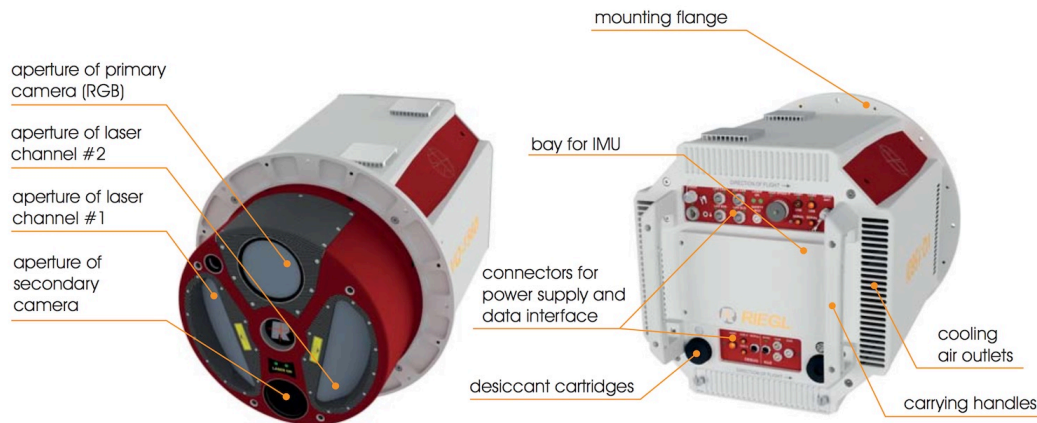


Figure 19: RIEGL VQ-1560i equipped with two laser scanner sensors

2.2.2 Full Waveform

Simple linear-mode systems provide only 3D coordinates. Processing the surveyed 3D point cloud, any segmentation and classification method has to rely solely on geometric information. With systems that can record the full waveform of each pulse received, instead of only a discrete number of returns, each analog return is digitally sampled at fine regular intervals, for example 1 nanosecond, and therefore can be further characterized by the amplitude, width, and cross-section. Based on the height of surveyed object and fixed sample interval, 64, 128, or 256 samples are recorded for each pulse sent. Apparently this survey generates a conspicuous amount of data that needs improvements in storage capabilities and processing power. This combination of geometric and thematic information triggers new possibilities in 3D segmentation, acquiring more attribute about ground features, producing a reliable classification of objects (Wagner et al., 2006) through the delivery of a virtually unlimited number of returns for each sent pulse. This is particularly useful in modeling vegetation and its details. Furthermore, from the digitized waveform is possible to extract data regarding surface roughness, slope, land cover and even derive products such as DEM with spatially variable predictive uncertainties or error maps with an error estimate for each point in order to produce a more rigorous quantitative analysis of data (Jalobeanu and Gonçalves, 2014).

2.2.3 Single Photon

New sensors now available on the market use a technology called Single Photon LIDAR (SPL) that initially was developed for Earth-to-satellite ranging. Each pulse is divided in a hundred of smaller beams and due to the array sensitivity to single photon events, the system greatly reduces the power dissipation requiring a minimal amount of energy (Niclass et al., 2005). Furthermore, the final pulse can reach a significantly higher rate, allowing the platform to move faster while maintaining a very high point cloud density at ground level, providing a greater detail for surveyed objects. SPL (Figure 20) is an efficient instrument for data collection and is becoming a cost-effective alternative to existing LIDAR systems for large area mapping thanks to its ability to produce a very dense and detailed three-dimensional point cloud over large areas in short timeframes (Swatantran et al., 2016) reducing the final cost per data point by an order of magnitude. The raw data can contain a considerable amount of noise, which can be efficiently filtered using different methods with high accuracy and great efficiency (Tang et al., 2016).



Figure 20: Leica SPL100 single photon LIDAR

2.2.4 Geiger-Mode

Geiger-mode LIDAR (Aull et al., 2002) has been only recently made available in commercial market after being used in the defense sector for over a decade. It uses a different approach and it's able to acquire dense point clouds with a high sample rate from higher altitudes providing a very good ground coverage across the survey area. As for drawbacks, it has minor performances when flying in daylight and the raw data present a higher level of noise compared to linear-mode LIDAR. It uses an even larger array for data collection, usually with a 32x128 matrix array containing 4096 detectors, and it can collect data from multiple angles reducing the chance of occlusion in the surveyed scene (Figure 21).

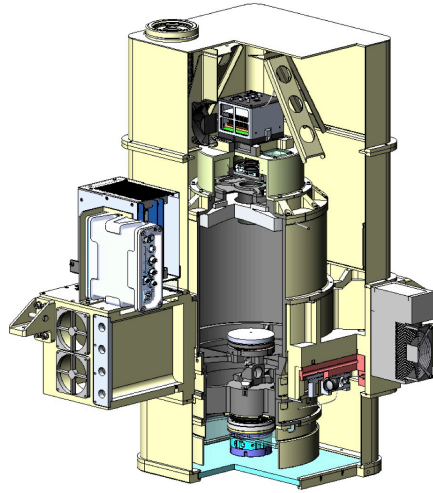


Figure 21: Geiger-mode LIDAR scheme (HARRIS)

2.2.5 Flash

Also Flash LIDAR cameras are structured with a matrix array of pixels, counting the highest number of detectors, in which each of them measures the time the pulse takes to travel to the target and be reflected into the camera sensor, providing a 3D depth and intensity of the image acquired (Figure 22). The range of the objects appearing in camera FOV is calculated and a 3D point cloud is generated at high speed. These sensors are still in development due to their high complexity for aerial surveys (Liu et al., 2009). They reached a wide diffusion in the gaming market through the introduction of KINECT platform, which is also interesting for close range and indoor mapping applications (Khoshelham and Elberink, 2012).



Figure 22: ASC Peregrine 3D Flash LIDAR Vision System

The choices for the proper instrument will depend on different sensors capabilities, flight planning, the size of the survey area, desired data density at ground level, delivery timeframe and also the economic budget available for instrument use (Table 23).

	Linear	Photon	Geiger	Flash
Altitude AGL	150-1500m	1000-8500m	4000-11000m	500-2000m
FOV	45-60°	10-40°	30°	5-10°
Detectors	<10	100	4096	16000
Points/s	100-800k	200-350k	200-400M	325-500k
Coverage km²/h	50-180	170-500	1000-1600	40-160

Table 23: Main parameters for different airborne LIDAR technologies set to reach a point cloud density of 8 points per square meter (HARRIS)

2.2.6 Multispectral

One last airborne LIDAR instrument for airplane or helicopter platform that will be here described is a multispectral laser scanner, produced by Optech, named Titan Multispectral LIDAR (Figure 24).



Figure 24: Optech Titan Multispectral LIDAR system

It collects valuable information using three separate active imaging channels with different wavelengths: 532nm, 1064nm, 1550nm (Figure 25).



Figure 25: Example of survey with Optech Titan Multispectral LIDAR with point clouds acquired at different wavelengths, from left to right: 532nm, 1064nm, 1550nm

Each channel, one of which is at Near Infrared (NIR), work at a 300 kHz frequency, acquiring a global point cloud at 900 kHz. The multispectral data can be used for disaster response, land cover classification, environmental modeling, forest inventory, vegetation classification and even shallow water bathymetry.

2.3 Sensors For Remotely Piloted Aircraft System

2.3.1 Light Detection And Ranging Sensors

With recent advancements in sensor technology and RPAS payload capabilities, the LIDAR market for RPAS is expanding. RPAS platforms are in fact being increasingly used as a low-cost alternative to other aerial platforms in order to obtain valuable data for small areas or individual buildings, in order to produce maps and 3D models (Nex and Remondino, 2014).

Both LIDAR and RPAS technologies are evolving and the union of the two is still at its beginning. As the technology will advance in both sectors, it will lead to new developments and applications. Until some years ago, LIDAR sensors were confined to manned platforms such as airplanes and helicopters due to the weight of those sensors and the power needed to operate them. Only recently, some compact, lightweight, and low-energy LIDAR instruments have become available and every year active sensors and high-grade IMU are getting smaller and cheaper (Colomina and Molina, 2014).

For example, RIEGL VUX-1 which was commercially available only in the last year. It is a very compact instrument (227x180x125 mm) and with a weight of just 3500 grams can be mounted on a good number of fixed-wing and rotary-wing RPAS platforms. Using a rotating scanning mirror it can capture up to 200 parallel scan lines per second with time-of-flight measurement rate up to 500 kHz with an accuracy of 10 mm and provides internal storage with several hours of data collection in a 240 GB Solid State Disk. Its FOV is 330° and it can operate up to an altitude of 300 meters above ground level providing full waveform recording. An even more recent variation of this instrument is the more compact RIEGL

miniVUX-1 that weighs only 1550 grams, with a 360° FOV, and it can acquire data up to 100 kHz (Figure 26).



Figure 26: RIEGL VUX-1 and RIEGL miniVUX-1

From another producer, the YellowScan Mapper was presented in 2014, with a maximum flying height of 100 meters and a pulse frequency of 40kHz. Other parameters are the FOV of 100° and it can record up to three values per pulse sent (Figure 27).



Figure 27: YellowScan Mapper

There is a good number of RPAS instruments build upon simultaneous localization and mapping (SLAM) techniques equipped with Velodyne systems such as HDL-32 (1 kg) or the smallest and cheapest VLP-16 (0,8 kg) that can perform simultaneous positioning for the platform and mapping for the surveyed area (Moosmann and Stiller, 2011).

Velodyne VLP-16 has 16 channels with a 360° FOV and can acquire data at 300 kHz using 16 separate channels with 2 returns per pulse sent and a range of 100 meters. These instruments can reach a range repeatability under 1 centimeter with a beam divergence under 3 mrad. Among the instruments equipped with

Velodyne LIDAR it is possible to mention YellowScan Surveyor, KAARTA Stencil, and Phoenix Lidar System Alpha AL3-16. These systems can be mounted also on backpacks to build a MMS, boats or cars, and in fact they can be a part of self-driving car systems (Figure 28).



Figure 28: YellowScan Surveyor, KAARTA Stencil, Alpha AL3-16

2.3.2 Digital Camera Sensors

A promising segment of the market is today related to UAV-mounted camera sensors due to recent developments. Having to deal with a constrained payload, weight is a fundamental parameter for UAV photogrammetry, while it is not a strict limit for photogrammetry from a manned airplane or helicopter. It must be limited in order to maintain flexibility in the selection of flight height, duration, and speed.

Especially in rotary-wing platforms, the sensor is not directly connected to the aircraft. Instead, a gimbal is used to support the sensor, as a pivoted mechanism allowing rotation of the supported sensor around a certain number of axis. The use of gimbals in remote sensing allow the computation of a pre-determined path and trajectory to keep the line of sight of the camera targeted to the surveyed object (Sun et al., 2008). In particular, gyrostabilized gimbals are also employed in order to free the sensor from any vibrations transmitted by the RPAS platform (Figure 29). Furthermore, maintaining a remote control on the gimbal movements, the ground operator can chose in real-time during the survey where to point the sensor in order to acquire nadiral imagery or oblique imagery being able to observe also facades of buildings in order to generate a complete 3D city model containing details and texture data for each element of the surveyed structures, developing specific methods to avoid problems arising from occlusions (Rau and Chu, 2010).

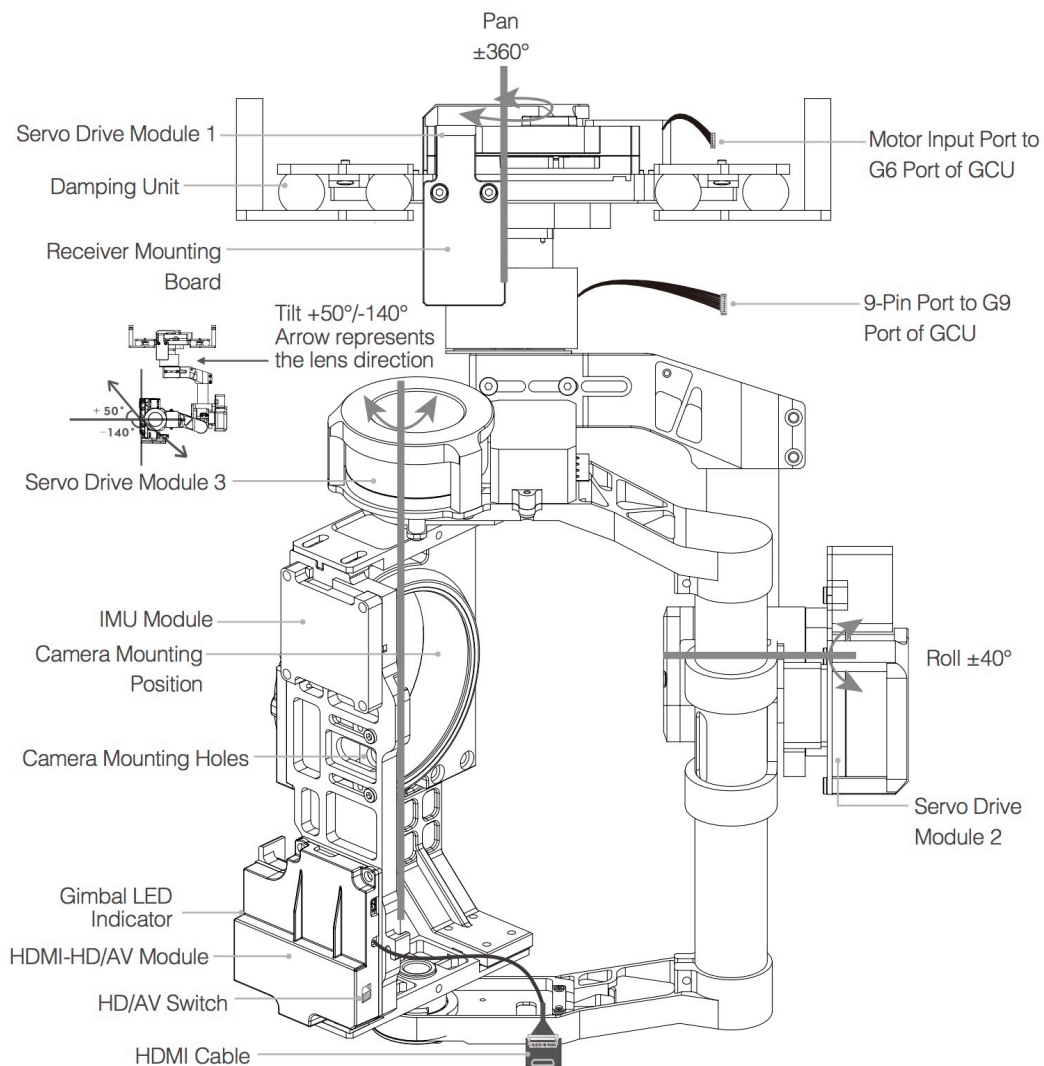


Figure 29: DJI 3-axis gimbal functional diagram demonstrating angles for pan ($-360^{\circ}/+360^{\circ}$), tilt ($-140^{\circ}/+50^{\circ}$) and roll ($-40^{\circ}/+40^{\circ}$)

Certain research studied the possibilities of specific sensors, such as hyper-spectral camera, and new possibilities that arise with surveys performed from a RPAS platform accessing areas without disturbing the surface cover and acquiring data from pointing the sensor at different angles to easily assess particular effects over any land cover (Burkart et al., 2015).

The RPAS platform can guarantee the possibility to maintain a close distance from the sensor to the object to survey when it is needed. Thanks to the control over the gimbal it is possible to acquire in a single flight both vertical and oblique imagery in a short timeframe. It is verified that the simultaneous use of images with a vertical and inclined axis in the generation of a dense 3D point cloud has reduced the uncertainty of the final model (Bolognesi et al., 2015).

In the last decade, a growing number of Digital single-lens reflex camera (DSLR) were replaced on the market with more compact mirrorless interchangeable lens camera (MILC) thanks to their lowest size and weight, maintaining the same image quality thanks to large sensors.

A good number of low-weight cameras that can be equipped on a UAV are nowadays available, with various sensor size, resolution, pixel pitch and focal length (Figure 30). However, low-cost sensors may have low performance when it comes to the impact of rolling shutter, compared to the performance of high-level sensors with global shutter. This affects the quality of results if these sensors are deployed in UAV platforms flying at relatively high speed (Vautherin et al., 2016).



Figure 30: Example of DJI Matrice 600 equipped with Ronin-MX gimbal

In the process of selecting the proper camera for the survey, a few important parameters must be considered such as weight and sensor properties such as size and pixel pitch. The sensor size is directly correlated to the Ground Sample Distance (GSD). Pixel pitch, instead, is the physical dimension of each pixel in the sensor and is usually computed as the physical dimension of the sensor divided by the linear resolution of the sensor itself along that dimension. A larger pixel pitch allows the acquisition of crisp data with less noise even in low-light scenes. A few examples of some cameras that can be lifted by commercial RPAS are listed in the remaining part of this section.

The model iXU 1000 from Phase One is a professional optical camera suited for RPAS integration with a sensor that delivers 100 megapixels providing an excellent GSD even at higher flight altitudes. It is, in fact, a true metric calibrated camera specifically designed to withstand vibrations and different weather conditions when deployed on a RPAS platform. It is also available with an optional configuration for near infrared (NIR) surveys (Figure 31).



Figure 31: Phase One iXU 1000

X1D from Hasselblad has a medium-format 50 megapixels sensor in a compact MILC body. It weighs over 1000 grams with one of the two lenses available (35mm or 70mm) which is compatible with a good number of RPAS payloads, delivering a great FOV for different applications at a more reasonable price (Figure 32).



Figure 32: Hasselblad X1D

Sony A7 has a full-frame 24 megapixels sensor retaining compatibility with a large set of lenses available on the market, being able to adapt with a good versatility at different use cases. Also this model is a MILC that weighs under 500 grams without the lens. It has a good value for money and can deliver high-quality images (Figure 33).



Figure 33: Sony A7

Sony A6300 is equipped with a smaller APS-C sensor but still retains an excellent 24 megapixels resolution at almost half the final price from the full-frame model in a smaller and lighter body. Also this model is a MILC and it is the last option in this overview to offer different focal length based on the survey choice (Figure 34).



Figure 34: Sony A6300

Zenmuse X4S is a camera developed exclusively for the RPAS market by DJI with a 20 megapixels resolution and a 24mm equivalent lens with 84° FOV. It has good image quality for a 1-inch sensor, and the optics assure low dispersion and low distortion. The image acquired can be recorded in raw format in order to avoid JPEG lossy compression (Figure 35).



Figure 35: DJI Zenmuse X4S

Hero 5 Black is the most recent high-end action camera available from GoPro, the popular leader action camera market (Figure 36). Its lightness, around 100 grams, it's good for micro UAV photogrammetric surveys and with its low payload can increase flight time. The biggest limitation is the size of the sensor, the resolution and the large distortion effects caused by a very short focal length. However, being a low-cost and low-weight optical sensor, also deployable in underwater surveys (Capra et al., 2015) it gathered interest from the scientific community and a lot of researchers have focused on the critical process of this sensor calibration (Balletti et al., 2014).



Figure 36: GoPro Hero 5 Black

With all the information gathered from the previously described sensors, it was possible to perform a comparison based on precise data in order to better understand the deployability of a different camera based on payload capabilities, resolution needs, impact on GSD (Table 37). Also, a graphical representation of the different sensors sizes was carried out for further comparison and to better

understand the great differences in sensing surfaces that are possible to obtain with the presented instruments (Figure 38).

	Phase One iXU 1000	Hasselblad X1D	Sony A7	Sony A6300	DJI Zenmuse X4S	GoPro Hero 5 Black
Weight [kg]	0,93	0,73	0,47	0,40	0,25	0,12
Resolution [MP]	100	50	24	24	20	12
Resolution H [pixel]	11608	8272	6000	6000	5472	4000
Resolution V [pixel]	8708	6200	4000	4000	3648	3000
Sensor H [mm]	53,4	43,8	35,8	23,5	13,2	6,2
Sensor V [mm]	40,0	32,9	23,9	15,6	8,8	4,6
Pixel pitch [µm]	4,6	5,3	6,0	3,9	2,4	1,5
Price	€€€€	€€€	€€	€	€	€

Table 37: RPAS camera specifications comparison

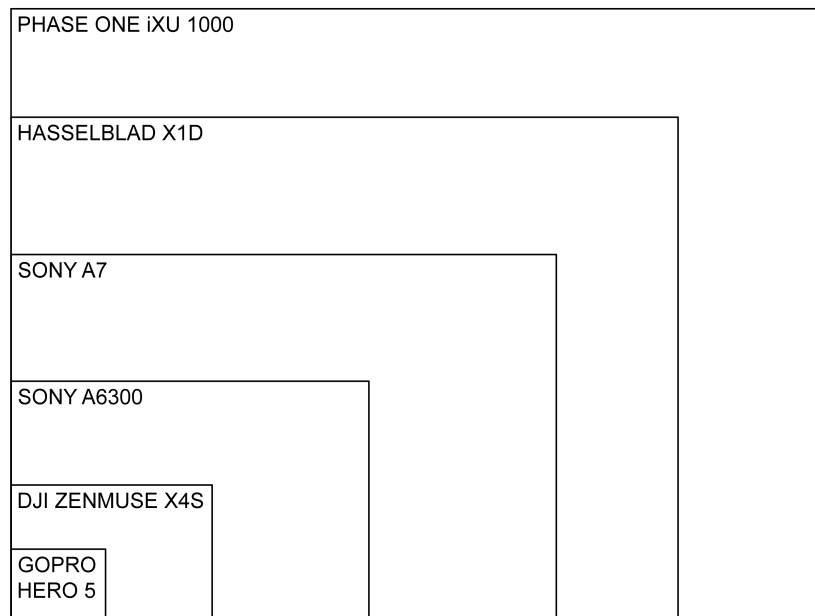


Figure 38: Graph showing relative sizes of camera sensors

2.4 Discussion

The described sensors are in some cases complementary regarding the survey detail, survey coverage and spectral information. In some studies, such as in Stal et al. (2013) data acquired from aerial imagery is compared to products derived from LIDAR and compared qualitatively and quantitatively.

With the combination of the good height assessment accuracy of the laser scanner and good planimetric accuracy of aerial images, both high accuracy and higher automation in data processing can, in theory, be obtained (Shan and Toth, 2008).

From LIDAR surveys, for instance, it is possible to obtain a cleaner point cloud and a complete information regarding vegetation and objects below it. Furthermore, it is a sensor not dependent on light conditions.

Regarding the case studied in the context of this thesis in urban applications, a few critical issues such as occlusions and irregular point density have an impact on the final quality of 3D city models.

Regarding occlusion, it is a common problem for sensors mounted on airborne platforms applied in surveys for urban areas. As previously said, the laser scanner can acquire data even from objects hidden behind vegetation, penetrating the foliage. Nevertheless, the final result depends on the leaf surface and foliage density. Furthermore, neither LIDAR or photogrammetry techniques can avoid occlusions due to solid objects that pose in between the sensor and the complete acquired scene. In order to have complete data for the area, even for the building facades, sometimes a terrestrial survey or a low-height flight must be taken into account, with an oblique acquisition.

Furthermore, there are some variables that contribute in generating a point cloud with an irregular density. It must be considered that, for instance, LIDAR sensors emits a signal that is reflected by the surveyed surface and the final size of each pulse footprint or distance measured on the ground between consecutive pulses is correlated to the platform altitude and technical specification of the LIDAR instrument. Furthermore, some returns are discarded for their weak intensity caused by an unfavorable angle of the surveyed surface. The final result is a point cloud with irregular displacement of surveyed measures and the 3D models that are later generated from the dataset can suffer from fragmentations and holes lowering the global accuracy of the results. Regarding possibilities for direct survey and georeferencing from an aerial platform, without the use of Ground Control Point (GCP), it is feasible if supported by accurate Inertial Measurement Units (IMU) (Mostafa and Hutton, 2001).

2.5 Data Fusion

One of the key points of the research described in this thesis is data fusion in order to find the proper way to use any data available in the case study area inside the interpretation processing. As it was illustrated in previous sections, it is possible to process different data acquired with different sensors at a different distance from the desired object. For instance, a point cloud acquired with LIDAR sensors can be integrated with aerial thermal imagery and ground surveys in order to determine a better model for the environmental conditions of the area studied, providing a DSM with a high spatial resolution and a detailed model for Sky-View Factor (Mandanici et al., 2016).

The presented research involves mainly around data in the form of point clouds acquired from airborne platforms. Nevertheless, this data can be integrated with information obtained from high-resolution images acquired from satellite and other laser scanner data acquired from a terrestrial platform. Furthermore, other possibilities are now offered by sensors that can be mounted on a RPAS. One of the challenges in data fusion is considering the accuracy of different data, that vary mainly depending on the distance of acquisition and generally it is inversely proportional to how wide is the area covered by the acquisition.

One of the topics of research concerns the study of best practice to integrate geospatial data with different characteristics, acquired from different surveys. Use of accurate data and updated metadata is mandatory, within the same spatial and temporal reference system. Both the scientific community and technicians need precise and up to date geographical data for different purposes.

2.5.1 Case Study

The case study here presented considers data acquired in two areas within the city of Bologna, as detailed in Figure 39 and Figure 40.

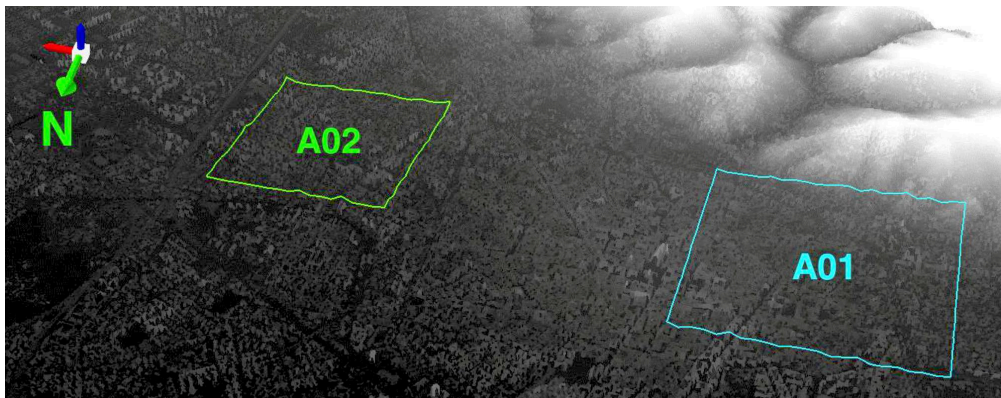


Figure 39: Two case studies represented over the DSM of the city

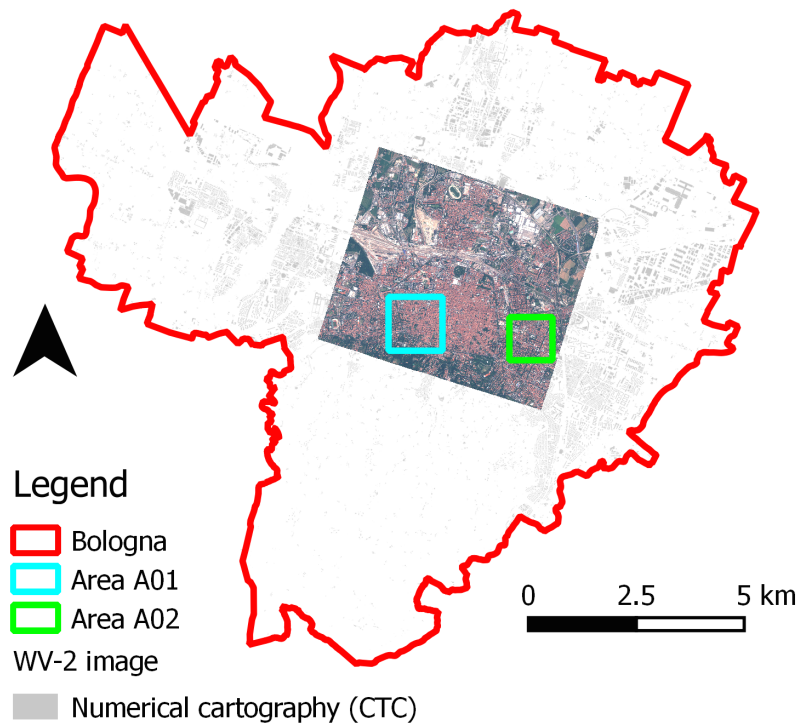


Figure 39: The two area studied in the Bologna case study

There were available: a very high-resolution multispectral satellite image, a 3D point cloud acquired by aerial laser scanner and a digital cartography, generated through aerial photogrammetry and updated by the Municipality of Bologna, used as a geometric reference (Figure 41).

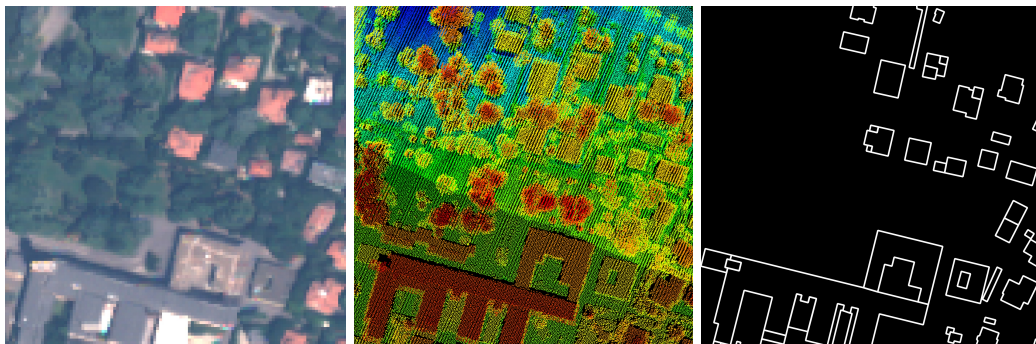


Figure 41: Very high-resolution multispectral satellite image, 3D point cloud acquired by aerial laser scanner, digital cartography used as reference data

2.5.2 Integration Of Remote Sensed Data

The information obtained by remote sensing data processing has been included within the Geographic Information Systems in order to integrate and combine them with other textual and descriptive information in a sustainable land use

planning perspective. The main problems in detailed and accurate urban area representation by using remote sensing technology result from the spatial and spectral heterogeneity of the urban environment typically composed of built-up structures (buildings, transportation areas), various vegetation covers (e.g. parks, gardens, agricultural areas), bare soil zones and water bodies. Remote sensing resources such as Very High Resolution (VHR) images and LiDAR data, together with new image analysis techniques, have improved the mapping and analysis of urban areas.

Processing all the data available it was possible to orthorectify the satellite image using a digital surface model obtained from LiDAR data and obtain elevation information from the laser scanner by subtracting the digital terrain model from the digital surface model, in order to evaluate the heights and volume of each building. It was also possible to compare the data with the existent digital cartography (Figure 42).

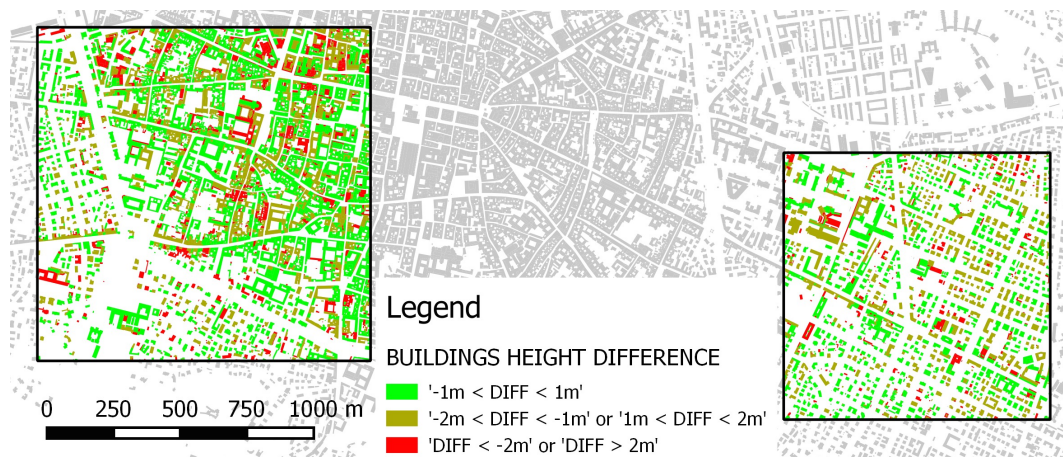


Figure 42: Comparison between building elevation as recorded in digital cartography and elevation processed from LIDAR data

Using the data obtained from the multispectral image it was possible to perform a classification of roofing materials of each building (Figure 43).

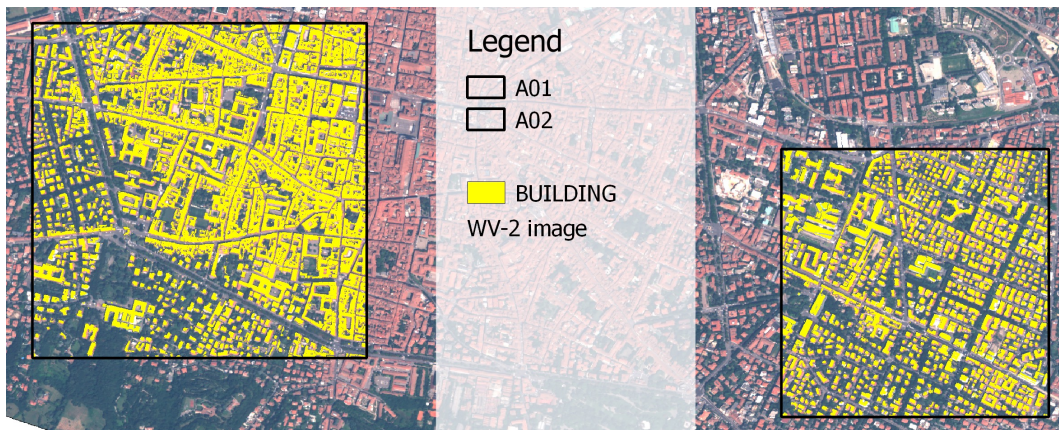


Figure 43: Classification of buildings

It was possible to produce a workflow for the simultaneous use of heterogeneous techniques such as satellite imagery and the aerial laser scanner in order to update an existing database while providing new information at urban scale. Bologna city has been considered as an example, due to the richness of available data, testing the procedures to extract and classify buildings in two specific areas. Two subareas have been in particular analyzed in order to evaluate the performance of the whole workflow: the first refers to the historic district with its complex cluster of extremely close buildings, and the second includes territory at the foot of the hills, where the digital surface/terrain model constitutes an important information.

An object-based classification of the buildings has been performed, taking in account geometric and radiometric properties derived respectively from multispectral satellite imagery and LiDAR aerial acquisition, the latter used in the segmentation process also to avoid problems deriving from the image orthorectification. The results, compared with the available large scale numerical cartography, show a good level of accuracy in the footprint of the identified buildings (Figure 44).

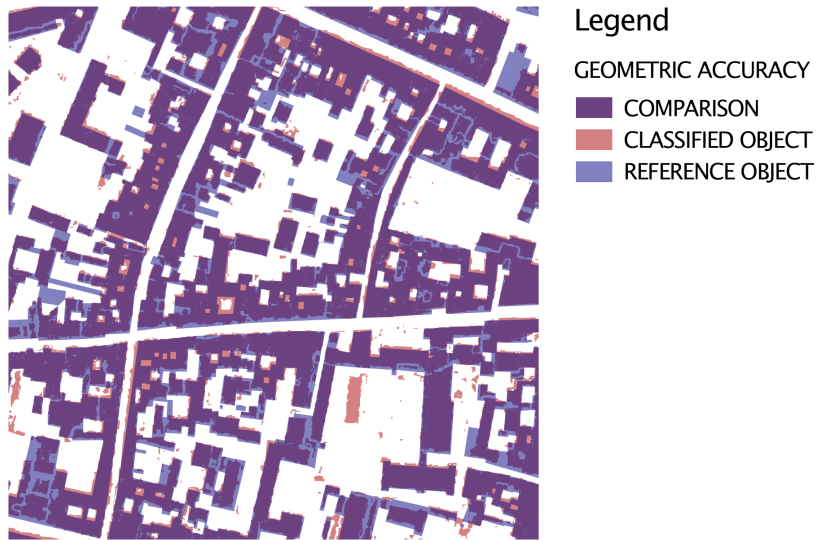


Figure 44: Geometric accuracy for the buildings processed and classified against the reference data from digital cartography

Furthermore, the use and integration of multispectral data from the WorldView-2 sensor have been indispensable to classify the materials of each building roof. The obtained map with the building's classification, according to their roofing material, have been further used to derive an additional level of information in the available numerical cartography (Figure 45).

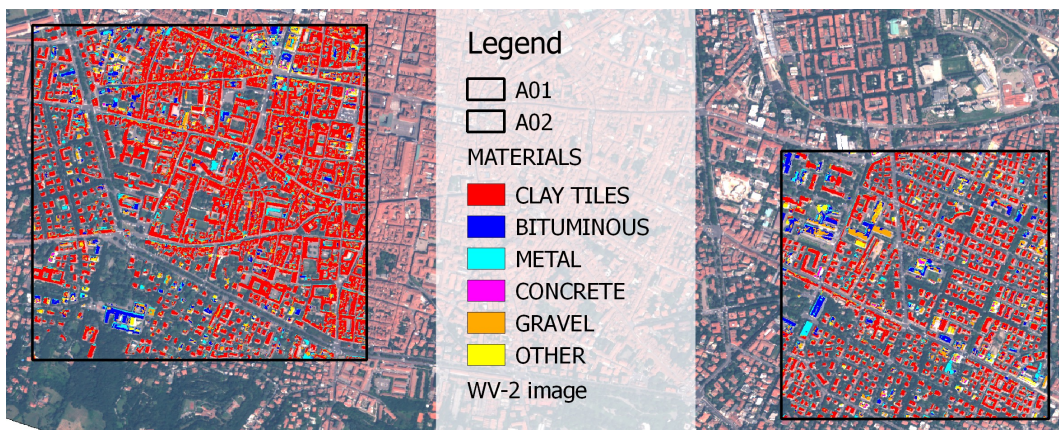


Figure 45: Classification of roof materials (Franci et al., 2014)

The experience here described shows different thematic maps produced in a GIS environment from the integration of data acquired from different platforms and sensors for an urban application. One of the critical issues was to properly co-registered all the different geospatial data. This created an added value updating and enriching a pre-existent numerical cartography, delivering precious information useful in a Smart City perspective, where accurate and up-to-date databases are crucial for a number of applications at urban scale such as energy

performance indicator, traffic analysis, environmental monitoring (noise, pollution) and sustainable planning. All the data and thematic maps provided in this section were processed in collaboration with an expert colleague expert responsible for all the classification of multispectral imagery and finally published in Franci et al. (2014).

2.6 Challenges And Perspectives

Our technology-driven world is changing and the number of sensors will further grow at a rapid pace. This section tries to describe the possible consequences and the related challenges and problems that will arise from the spread of a few new technologies that will both use and acquire 3D data, especially in the urban environment: RPAS and self-driving vehicles.

2.6.1 Growing Trend In Unmanned Aerial Vehicle Applications

RPAS platforms and sensors were described in detail in the previous sections, but there is a clear growing trend both in the commercial market and in research field as the platforms are more capable and the sensors are improving their resolutions (Figure 46).

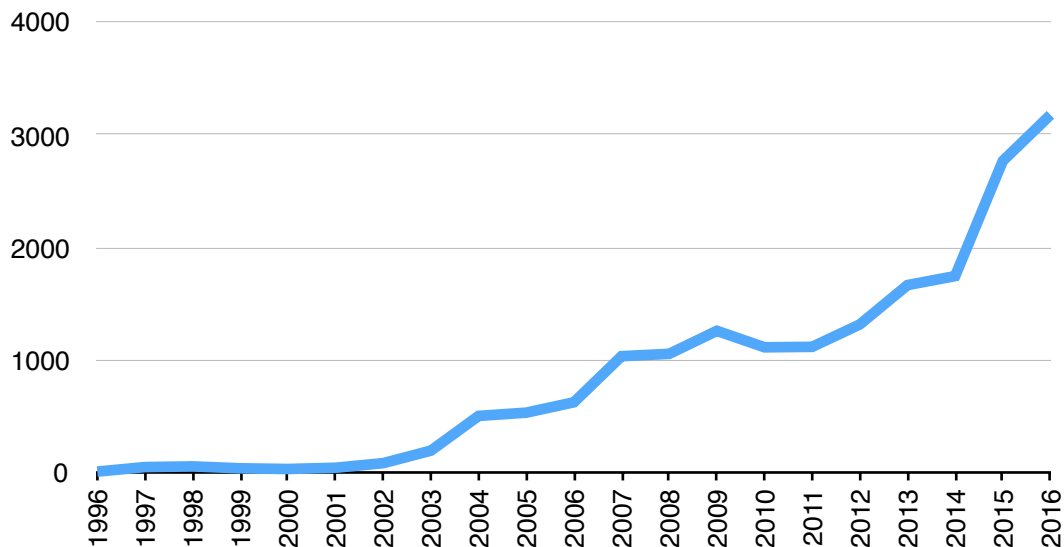


Figure 46: 'UAV' used as a keyword in scientific literature indexed in Elsevier's Scopus, the largest abstract and citation database of peer-reviewed literature.

Gartner, the world's leading information technology research and advisory company, confirms that the global market of UAVs for personal and commercial use is growing very rapidly and it is expected to reach more than \$6 billion in

2017 and grow to more than \$11 billion by 2020. Almost three million drones will be produced in 2017, 39 percent more than in 2016.

The German market research company Drone Industry Insights analyzed in 2016 the UAV environment providing a comprehensive picture of the global drone ecosystem in its different components: agriculture, analytics, communication, delivery, electronic components, engineering, governmental, inspection, insurance, integration, mapping, navigation, operators, recreational, research activities, retail, software development, etc. Overall more than 700 entities were cataloged in these categories (Figure 47). Moreover, there are still plenty of niches and specific use cases to be developed in the near future. This ecosystem is strongly technology driven and new applications will emerge as the hardware will become more capable. Furthermore, advanced drone operation regulations, that are nowadays still in development, will allow new use cases with a high rate of automation.

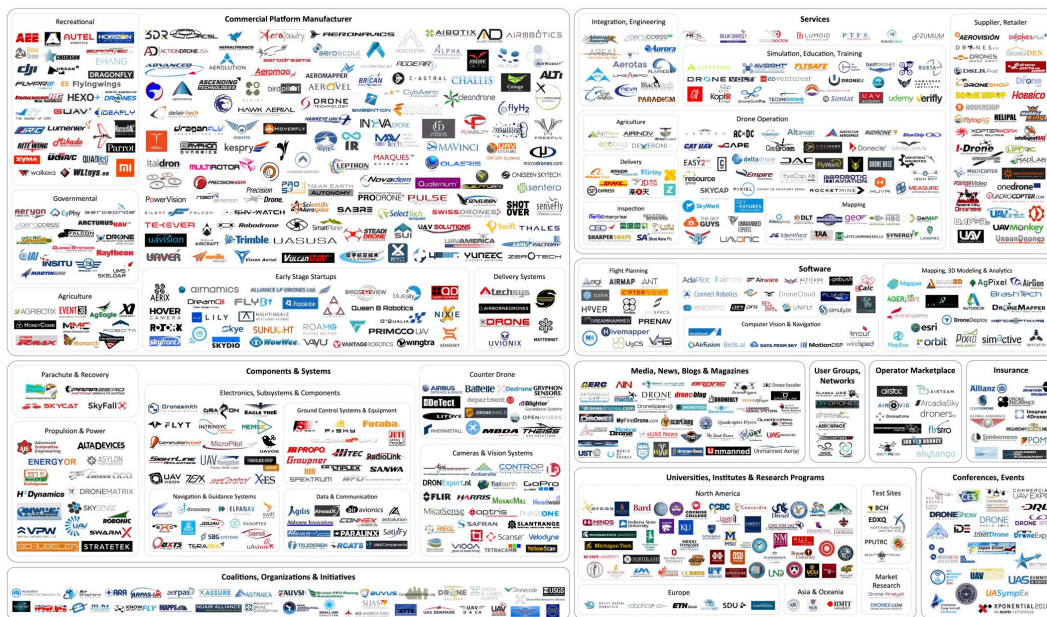


Figure 47: UAV ecosystem (Drone Industry Insights, 2016)

2.6.2 Urban Geospatial Data And Self-Driving Vehicles

Regarding self-driving vehicles, detailed and accurate maps need to be created and maintained updated. First of all, it should be noted that these systems usually can reach a good relative sub-metrical accuracy, most important for navigation purposes, but a worse absolute accuracy due to derive problems from inertial platforms or multi-path problems for GNSS receiver in urban canyons. The integration of data acquired from these platforms with those obtained from other sources will, therefore, be a challenge. On the other hand, this new huge

volume of data can be precious in some remote sensing scenarios providing a great amount of constantly updated metric data.

These technologies are strongly accelerated by the customer market. There is a solid increasing demand for navigation with a complete visualization of the surrounding environment, useful to both human and autonomous navigation. Therefore, we will see an increase in data acquired from different sensors (Toth and Józków, 2016).

In the last decade competitions organized by the Defense Advanced Research Projects Agency (DARPA) for military purposes obtained promising results and nowadays the first tests of self-driving vehicles are carried out on public roads under human supervision. These vehicles use on-board sensors such as GNSS receivers, laser scanners, radars and cameras to track other vehicles, detect obstacles and localize themselves in a road model (Urmson et al., 2008).

Some of the sensors that are today on a good part of the self-driving test vehicles are Velodyne scanners (Figure 48), wide angle camera and a combination of GNSS and IMU.



Figure 48: Sensors today mounted on experimental self-driving vehicles: Velodyne HDL-32E (left) and HDL-64E (right)

The dense point cloud of data collected from a fleet of self-driving vehicles can be used as input for a good number of applications: human-driven car navigation, inspection of the road conditions, smart city management and self-driving cars themselves. Nowadays acquisition is mainly focused on major urban areas in order to build a complete 3D city model for navigation. At the same time, machine learning algorithms reduce the car's dependency on pre-existing maps (Figure 49).



Figure 49: Generated map from Velodyne HDL-64E in a test with SLAM techniques (Moosmann and Stiller, 2011)

Self-driving vehicles are equipped with an array of sensors in order to recognize the surrounding environment. A pre-existing 3D city model can improve positioning further from what is achievable with Global Navigation Satellite System (GNSS) in the urban environment, providing additional context for the information captured by the sensors, directly in the reference 3D model and allowing the vehicle to distinguish anomalies in regular driving conditions.

Nowadays, one of the today's biggest mapping company, HERE, uses a fleet of more than 200 human-driven cars to collect dense point cloud data about roads around the world in order to create a reference 3D city model to enable self-driving navigation.

Each vehicle is equipped with the following sensors: Velodyne HDL-32E, four 24 wide-angle megapixels optical cameras, GNSS and IMU. The combined sensors acquire approximately 140 GB of data each day, generating almost 30 TB of data among the full fleet. Between 2010 and 2015, 5 million kilometers of roads were mapped in 30 different countries (Ristevski, 2017). Once the hard drives are full, they are physically sent to processing centers, highlighting two of the infrastructural challenges still existing today: it is possible to collect a huge amount of data, but transmitting and processing the data into meaningful products is non-trivial.

On the other hand, for comparison and according to Intel and based on today's estimation, an averagely self-driven car will generate around 4 TB of data each day coming from hundreds of onboard sensors, the most part coming from cameras and LIDAR systems.

Chapter 3: Processing Algorithms And Storage

Nowadays, even if sensors described in the previous chapter can rapidly acquire enormous quantities of precise geospatial data, there is still a great challenge in the scientific community in order to study efficient and accurate automatic detection and interpretation algorithms. In raw geospatial data obtained from remote sensing instruments there isn't any semantic information associated. Consequently, the previously acquired data must pass through different steps of processing in order to become meaningful for researchers and stakeholders. In particular, point clouds collected in urban areas contain a great number of points at a variable density collected over objects with a different level of complexity and variability, creating a great challenge for an automatic procedure for filtering, classification, and modeling.

In recent years, great efforts have been made in the scientific community in order to develop a workflow of efficient and automated procedures in order to extract, from acquired data in the urban environment, roof lines and slopes in a complete automated processing (Rottensteiner et al., 2014).

The vast size of the data acquired during an aerial survey, make it impossible to carry out a manual processing within a reasonable time and with reduced costs. It is thus necessary to study and develop new automatic or semiautomatic methods for processing such data. In addition, a further advantage in the use of these procedures is that the products obtained by processing through an algorithm will be of constant quality over time because of their determinist nature.

Moreover, as it will be described in the last sections of this chapter, it is now of paramount importance to use efficient methods to properly store these increasingly massive amounts of data.

3.1 Software

New techniques and procedures for automatic and semi-automatic extraction of information from remote sensing data are increasingly developed, following a great scientific and commercial interest. Several algorithms are subjects for the experimentation here described and they are implemented in different software, COTS (Commercial Off-The-Shelf) or FOSS (Free and Open-Source Software), able to detect the geometry of buildings inside a point cloud. This kind of data can be acquired from aerial LiDAR or photogrammetric survey. Point cloud processing is a non-trivial issue: processed data can indicate great differences depending on the precise workflow followed with a specific software and

therefore on different algorithm procedures. Alternative implementations can, in fact, deliver different performance improving processing speed, memory efficiency or reliability of the results.

In this chapter, different algorithms to process dense point clouds will be compared for the extraction and classification of thematic information. The algorithms are implemented in different software, both COTS and FOSS: GRASS GIS, ENVI LiDAR, and LAStools. These software are structured to meet different needs in the processing of geospatial data. The procedures have been tested with a common dataset and the results are analyzed in a GIS environment. Additional considerations are carried out to evaluate different software functionality, comparing its performance and features.

In the case studied different software is used and each one shows advantages and drawbacks related with their different approach and design.

- ENVI LiDAR (Harris Geospatial Solutions, 2017): a software designed for LiDAR data analysis with fast and simple processing that can deliver precise results. It is a commercial software and their algorithms are not in public domain, and also the scientific community has no further information about the methodology for processing. Only some parameters can be changed in order to adapt the processing to the specific case study.
- LAStools (Isenburg, 2017): a suite of various software, each developed specifically for a specific task in LiDAR data processing. Some of the algorithms are open source and it was possible to achieve good results within a brief processing time. Several parameters can be set in order to adapt the processing to the specific case study.
- GRASS GIS (Neteler et al., 2012): an Open Source Geographic Information System software that can rely on a large number of algorithms and plugins extending its original capabilities in order to adapt the processing also to point cloud data. It is not the most efficient solution, considering that the software is not designed for LiDAR data processing. The processing time is usually longer and it is also longer the preliminary phase needed to import the point cloud. Being Open Source, it uses well known and defined algorithms that can be analyzed and therefore it is possible to have a complete control on the result.

3.2 Dense Point Cloud Processing

3.2.1 Case Study

A point cloud used for the comparison was acquired in the urban area of the city of Vaihingen, in Germany. It is a dataset acquired and published with the aim to

create a common benchmark in order to evaluate different algorithms to process data acquired by airborne sensors, within the initiative "ISPRS Test Project on Urban Classification and 3D Building Reconstruction "(Rottensteiner et al., 2012). These data are made available to the scientific community in a dedicated website, uploaded in LAS format (Figure 50).

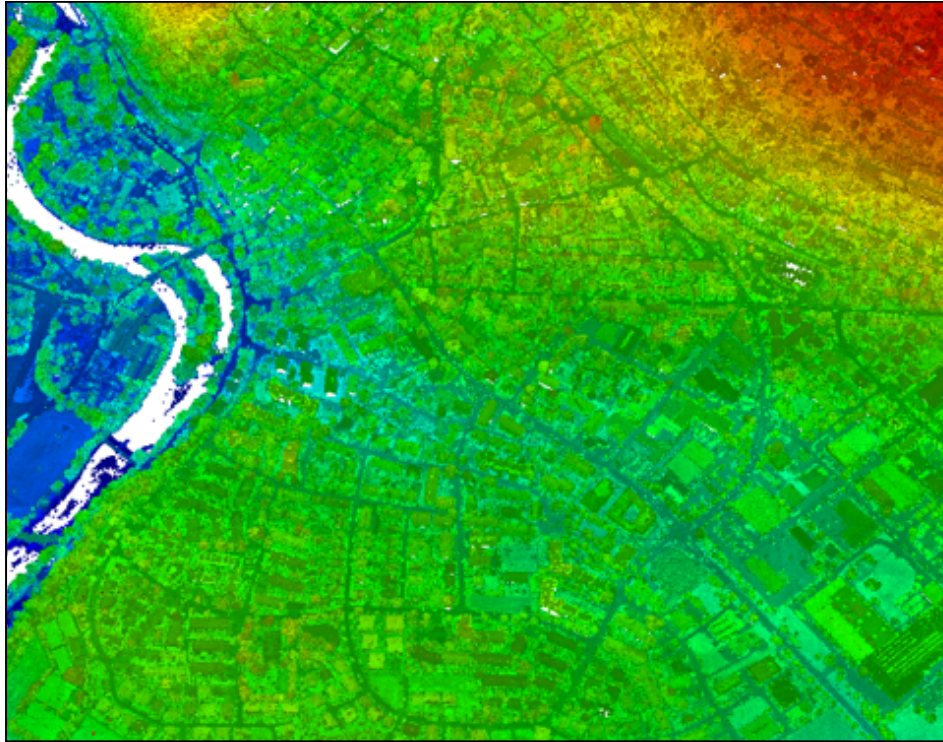


Figure 50: Point cloud for the city of Vaihigen represented in shades proportional to relative elevation

In particular, the point cloud here analyzed was acquired by Leica ALS50 airborne laser scanner. The entire test subject area is contained in 5 strips acquired August 21, 2008 with a flight altitude of 500 meters above the city (Figure 51).

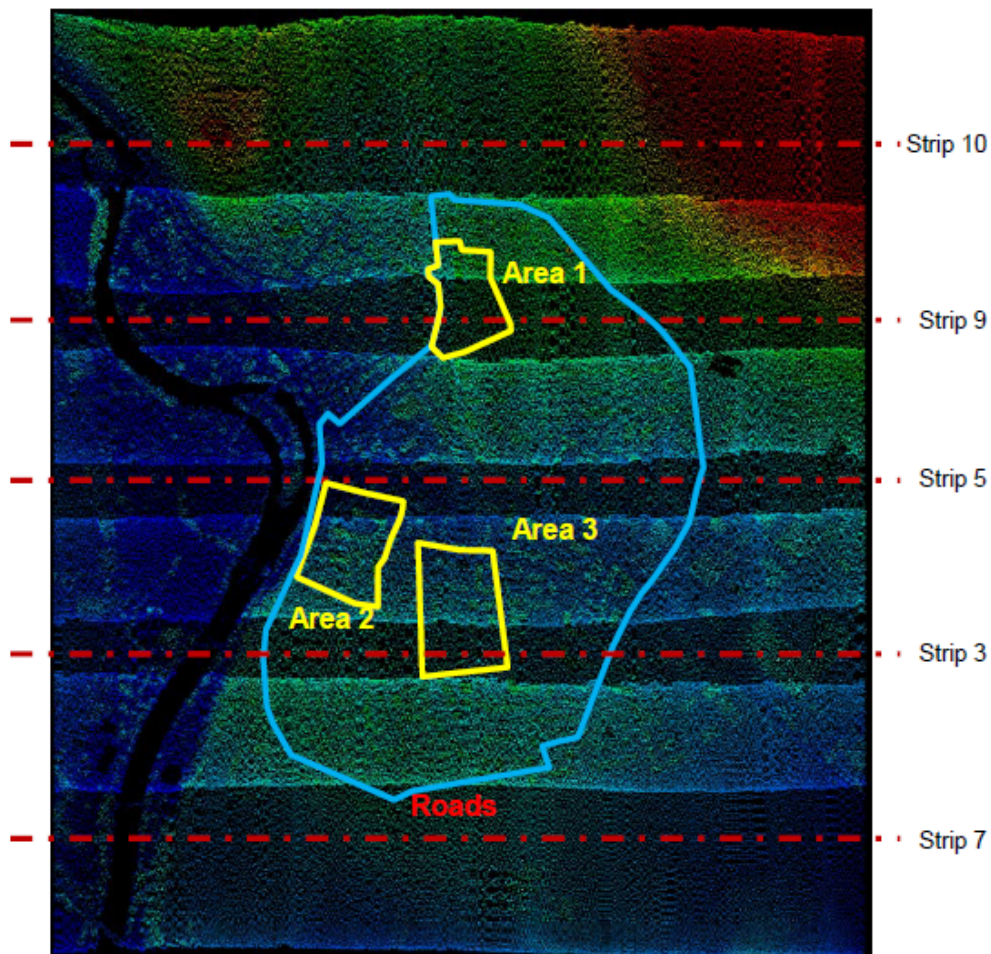


Figure 51: Overview for the laser scanner strips acquired over the case study area in the city of Vaihingen, Germany (Rottensteiner et al., 2012)

The result is a point cloud with an average density of almost 7 points per square meter, and a minimum of 4 points per square meter in those areas where there is no overlap between adjacent strips. These strips were processed in advance removing georeferencing systematic errors.

The surveyed area furthermore divided into three smaller parts, the test areas, which present different features. The area "1" is located in the heart of the city and is characterized by a number of historic buildings close to each other and consist of complex geometries. The area "2" is instead characterized by some high residential buildings, surrounded by vegetation. The area "3" is also residential, and instead includes buildings with more compact dimensions, well spaced, but equally surrounded by vegetation (Figure 52).



Figure 52: Details for each of the three area selected in the city of Vaihingen, from left to right: Area 1, Area 2, Area 3 (Rottensteiner et al., 2012)

3.2.2 Grass Gis Processing

First, using GRASS GIS, subsequently to the phase that allowed to import data, some steps were followed in order to process the point cloud to extract vector features representing buildings. It should be emphasized that, being a proper GIS application, the introduction of functionalities for point cloud processing in GRASS GIS should be considered as an appendix of the software and not the core function. This still allows the user, after appropriate treatment with a series of procedures to conform the data, to load LIDAR data inside a specific workflow from standard formats such as LAS. The data will be then processed as a simple 3D point vector layer. The first next step, through `v.outlier` command, allows to remove any noise generated by blunders, still contained inside the point cloud. The parameters for this step are obtained from experimental studies (Brovelli et al., 2004). Then, with the `v.lidar.edgedetection` command, it is possible to detect the border of the objects in the point cloud. The thresholds are specially defined based on the context of analysis and the result is a segmentation of the point cloud into several categories: soil, border and unknown. All variables were stressed to assess its impact on the processed result (Figure 53).



Figure 53: Comparison in GRASS GIS between two different parameters, highlighted in different colors, for object border definition in the point cloud

Subsequently, the `v.lidar.growing` algorithm is used to identify the inner area of each previously identified object. The result is then classified into four categories, differentiating the ground points from those belonging to objects, which are at the same time differentiated into single pulses and multiple pulses. In conclusion, the last step involves the use of `v.lidar.correction` command to extract objects such as buildings.

3.2.3 Lastools Processing

Using the `LAStools` software package has been possible to test the same dataset, by loading the information following a straightforward procedure. The first operation is performed through the application `lasground` for defining the DTM in the area of interest, dividing the point cloud into two categories: points belonging to the ground and points not belonging to the ground, according to context-base parameters. Then, with the tool `lasheight`, it is possible to eliminate some outlier outside an interval related to the ground level. Subsequently, `lasclassify` carries a classification directly on the point cloud obtained from the previous steps, distinguishing the points belonging to buildings and vegetation (Figure 54). In conclusion, the polygons that identify the perimeters of the buildings are being generated through the `lasboundary` procedure that identifies,

through a concave hull algorithm, the islands in which the points of the cloud are grouped.

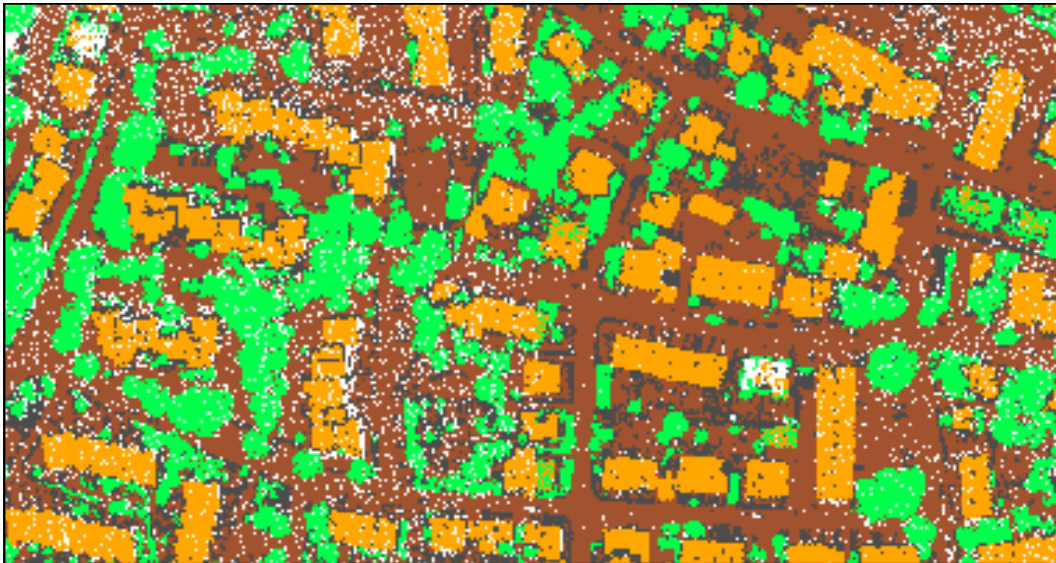


Figure 54: LAStools algorithm classification with points highlighted in different colors: buildings in orange, vegetation in green, ground in brown (Lambertini et al., 2016)

3.2.4 Envi Lidar Processing

The last software under test was ENVI LiDAR. It has been possible to load the data and set the required parameters. The first threshold concerns the definition of the minimum area to set within the point cloud to define the roof surface for each building. Additionally, after having defined the DTM also in this case, all the points located at a relative elevation from ground level under a certain threshold are filtered out. In addition, it is also defined the threshold for the maximum inter-distance between adjacent points, which lie in the same plane of each slope. Similarly, the last threshold value corresponds to the maximum tolerance allowed to represent flat surfaces. Consequently, any surface that includes a curvature will be represented as a succession of planar simplified areas. Additional variables relate to the best definition and analysis of vegetation, not the subject of this work. The end result, in this case, is not only the fingerprint representation to the footprint of the building, or its overall size, but also consists in a complete three-dimensional representation of the slopes of each roof, oriented and sized appropriately according to the information contained in the original point cloud (Figure 55).

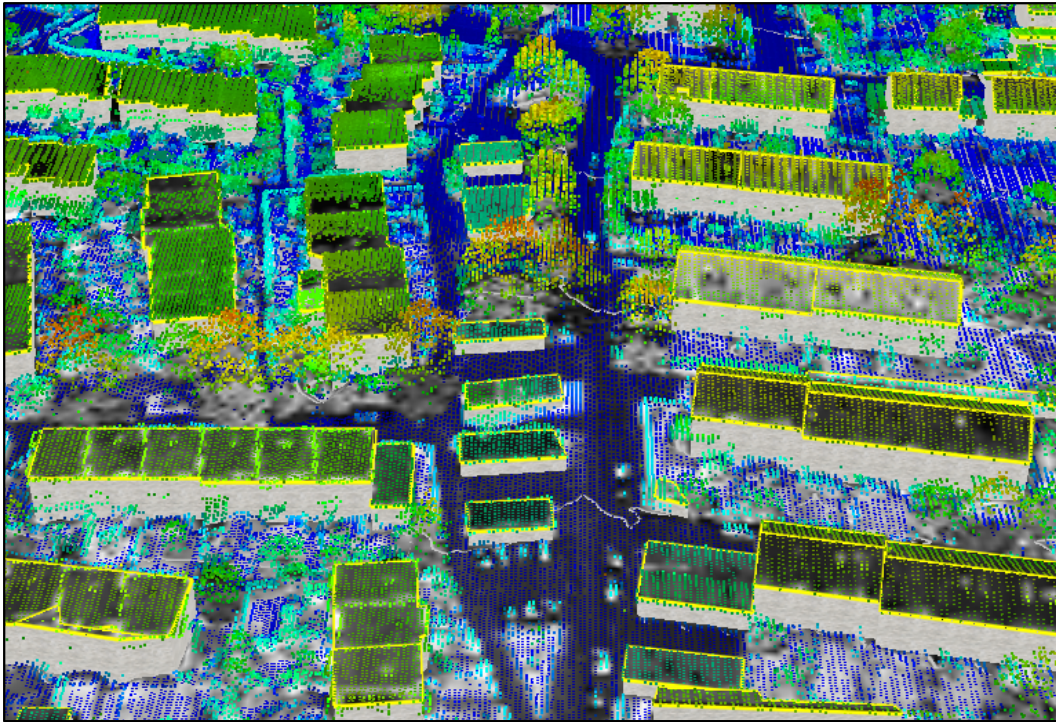


Figure 55: Tridimensional visualization of building extracted with ENVI LIDAR (Lambertini et al., 2016)

3.2.5 Results Comparison

The results have been analyzed in the form of digital cartography in a GIS environment. In a first qualitative analysis, it has been observed that in some cases different geometries of the same building have been produced, in particular highlighting how some algorithms produce an incorrect footprint in the most critical circumstances such as those of tall vegetation proximity, or when the building geometry is, in fact, more complex. Comparing different procedures it is possible to perform further considerations based on the total number of buildings properly reconstructed for the great part of their surface in the different areas analyzed for the city of Vaihingen. The area marked as 1, with data acquired over the city center, comprehends a total of 27 buildings. The area marked as 2, with high residential structures, has 9 separate structures. The area number 3, which is also residential, is characterized by 40 well-spaced compact buildings. It was possible to distinguish three cases: the buildings completely correctly recognized marked as “correct”, the buildings recognized only in some part of the structure with minor problems and marked as “partial”, and lastly the building that haven’t been recognized at all or whose surface were wrongly overestimated and therefore marked as “missed” (Table 56).

	GRASS GIS			LAStools			ENVI LiDAR		
AREA	1	2	3	1	2	3	1	2	3
Correct	51,9%	77,8%	57,5%	59,3%	100,0%	87,5%	59,3%	100,0%	77,5%
Partial	25,9%	11,1%	12,5%	33,3%	0,0%	2,5%	7,4%	0,0%	2,5%
Missed	22,2%	11,1%	30,0%	7,4%	0,0%	10,0%	33,3%	0,0%	20,0%

Table 56: Quantitative analysis for building modeled from the point cloud (Lambertini et al., 2016)

As it is possible to observe from the results, a better performance was achieved in particular in residential areas ("2" and "3"), by specialized software in the processing of LiDAR data: LAStools and ENVI LiDAR. It is also possible to highlight additional considerations related to the various software features. In fact, performance and capability of user intervention in selecting the appropriate parameters for the data processing were compared. Also, the products generated as output from the different software differ by type and purpose. For example, a peculiarity for the ENVI LiDAR software regards the greater control in the process of Quality Assurance that allows a trained human operator to review the results obtained from the automatic analysis.

Nevertheless, in all the cases analyzed, it was still possible to export vector geo-referenced polygons representing the footprints of buildings and overlap this new layer produced with other geographical information. The experimentation was carried out as a methodology for software and procedures comparison, looking for a tool that can be effectively inserted into a workflow for the analysis of large amounts of data. It was possible to verify that the procedure for the automatic extraction of buildings from point clouds, with all the software analyses in this work, is accessible for users with enough experience in the treatment of geographic data. In particular, it was evident that any application that shows to the user a more simplified and immediate interaction, on the other hand, shows less chance for deep analyses by means of a complete choice over variables and parameters calibrated according to different needs. This is especially true for the most specialized software. They give more control to the user on the final result and therefore requiring a steep learning curve and a greater experience to complete the required workflow.

3.3 Point Cloud Workflow

The availability of software packages that allow extracting, virtually in automatic mode, 3D features, and in particular buildings, from high-density point cloud is very attractive for a variety of applications in urban areas. A precise 3D roof's

model can be easily extracted and with it all the information about the surface area and orientation of each slope. One of the main problems is that, in order to reduce to a minimum the manual intervention in the presence of complex geometries of the roofs, it is crucial to acquire a dataset with a good point cloud density. Therefore it is appropriate to schedule specific survey aimed to obtain the proper density of data to process. Only with high-density data it will be possible to produce an appropriate 3D model, based on the desired level of detail. (Africani et al., 2013)

Furthermore, and increased automation in the workflow is fundamental in order to carry out a fast processing when there is urgency for fast delivery of results: rapid mapping and rapid response with easier management of emergencies having pre-event data available.

In the last years, technological progress and proposal of new methods laid the foundations for the introduction of algorithms derived by the application of artificial intelligence in order to process a huge amount of data. Using artificial intelligence and some training data, different approaches who rely on deep learning techniques are exploitable for remote sensed data processing. Even integrating data acquired from a large number of sensors that record different physical phenomena at different spatial, radiometric, spectral or temporal resolution. In the field of deep learning, new Deep Neural Networks (DNN) and Convolutional Neural Network (CNN) are researched and developed for an effective and completely automated analysis of geospatial data. New DNN algorithms are now developed for object detection, classification, quality assessment of remotely sensed imagery and point clouds (Vetrivel et al., 2017). In fact, in a semantic characterization of point clouds and their derived products, any reconstructed elements produced in the final 3D models should semantically correspond to a specific object and category in order to provide an added value to the delivered model.

3.4 Point Cloud Storage

Nowadays LAS is a public file format and an industry standard for LIDAR data, in order to improve data exchange and interoperability. It is maintained by the American Society of Photogrammetry and Remote Sensing (ASPRS) and it supports any kind of 3-dimensional data expressed in coordinates X, Y, Z. It is a non-proprietary binary format used by almost any software developer as an alternative to generic ASCII (American Standard Code for Information Interchange) files which would be less performant compared to LAS in the data reading phase and even inefficient in storing data presenting larger file sizes. LAS files comprehend and header with information regarding the data contained

in the dataset such as the software that recorded the file with the timestamp for creation date and time, the global number of point records distinguished by returns, eventual offsets or scale factor and definition of the three-dimensional bounding box of the data contained in the file. The LAS 1.4 Specification was approved by the ASPRS Board at the end of 2011 and is still the most recent version of the protocol.

Even if a LAS file is more performant and storage efficient compared to an ASCII file, some procedures have been developed in order to further reduce the LAS file size to a more compressed file format aiming to reduce the need for storage of huge files for large surveys and also lowering the requirements and time needed to copy or transfer a large LIDAR data archive over a network. With these premises, Martin Isenburg from rapidlasso developed LASzip, a library specifically devoted for the compression of LAS data in LAZ files. It has a LGPL-license and therefore any software developer can use it to process LAZ files in the same way they are able to work with LAS data. Furthermore, LASzip algorithm is completely lose-less but still, it can compress a standard LAS file into a more compact LAZ lowering the storage requirement of approximately one order of magnitude.

Larger point clouds are also stored in a database structure, instead of a file-based solution such as LAS or LAZ. Government and entities are beginning to deal with massive dataset acquired over entire nations. This is the example described by van Oosterom et al. (2015) in which they stressed the national height map of the Netherlands (AHN2). The point cloud has a density up to 10 points per square meter, extending in the entire country, with a total of 640 billion points recorded over several TB of storage.

3.5 Voxel Models

The word voxel is based on the abbreviation of vox for volume and element. In the same way that the word pixel is based on the abbreviation of pix for picture and element. Therefore, a voxel is a unit spatial information that defines data acquired in three-dimensional space, at the same way in which a pixel refers to data projected on a two-dimensional plane (Figure 57).

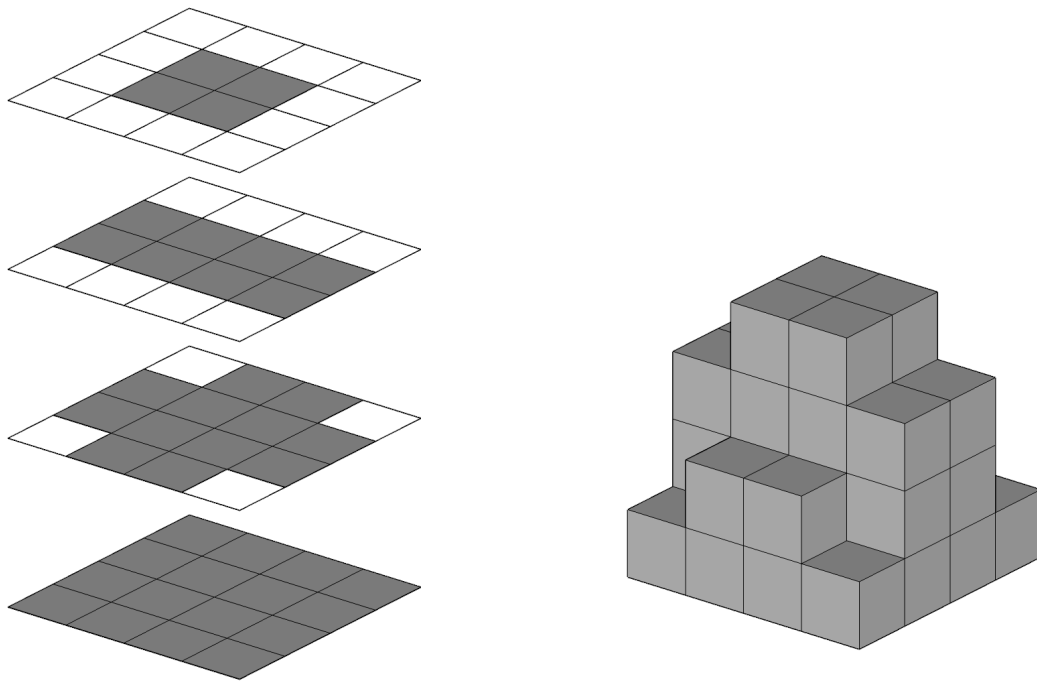


Figure 57: the concept of a voxel model (right) as a sequence of pixel images stacked one on top of the other (left)

The determination of coordinates passes from a couple X, Y indicating row and column to a triplet X, Y, Z adding information regarding the volume of objects represented in the dataset. Furthermore, each voxel can contain information regarding color, intensity or any data sampled from the sensor. Any eventual space between voxels is represented with empty data since there is a strict continuity in the 3D matrix that defines the voxel-based representation. This kind of dataset is widely used in the medical area to view from different angles results acquired with Magnetic Resonance Imaging (MRI).

In the case of a voxel model representing a building, the data contained in each voxel could semantically represent the construction material.

3.6 Big Data Challenge

In a speech in 1998, the American politician and environmentalist Al Gore envisioned a future where people could interact with a virtual 3D model of the world, called Digital Earth, and through it access a great amount of information (Gore, 1998). This vision guided by technology has gradually transformed into real products such as NASA World Wind and Google Earth. In fact, huge organizations such as NASA and Google collect from Terabytes to Petabytes of data each day, with a large portion of spatiotemporal data in the form of imagery. The rate at which this data is being generated exceeds the ability to analyze and

extract and understand information. Efficient management and analytical infrastructure for big spatial data are needed and performing spatial data mining algorithms (Vatsavai et al., 2012). Nevertheless, spatial analysis becomes complicated with the wide use of disruptive technologies such as embedded sensors, crowdsourced data and social media (Auferbauer et al., 2015). Furthermore, as previously discussed in the storage section of this chapter, acquisition with a high density of data and large extent for the surveyed area need particular structures and configuration of both hardware and software.

Big Data collection and machine learning is changing approaches also to business management (Yang et al., 2015) as they are now processing datasets regarding geographical locations and demographical factors in order to invest more wisely. Structured analysis leveraging a wide range of parameters become accessible using a GIS. Geographical information such as a complete 3D city model can be used as the base to connect any auxiliary data giving a complete understanding of the environment. In a non-comprehensive list of business that can benefit from these GIS analyses are insurance, retail, logistics, construction companies, real estate and marketing in general.

In general, geospatial data plays a major role in Big Data providing benefits to users and communities (Lee and Kang, 2015). New datasets in form of point clouds are acquired at a growing speed and new algorithms are needed to process the acquired data efficiently (Cao et al., 2015).

Sensors are only one of the multiple data sources for Big Data, among machine data, transactions data, Internet of Things data and Web&Social data (Hashem et al., 2015). Nevertheless, only the integration and transversal analysis of details coming from different data sources can deliver a new level of enriched knowledge, in particular at a Smart City level, where the key is inter-modality and interdisciplinarity. Furthermore, a great number of scenario and concepts need a deep analysis of Big Data to deliver an efficient result: Digital Earth (Craglia et al., 2012), disease spreading (Allen et al., 2016), disaster prevention (Pradhan, 2013), climate analysis (Tehrany et al., 2015) and many more.

Chapter 4: Analysis At Different Urban Scales

4.1 Level Of Detail

The Level Of Detail (LOD) of a 3D city model may be considered as the most relevant parameter. It represents the correspondence of the model to the real-world (Biljecki et al.,2014). The CityGML standard from the Open Geospatial Consortium defines five different levels of detail. The concept is intended for different thematic classes of objects. Nevertheless, its primarily focus are buildings, which are described through five classes with increasing geometric complexity.

In this chapter, a number of case studies will be presented and described in details with their different workflow aimed to produce 3D models with a required LOD based on context. Therefore, different techniques to reach the desired LOD will be discussed.

First of all, it is necessary to introduce a definition of the different LOD ad described by Kolbe (2009) in CityGML (Figure 58).

- LOD0: a simple representation of footprints, typically used in a GIS environment
- LOD1: a simple prismatic model that can be obtained with the height extrusion of the building footprint contained in a LOD0 model using the elevation of the object as the only further parameter, without any definition of the roof structure
- LOD2: a slightly more complex model with schematic roof shape. In particular different model, components can be classified in semantic classes such as facades, roof slopes, etc.
- LOD3: an architecturally detailed model which comprises small items such as windows or doors and is overall more complex than LOD2.
- LOD4: it completes the previous level of detail including not only the exterior part of the model but also interior items such as internal walls and furniture.

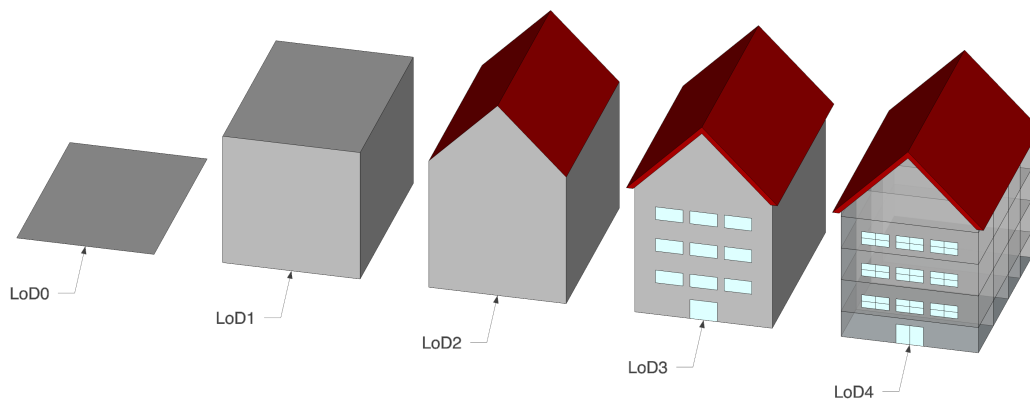


Figure 58: Differences of the first five LOD as defined in CityGML

In Biljecki et al. (2014) is suggested that interior and exterior reconstructed elements of the 3D model should be kept separate because the number of applications that make good use of the sole exterior geometry is larger compared to all indoor applications. Nowadays the greatest part of available 3D city models is composed only of data acquired over the external surface without any information regarding the interior. As it is easily understandable and deductible by previously discussed chapters, it is still faster to acquire external data for buildings over a large area, even an entire city, rather than gathering precise geometrical information for the indoor spaces of each building. In fact, acquisition methods and sensors used to survey data from outdoor and indoor spaces are usually different, in particular regarding the choice of the platform, being respectively airborne platforms and terrestrial platforms. Nevertheless, in some scenario, this data should integrate in order to create a complete model.

CityGML itself is an Open Data model in XML format created to delivery information intrinsic in the virtual 3D representation of city models (Kolbe et al., 2005) and it also complements Building Information Models (BIM). All the topics previously discussed find here a common denominator in the intrinsic new possibilities arising from the integration of point cloud data in a series of products. For example, 3D models at a certain LOD, automatically derived from point clouds through several techniques may be used for as-built documentation (Tang et al., 2010). Furthermore, any development and diffusion of BIM will result in a major contribution for producing and updating 3D city models.

In this chapter analysis at different scales and different LOD will be carried out: from a complete urban scale to a single building detail.

4.2 Roof Planes From Point Cloud

4.2.1 Case Study

Düsseldorf is the capital city of North Rhine-Westphalia (NRW) state in Germany, developed near the banks of the Rhine river. The population counts more than 610000 people spread over 217 square kilometers of the city (Figure 59).



Figure 59: Aerial three-dimensional overview visualization for the Düsseldorf case study

In 2016 the NRW state was the first in Germany to support the release of open and free geospatial data of the state and municipalities on their portal in order to produce a real benefit to the community of users of geospatial data, researchers and also citizens. The data is also available in the form of raw LiDAR point clouds and machine-readable formats. Furthermore, the database released includes the data of the real estate catalog, such as corridors and buildings, as well as the country-specific data of the national survey, such as topographical maps, aerial photographs or digital terrain models, carried out by the 53 districts and town districts (Figure 60).

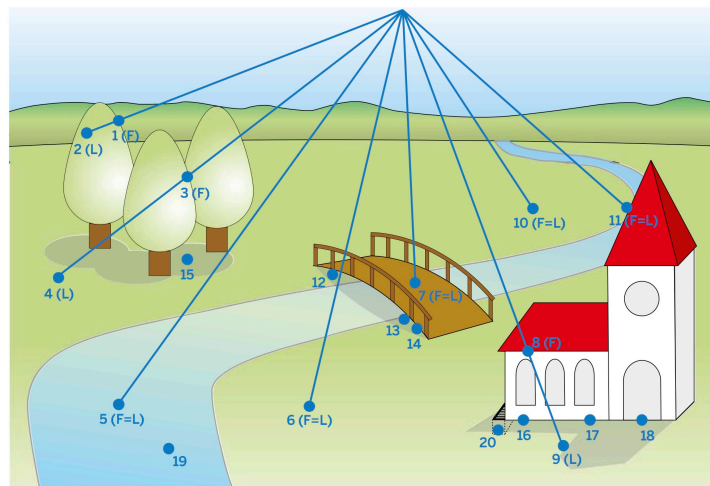


Figure 60: Scheme provided by NRW with indications regarding point cloud classification and differentiation between first pulses (F), last pulses (L), and other ad-hoc categories

4.2.2 Data Analysis

A series of files, available as Open Data in NRW website. The data contained in the files is delivered in tiles aligned in a grid, differentiated between raw data for DSM and filtered data for DTM. The DSM dataset, called DOM, contains also only first pulses (FP). The files are compressed in a ZIP folder when downloaded from the repository. Inside the compressed folder, the data is delivered in a simple ASCII file in text format with East, North, Elevation coordinates rounded to centimeter resolution with two decimal digits. The coordinate reference system is EPSG:5555, a composition of ETRS89 / UTM zone 32N with DHHN92 elevation data.

A certain number of ASCII files for the area of interest were considered:

- dom1l-fp_32343_5675_1_nw.xyz
- dom1l-fp_32343_5676_1_nw.xyz
- dom1l-fp_32343_5677_1_nw.xyz
- dom1l-fp_32344_5675_1_nw.xyz
- dom1l-fp_32344_5676_1_nw.xyz
- dom1l-fp_32344_5677_1_nw.xyz
- dom1l-fp_32345_5675_1_nw.xyz
- dom1l-fp_32345_5676_1_nw.xyz
- dom1l-fp_32345_5677_1_nw.xyz

All those files were fused in a unique dataset with the CAT application from the command line and then converted in a unique compressed point cloud file such as LAZ with LASzip compressor from LAStools suite reducing the dataset storage requirements (Figure 61).

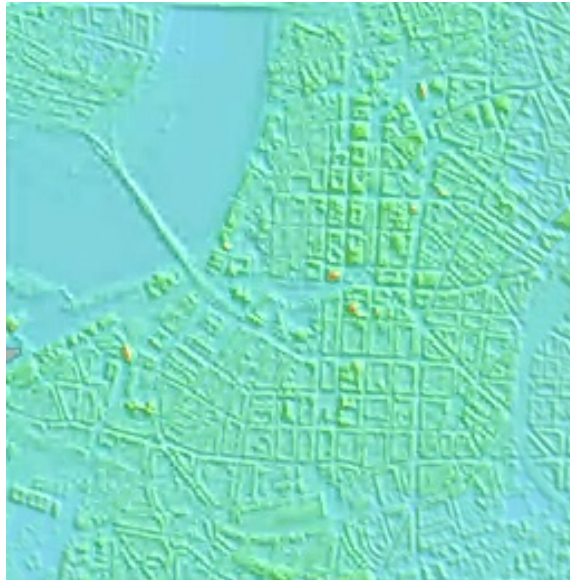


Figure 61: Hillshade for the point cloud subset

It was possible to observe and process all the data for the case study. The density of the data isn't constant along the surveyed area, reaching higher values in the overlapping of adjacent strips. As a first step, the DSM and DTM were computed for the entire area of interest (Figure 62).

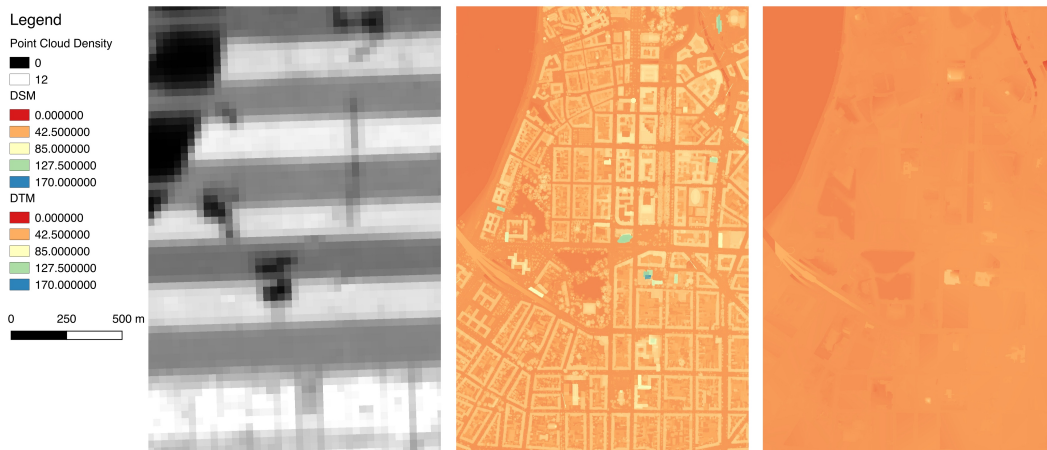


Figure 62: Data processed for the study area, from left to right: point cloud density, digital surface model, digital terrain model

In a detail for a specific building, it is possible to observe the full pipeline of processing, starting from the raw point cloud data, highlighted with colors proportional to the elevation of the data, to a sequential step of classification of the point cloud in points surveyed over the building roof (yellow), ground (orange) and vegetation (green). Finally, a 3D model is computed on the points attributed to the building slopes (Figure 63).

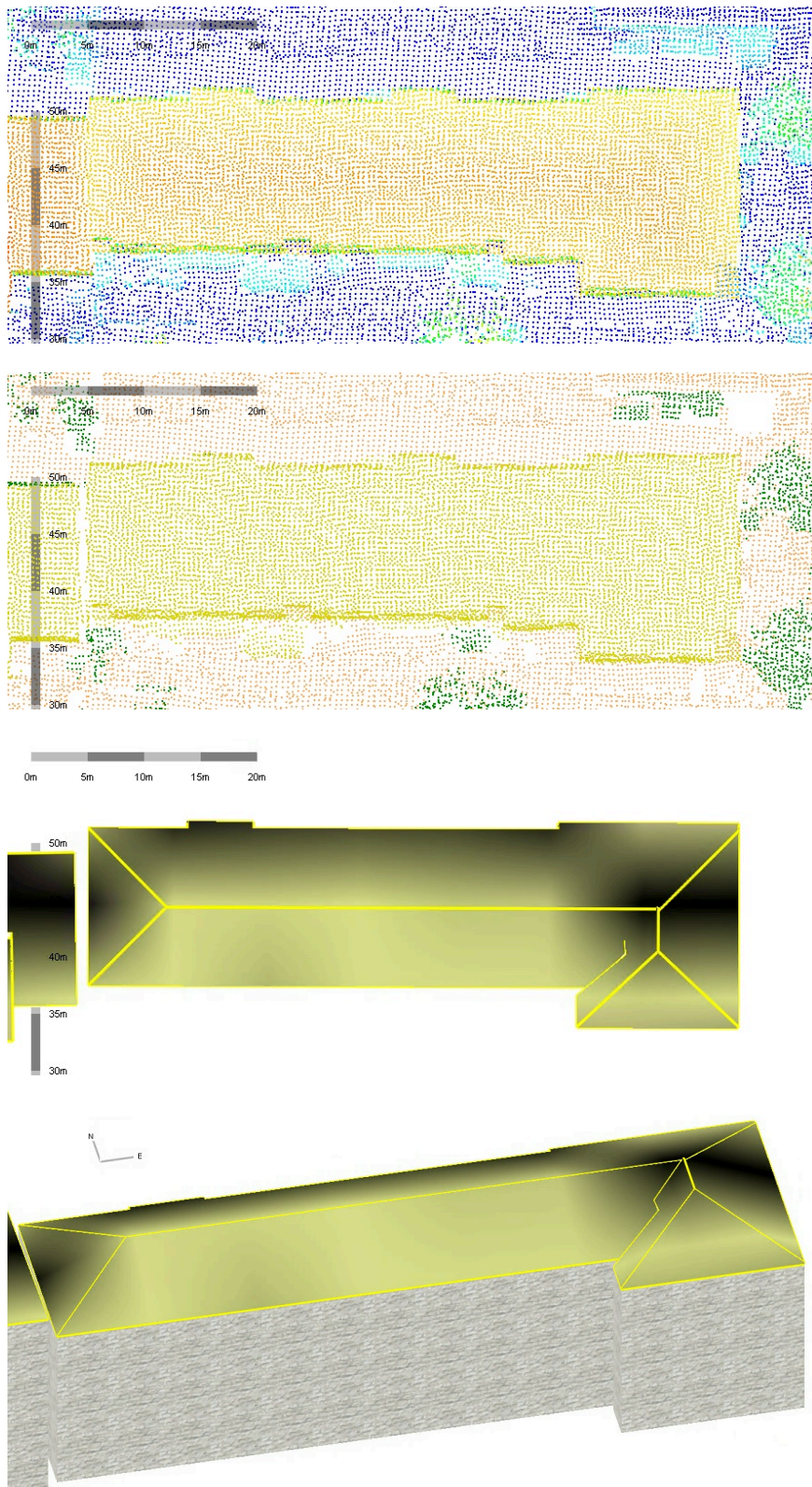


Figure 63: The full pipeline of processing described in the sequence of workflow for a specific building

Data belonging to the facades is also recorded in the FOV of the LIDAR sensor, as can be seen in detail from cross sections (Figure 64).

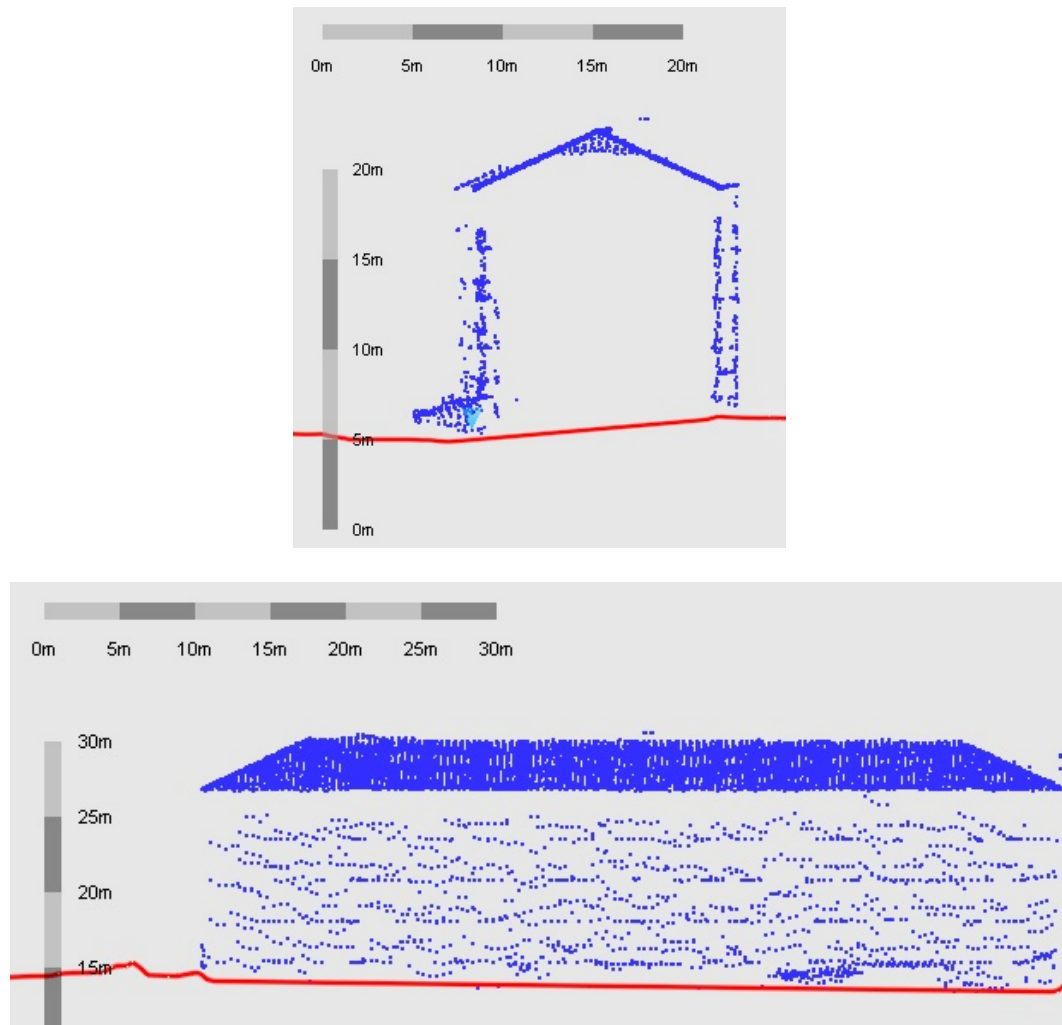


Figure 64: Cross Sections from the specific building

The highlighted data is partially recorded over balconies and partially over wall surfaces, as can be observed from the reference building image acquired from a terrestrial platform (Figure 65).



Figure 65: Reference building acquired from Google StreetView

The structure of the urban texture in the study area is compact and regular, as it is possible to observe from the enlarged detail of the DSM extracted in Figure 66.

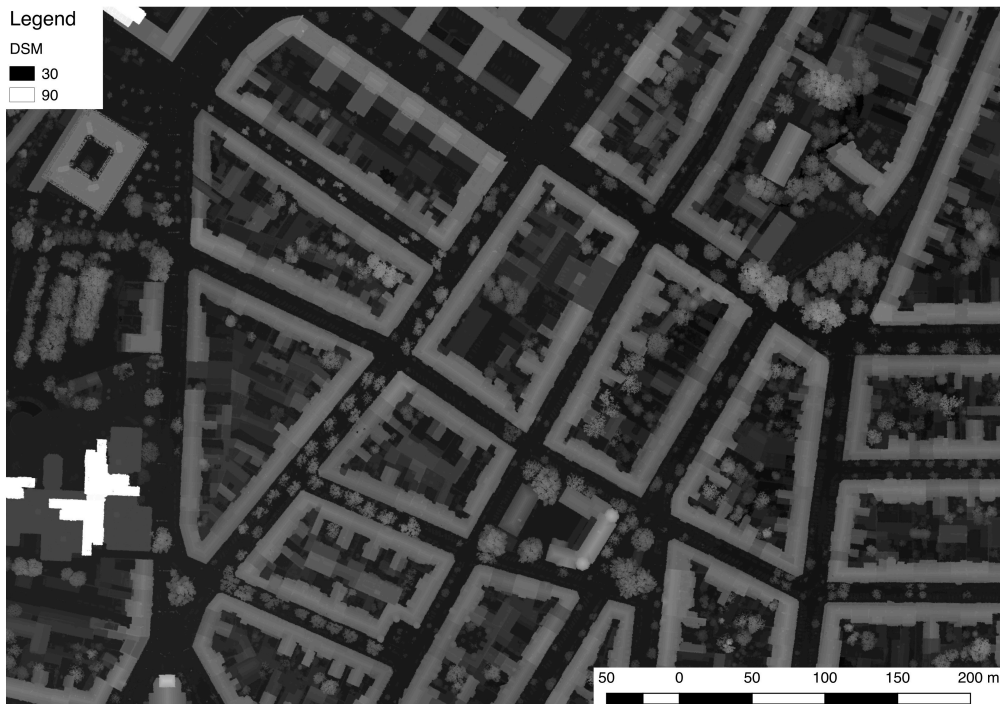


Figure 66: DSM for a central area of the city

The reference data used in the Düsseldorf case study is ALK NRW, the cadastre map delivered and maintained by North Rhine-Westphalia State (Figure 67) showing a good comparison with the data extracted from point cloud processing.

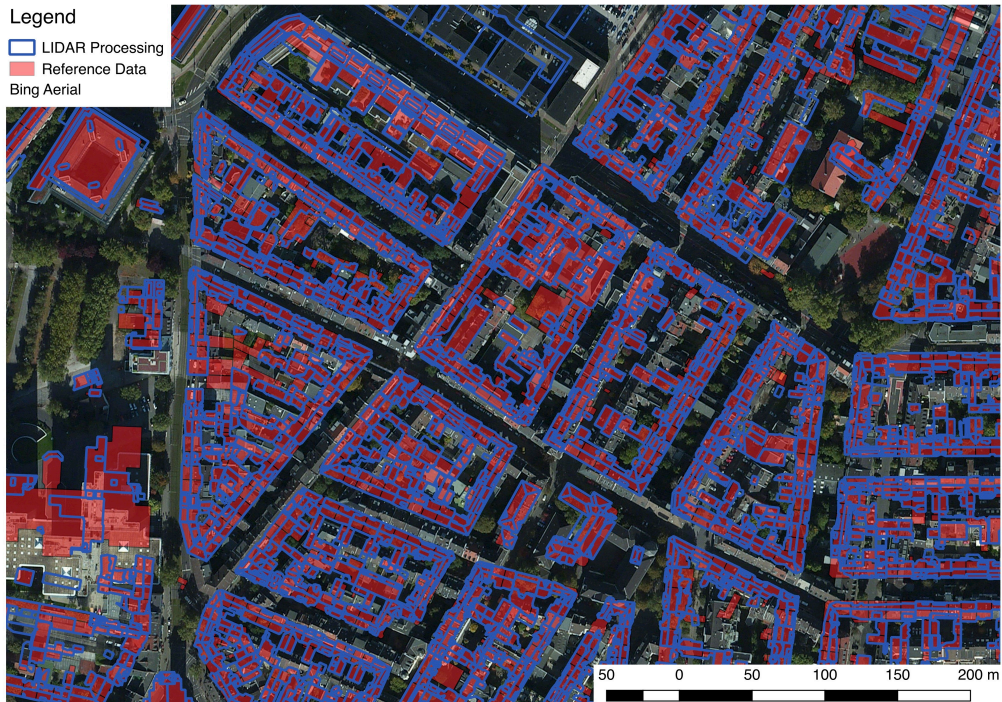


Figure 67: Building slopes processed from LIDAR data against reference data for buildings and aerial image in the background

A final LOD2 model can be computed with the data processed from the LIDAR survey (Figure 68).



Figure 68: LOD2 3D city model

The resulting vector can also be exported in a standard Drawing Exchange Format (DXF) file for further use in CAD software (Figure 69).



Figure 69: CAD 3D models of roof slopes

4.3 Solar Radiation On Roof Planes

Identifying the right roofs to install solar panels inside a urban area is crucial for both private citizens and the whole local population. It is not an easy procedure because it depends on a large number of parameters: insolation, orientation of the surface, size of the surface, shading due to topography, shading due to taller buildings next the surface, shading due to taller vegetation and other possible problems typical of urban areas like the presence of chimneys. Accuracy of data related to the analyzed surfaces is indeed fundamental, and also the detail of geometric models used to represent buildings and their roofs. The complexity that these roofs can reach is elevated. This work was possible with the collaboration of technicians from Comune di Bologna and published in the International Archives of the Photogrammetry, Remote Sensing and Spatial Information Sciences (Africani et al., 2013). It uses LiDAR data to obtain, with a semi-automatic technique, the full geometry of each roof part complementing the pre-existing building data in the municipal cartography. With this data is possible to evaluate the placement of solar panels on roofs of a whole city analyzing the solar potential of each building in detail. Other traditional techniques, like photogrammetry, need strong manual editing effort in order to identify slopes and insert vector on surfaces at the right height. Regarding LiDAR data, in order to perform accurate modeling, it is necessary to obtain an high density point cloud. The method proposed can also be used as a fast and linear workflow process for an area where LiDAR data are available and a municipal cartography already

exist: LiDAR data can be furthermore successfully used to compare to a pre-existent digital cartography.

Knowing that a city is a central hub of energy consumption, among useful applications for GIS and 3D city models there is the study for energy consumption and production. This analysis can be conducted at an urban scale even to single buildings in detail. One example is Bologna Solar City, from Municipality of Bologna (Italy): a web application created to evaluate the placement of solar panels on roofs. It will be discussed in detail in the following section. Another example is to use LiDAR data and a derivative Digital Surface Model to produce a true orthophoto (Günay et al., 2007) that is useful in order to refine a detailed energy map relative to each building. This kind of analysis at building level was performed within EnergyCity, a project from Central Europe, to better understand the actual energy management and support strategies from the urban municipalities in order to reduce energy consumption and CO2 emissions (Bitelli et al., 2015).

4.3.1 Case Study

The Municipality of Bologna has a long experience in cartography and a good collection of data over the years in digital format. These data are continuously updated through different sources: georeferenced CAD drawings from executive projects, manual extraction of features from aerial orthophoto taken every year and surveys on the field are used to update the original large scale numerical cartography (CTC) made by aerial photogrammetry. In 2010, in order to help its inhabitants to reduce energy costs and save the environment, Bologna SIT office created a web application called Bologna Solar City (Figure 70) to search for renewable energy systems applied in the Bologna territory and to evaluate the placement of solar panels on roofs. The basic idea was to estimate the solar energy available on roofs. This evaluation is the sum of direct and diffuse solar energies and it was calculated with ArcGIS tools. The algorithm applied required several elements in input. First of all, a DSM of the city territory developed with a large number of altimetric information deduced from the municipal cartography. The other factors considered are, on a raster-based model, weather conditions, position, and shade of each location (Minghetti et al., 2011).

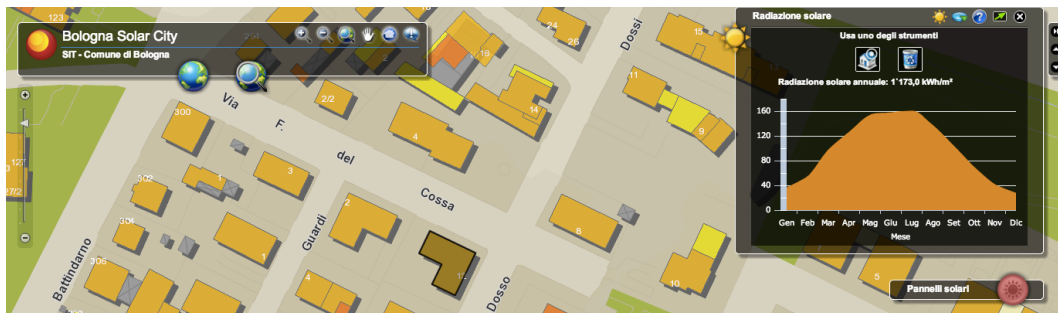


Figure 70: Bologna Solar City web application

The map services were published using ArcGIS Server and a user-friendly interface application was made available using ArcGIS API for Flex. Through this web application, it is possible to calculate the total solar radiation per building, thus estimating the potential yearly energy production and the reduction of CO₂ emissions.

The main simplification in Bologna Solar City was to consider all the roofs as flat, because in 1:2000 municipal cartography there are only two height information for each building: the bottom line and the height of the rain gutter. Unfortunately, the greatest part of roofs in Bologna, as well as in many other cities, are composed of a complex arrangement of different slopes, with many ridges and valleys. In order to perform an accurate analysis, different parameters must be considered: insolation, orientation of the surface, size of the surface, shading due to topography, shading due to taller buildings next to the surface, shading due to taller vegetation and other possible problems typical of an urban area like the presence of chimneys.

The accuracy of data relative to analyzed surfaces is indeed fundamental, and also the detail of geometric models used to represent buildings and their roofs. For this reason, the precise geometry has to be acquired in order to have a good evaluation of the solar potential of each part of the roof. To obtain this kind of information a DSM of the city could be very useful. This is obtained, in the presented work, from LiDAR data using point clouds acquired from airborne laser scanning. These points are loaded in ENVI LiDAR. This software can classify and also directly extract 3D features from the point cloud if the data density is adequate. One challenge is to integrate LiDAR data and digital 2D cartography taking in account that each dataset has a different origin, a different reference system and also a different acquisition epoch.

4.3.2 Point Cloud Processing

At the moment of writing this thesis there is no LiDAR data available to cover the whole city of Bologna, but only partial coverage. The chosen study area is Reno

district, one of the areas with full data coverage along with Porto district which is less interesting in the analysis of this paper, being partially covered by railway and Station of Bologna and being partially inside the historical center of the city, where the installation of solar panels on roofs has to follow strict rules.

The laser scanner used by Blom CGR S.p.a. in the flight that took place in 2009 was an Optech ALTM 3033 with the following specifications:

- Scan width (FOV): +/- 11 degrees
- Operational altitude: 1250 m altitude Above Ground Level
- Average distance between strip axis: 322 m
- Laser repetition rate: 33 kHz
- Horizontal accuracy: 1/2000 altitude = 0.6 m
- Vertical accuracy: +/- 0.2 m at the 1250 m altitude AGL

The dataset received is in LAS format in a projected CRS:WGS84 / UTM zone 32N (EPSG:32632). Elevation data is therefore referred to WGS84 ellipsoid. The LiDAR cloud is not particularly dense. The survey was not performed with 3D building extraction as the primary goal. Therefore, the average data density is only equal to 1 point per square meter with higher value where two adjacent strips (Figure 71).

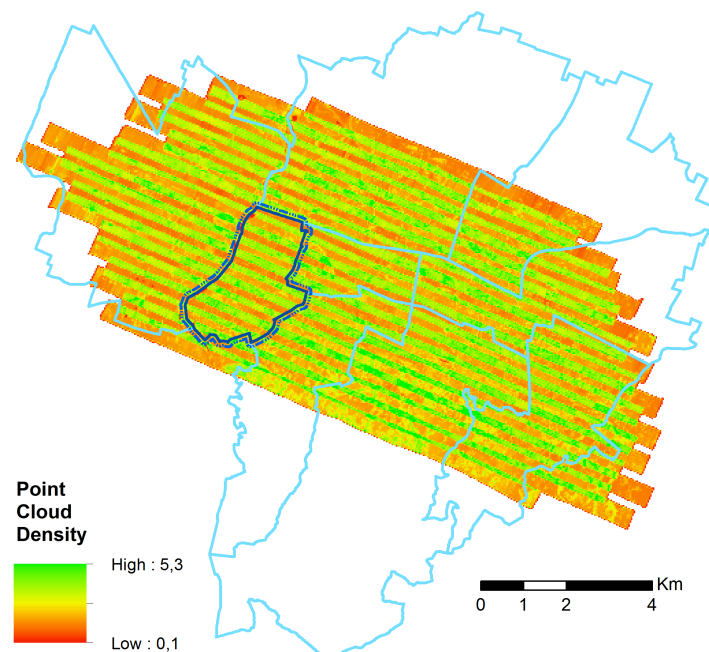


Figure 71: LIDAR data coverage with its density and Bologna district boundaries, highlighting the extension of the processing

In this work were also used vector data from digital GIS cartography (CTC) at a nominal 1:2000 scale, produced and maintained by Municipality of Bologna and now shared as Open Data: buildings perimeter, elevation points with orthometric height and district boundaries.

This dataset has a different CRS than LiDAR data: ED50 / UTM zone 32N (EPSG:23032) and orthometric height. In order to work in an accurate and coherent environment, all vector data were transformed into the same CRS as LiDAR data using ConvER3 GPS7, a free software from Regione Emilia-Romagna. It can use IGM (Italian Military Geographical Institute) grid to perform a rigorous transformation from different Coordinate Systems, including conversion from geoid to ellipsoid heights and vice-versa. The result is more accurate than transformation parameters inside GIS software.

The study here described uses the software ENVI LiDAR from HARRIS. The procedure firstly consists in importing all the 20 LAS files acquired over Bologna in ENVI LiDAR that converts them into a unique binary data file for a faster manipulation. The first operation to perform is to check data density through the work area.

ENVI LiDAR procedures operate to filter data and classify each point of the cloud. Then, through automated feature identification with manual tools for quality control, it is possible to extract different features as vegetation, power line vectors, and power poles, DSM and filtered DTM, building vectors with roof face and perimeter.

One relevant improvement over traditional LiDAR software is in the further analysis after point classification. With appropriate segmentation procedures is possible to create vectors and then interpolating surfaces among planes defined in the point cloud (Rottensteiner and Briese, 2002). The software, with a semi-automatic procedure among building's vectors, can identify the correct position, aspect and slope of each roof plane in the work area extracting consistent 3D building models geometrically correct.

4.3.3 Building Extraction

Within the urban environment where the study area is set, there are various problems related to features, like buildings from various periods with hipped or gabled roof often irregular and made more complex by the presence of heterogeneous elements. There is also a strong noise effect on point cloud data caused by vegetation that is located adjacent to the buildings on the fringes of urban roads. In correcting the slopes of the roofs the primary focus must be to keep their correct aspect rather than the exact representation of all the complexity that some buildings show as chimneys, dormers, and complex

geometries. It would not be technically possible to represent them due to the reduced density of the points, it is also not relevant to the objectives that have been placed in this research, which require taking greater account regarding the orientation of the surfaces analyzed with the aim of evaluating their solar radiation potential.

Regarding building extraction, some production parameters have been chosen to perform analysis on the dataset for the test area after extensive tests.

- Minimum area of 5 square meters for which will not be vectorized slopes of the building with a lower surface of the value set.
- Near ground filter width of 2 meters in order to filter out buses, trucks and train cars. Building planes less than 5 meters from the ground are not classified as buildings unless they have a width greater than this parameter.
- Buildings points range as the spatial variation of building's points: the value is used by the software's algorithm that scans for planar surfaces when the point density is not constant inside analyzed area or when there are some holes in the point cloud dataset. In this cases the value was set as high as 1.4 meters, increasing the risk to misclassify vegetation point into building class.
- Plane surface tolerance for curved roofs that are modeled using a series of successive planes. A new plane starts when the distance between the points being analyzed and the previous plane reaches this value, set to 0.5 meters.

Using ENVI LiDAR after the beginning classification procedure and the further building extraction procedure is then possible to use tools to ensure resulting feature representations are accurate. In the Quality Assurance mode is possible to interactively fine-tune point classifications and modify feature vectors such as building's roof shape using various tools such as cross sections.

Laser scanners detect points on antennas, chimneys, and every reflective surface. These points and other outliers are automatically filtered out from software algorithm as they become noise around the roof surface. With tools like Cross Section in ENVI LiDAR is possible to manually remove these points if they were not correctly classified (Figure 72).

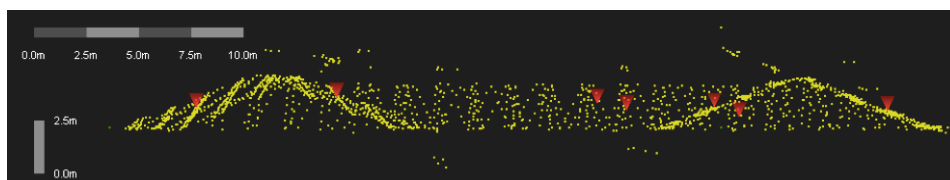


Figure 72: Cross section in the analyzed point cloud

Also, with Change Classification Code tool, points that were not classified as buildings can be assigned to the correct class. If the data density is adequate, it is also possible to set the selected points as a starting point for a new interpolating surface searching. This reduces limitations set on noise in the automatic process, thereby increasing the ability of ENVI LiDAR to set a plane at the designated point. Each vector can be manually edited, moving its vertices in every direction, to fit better to the local point cloud (Figure 73).

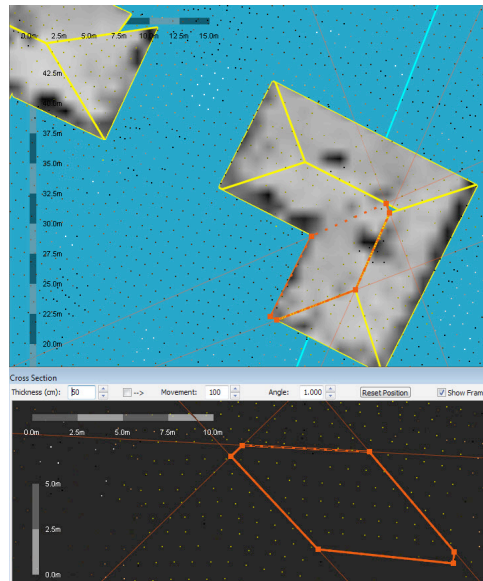


Figure 73: Manual adjustment performed by human operator

The final 3D model is composed of separate planes for each slope and rooftop, and it is possible to load the data in a 3D environment to compute the normal vectors to each surface (Figure 74).

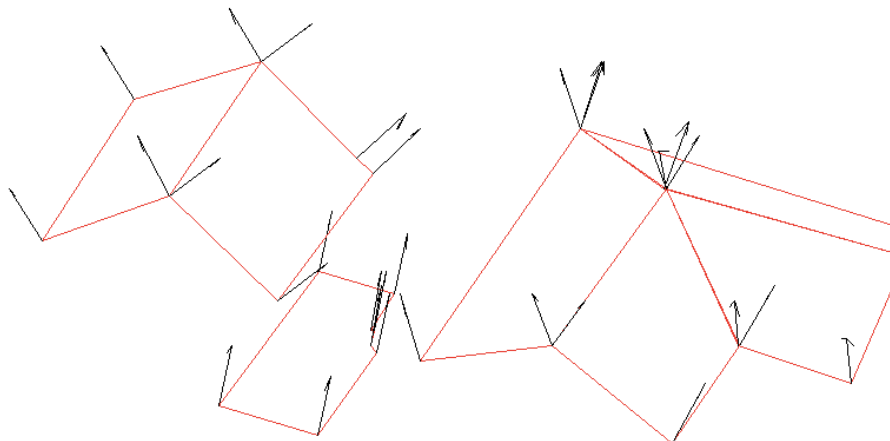


Figure 74: Vector roof models extracted from LIDAR data, displayed in a 3D visualization with the normal vectors applied to each separate slope

The municipal numerical cartography is loaded to perform a visual check. As can be seen some buildings were not recognized from the low-density point data cloud. In order to perform any comparison, it must be considered that in many cases LiDAR data can identify roofs areas, but especially where there is a pitched roof that extends over perimetric walls, the extension of that surface projected at ground level is wider than the area delimited by building's walls (Figure 75).

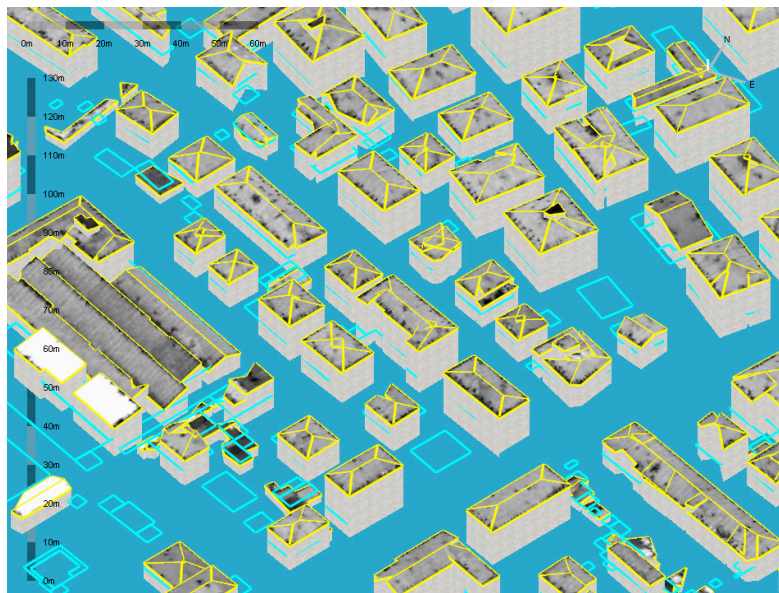


Figure 75: 3D extracted roofs along with buildings footprints from pre-existing digital cartography

Furthermore, in a traditional survey or in photogrammetry it is possible to identify quality-control elements in correspondence with the surface discontinuity as walls intersection or rain gutter line in roofs. Those two kinds of controls are not available in LiDAR data especially when there is a low density in points. In pitched roofs, the clearest discontinuity is the ridge roof line which position is determined by the intersection of the adjacent roof planes. An evaluation of planimetric accuracy can be performed comparing ridge roof lines in overlapping LiDAR strips (Vosselman, 2012). Those lines can be easily extracted from the data cloud with software like ENVI LiDAR. The final 3D model is equal to LOD2 (Figure 76).

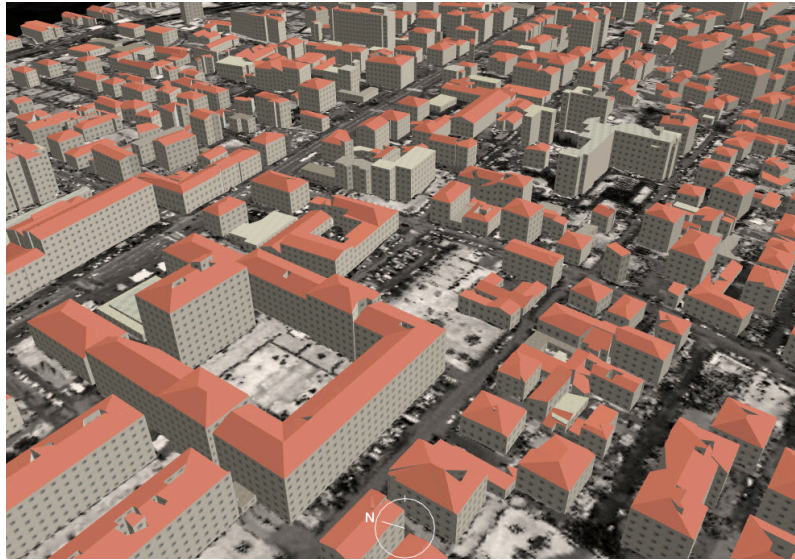


Figure 76: Final LOD2 model for the study area

In order to perform solar radiation analysis, one possibility is to directly use the Digital Surface Model produced from LiDAR data and buildings vector data from digital cartography as the mask for the DSM to analyze only roofs area. The LiDAR points must be first classified in order to remove vegetation points and possible outliers. Doing so, the DSM can be computed only on points belonging to buildings and ground level. But with data so low in density as 1 point per square meter the resulting DSM has a potential cell size of only 1 meter. Performing slope and aspect analysis at building level with so low detail brings in a lot of noise and salt and pepper effect that makes the data not suitable to identify every different surface of each roof. As it is possible to observe from Figure 77, there are also holes in the data that occur where the point cloud density goes below 1 point per square meter.

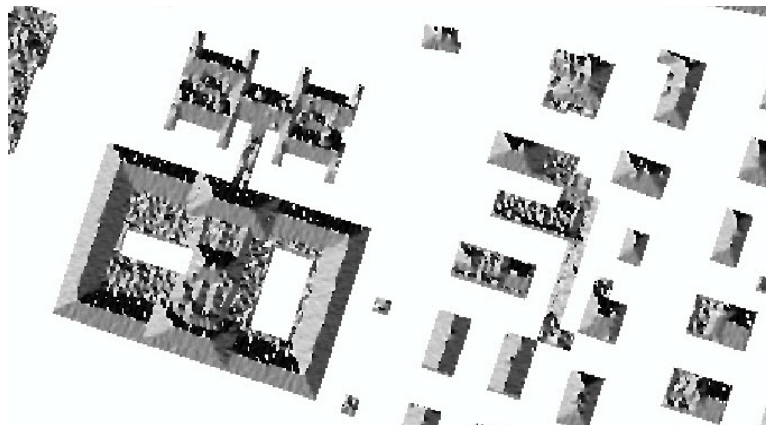


Figure 77: Aspect Map generated from LIDAR DSM masked with Municipality vector boundaries

To obtain a better resolution the point density must grow exponentially: the operative rule to obtain a certain pixel size in generated DSM is equal to 1 over the square root of point cloud density. Using a dataset with 4 points per square meter the raster resolution can be 0,50 meter; using a dataset with 16 points per square meter a raster resolution of 0,25 meter can be achieved (Beinat and Sepic, 2008).

To obtain slope and aspect values in ESRI ArcGIS environment, using a 3D vector exported as a Polygon Z(M) from ENVI LiDAR, the best option is to transform 3D data to a raster. Generating a DSM allows running 3D analysis tools like line-of-sight, viewsheds or solar radiation calculations. This transformation is performed creating first a Triangular Irregular Network (TIN) using the roof polygons as breaklines and using constrained Delaunay triangulation where no densification occurs and each breakline segment is added as a single edge. Then it's used a tool to generate a raster linearly interpolating cell z-values from the input TIN at the specified resolution of 0.5 meters that should be adequate given the instrument accuracy. Then Extract by Mask function is performed to delete values outside the modeled buildings, using the building's perimeter polygons obtained from ENVI LiDAR as a mask. With this final raster is possible to create derivative products like aspect and slope maps and use the resulting DSM to perform solar radiation analysis (Figure 78).

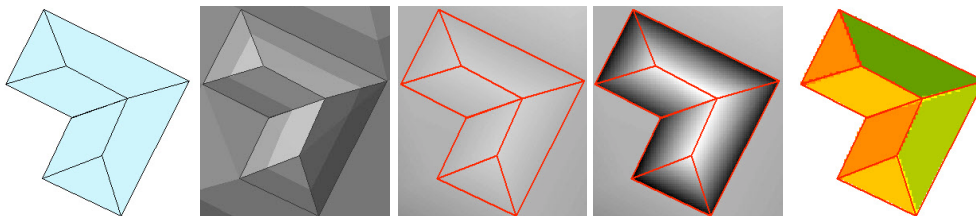


Figure 78: 3D vector obtained from LIDAR data processing, TIN model, raster model, masked model, aspect analysis

4.3.4 Solar Radiation Analysis

The ArcGIS Area Solar Radiation tool computes the global solar radiation on a surface for any time of day for each month of the year, investigating in every direction whether there are any obstacles, natural and artificial, and cross-referencing this information with the map of the sun and the sky map. The first is based on the position of the sun and calculates direct beam radiation; while the second is based on the atmosphere and calculates diffuse solar radiation. Reflected solar radiation is excluded from the calculation (Minghetti et al., 2011). In order to perform a comparison between the two different solar radiation values, sloped roof against the flat roof, the tool Set as Boxed was used: it calculates the perimeter of the roof at the rain gutter level and sets the roof to be flat. The global

value obtained for the sample flat roof was compared with the solar radiation value among different roof slopes (Figure 79).

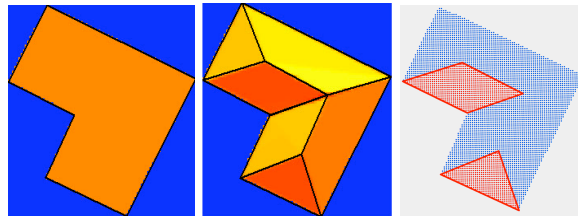


Figure 79: Boxed building model with flat roof, sloped roof, south-facing slopes highlighted in red

The global solar radiation on the sloped roof is 95% of the one obtained with the flat roof. But actually, only south-facing roof areas are suitable for solar panel installation. If the same ratio is computed considering only south faces from the sloped roof, the global solar radiation in the case studied is only equal to 28% of the amount of the flat roof model. As expected, the flat roof simplification tends to overestimate the solar potential of the building, while with proposed method that value can be computed with a good accuracy for each building.

In conclusion, the availability of software packages that allow extracting, virtually in automatic mode, 3D features, and in particular buildings, from high-density LiDAR data is very attractive for a variety of applications in urban areas, among which regarding assessments in the energy field. A precise 3D roof's model can be easily extracted and with it all the information about the surface area and orientation of each slope. The work has shown that a software of this kind can be in particular useful in studies devoted to the evaluation of solar systems installation on the rooftops (the example developed at Bologna Municipality has been described), or in analyses related to energy loss. Another secondary positive result is that this approach can help further validation of numerical cartography, derived from a photogrammetric database, adopted as the backbone of a municipal GIS. One of the main problems emerged is that, in order to reduce to a minimum the manual intervention in the presence of complex geometries of the roofs, it is important to have a dataset with a density much greater than that commonly available. Therefore it is appropriate to schedule specific LiDAR acquisition flights. In further analysis, if more detailed LiDAR data will be available, it will be possible to produce a better 3D roof model and estimate an even more accurate solar potential of each building, and also high vegetation will be taken into account and its shadow introduced in solar radiation computation.

4.4 Point Cloud Density

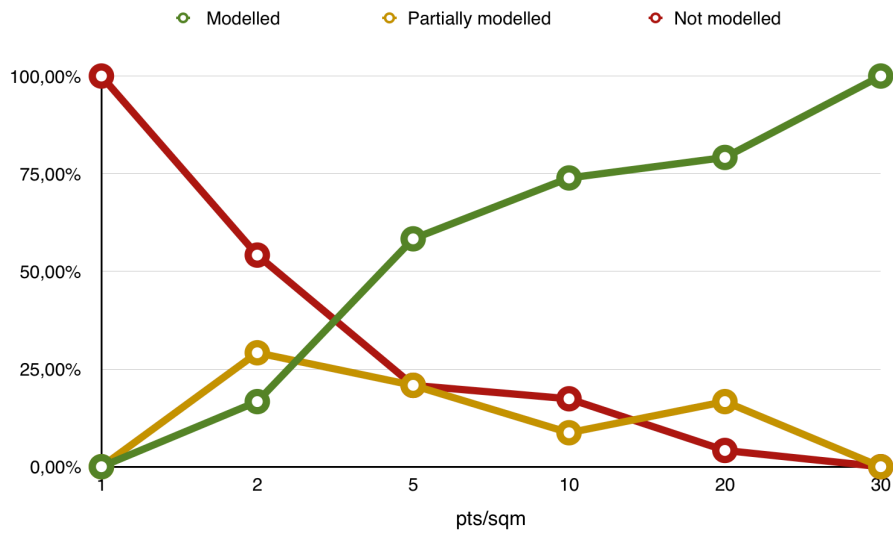
In another test area, with reference data for 24 buildings, the processing and performance with 2 algorithms from different software has been assessed in a test by Pasquali (2013) and discussed in his master thesis, undersigned as thesis advisor. The study stressed the influence of point cloud density at ground level on the derived processing in order to extract building roof planes (Figure 80).



Figure 80: Comparison of algorithm performance over different data density, from left to right: 30, 10, 2 points per square meter

With a density of 30 points per square meter, it has been possible to obtain substantially precise results. Furthermore, it was possible to even reconstruct the geometry of the various ancillary surfaces placed on the roofs of the buildings, such as the chimneys and dormers. With a decimated density at 20 points per square meter, the models obtained are less accurate, but still sufficient to identify almost all of the buildings in the surveyed area. With a density further reduced to 10 or 5 points per square meter, the results are necessarily less accurate than previous cases, but still improvable by careful application of some corrective action with the manual intervention of an operator. Finally, it was shown that with a density of only 1 or 2 points per square meter it is often not possible to extract and automatically model the geometry of the buildings by means of the algorithms under consideration.

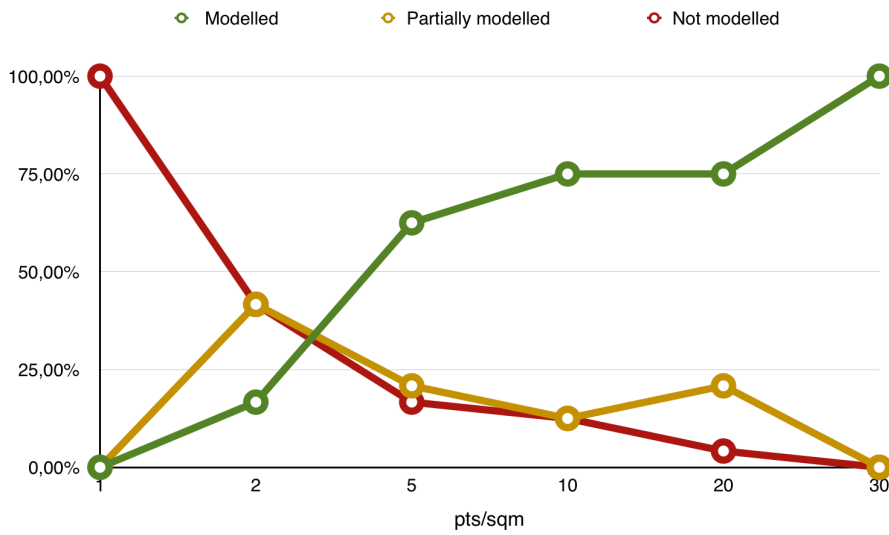
The test was carried out in a comparison between ENVI LIDAR (Table 81) and LAStools (Table 82).



Building geometries from ENVI LIDAR

Point Cloud Density (pts/sqm)	1	2	5	10	20	30
Modelled	0,00%	16,67%	58,33%	73,91%	79,17%	100,00%
Partially modelled	0,00%	29,17%	20,83%	8,70%	16,67%	0,00%
Not modelled	100,00%	54,17%	20,83%	17,39%	4,17%	0,00%

Table 81: Results from ENVI LIDAR processing point clouds at different density



Building geometries from LAStools

Point Cloud Density (pts/sqm)	1	2	5	10	20	30
Modelled	0,00%	16,67%	62,50%	75,00%	75,00%	100,00%
Partially modelled	0,00%	41,67%	20,83%	12,50%	20,83%	0,00%
Not modelled	100,00%	41,67%	16,67%	12,50%	4,17%	0,00%

Table 82: Results from LAStools processing point clouds at different density

4.5 Analysis At Building-Level

In order to bring the analysis at a LOD4, detailed information on each single building are needed: both outdoor and indoor data. This could be challenging for complex objects, such as historical buildings with irregular geometry. A full three-dimensional acquisition of both exterior and interior of those buildings is nowadays common in the field of cultural heritage from a sensor mounted on a terrestrial platform (Núñez Andrés and Buill Pozuelo, 2009; Guarnieri et al., 2013). These surveys along with other techniques allow to promote documentation and preservation operations and are critical to monitor the building after a particular accident, for example, a natural disaster, or in general to support policies of maintenance and restoration (Arias et al., 2007). This is achievable with different geomatic techniques, in a fast but also accurate manner. A laser scanner or photogrammetric survey of an ancient masonry building may be furthermore combined in a multidisciplinary context with other techniques, such as radar interferometric modeling, in order to study the dynamic behavior and produce an FE (Finite Element) model (Pieraccini et al., 2014).

A new approach was developed (Castellazzi et al., 2015) in order to deliver a full three-dimensional model of the building, following a linear and semi-automatic workflow that gives a fast pace to otherwise laborious operations. For instance, there are cases where urgent rehabilitation interventions are required in damaged structures affected by seismic events. The procedure presented in this section can process the acquired data available as a dense point cloud in order to deliver a numerical model suitable for a FEM (Finite Element Method) analysis for the building structure.

The result of a full three-dimensional survey is, in its simplest form, a dense point cloud. This is commonly achievable using ALS, TLS, digital photogrammetric techniques and Structure from Motion (SfM) approaches. The choice of the proper technique, the post-processing of the data and the combined use of multidisciplinary techniques (Sánchez-Aparicio et al., 2016) depends on the context and other parameters to consider that are not discussed in this context. In the case study for this LOD, several point clouds were acquired from a TLS with a precision in the order of a few millimeters, on the coordinates of the single points. Regardless of the technique chosen for the survey, a three-dimensional point cloud with comprehensive data acquired both from the exterior and from all the interior spaces of the building is expected as the input for the workflow described (Figure 83).

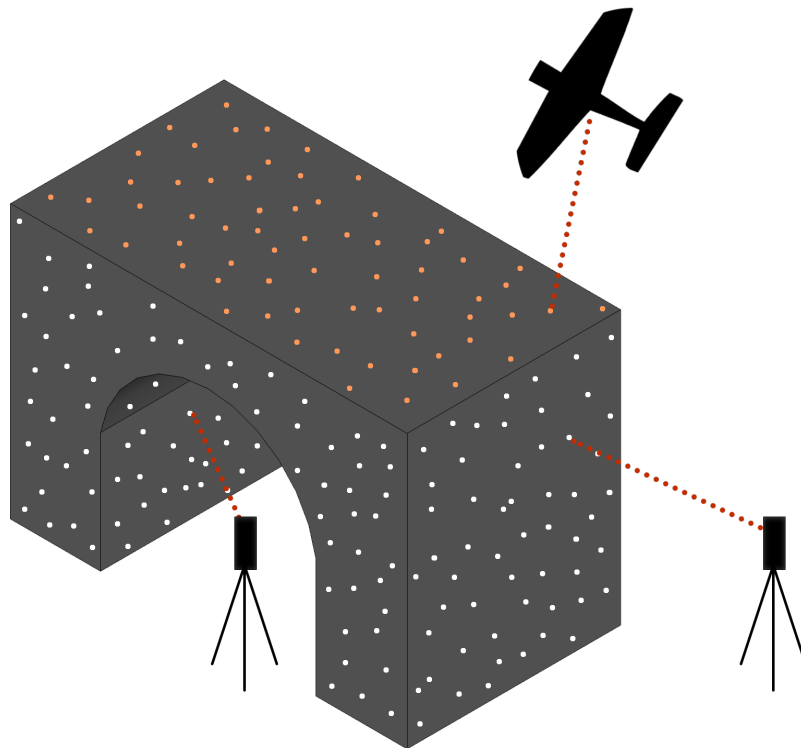


Figure 83: Point cloud and reconstructed model from data acquired both from terrestrial (white points) and airborne (orange points) platforms

Nowadays Building Information Modelling (BIM) interoperability has reached a significant level of maturity. Processing high-density point clouds derived both from photogrammetric and laser scanning surveys (Oreni et al., 2014), it's possible to produce very detailed BIM models. However, there is still the lack of complete algorithms able to perform an automated processing from point clouds to structural simulation based on FEM (Barazzetti et al., 2015). In another application, a validation for models reconstructed from point clouds, restricted to facades, was carried out (Truong-Hong and Laefer, 2013). Nevertheless, different experimental tests indicate that further work is needed to increase the level of automation, e.g. to better discriminate real openings from data occlusions (Tang et al., 2010; Hinks et al., 2013). Therefore, the BIM models automatically produced from point clouds cannot directly be used in FE software. In fact, several manual corrections are needed to avoid mesh local distortions or small elements and to guarantee the correct representation of complex architectural objects. Providing algorithms that are both robust and capable to operate with few manual intervention, in order to fill holes, close gaps and remove intersection, requires an appropriate interpretation based on the object investigated (Attene et al., 2013).

4.5.1 Voxel-Base Procedure

The procedure proposed in this section starts with a number of different point clouds, acquired from outside and inside the historical building with a heterogeneous distance from the instrument to the surface of the walls. All the data are then merged and georeferenced in a unique cloud with a more regular point distribution. A mesh is computed for the entire building, with inner and outer surfaces. One of the main problems in this phase is the presence of holes in the mesh, due to data missing in the point cloud for occlusions in the line of sight between the sensor and the surface to acquire; this problem is furthermore present for buildings damaged by natural disasters or in a serious state of decay. These holes do not allow to properly define, for a whole complex building, an accurately filled model using automatic procedures. In order to better analyze the polygonal model, our procedure aims to simplify a complex three-dimensional geometry into a series of two-dimensional closed polygons from sequential sections of the building obtained with a constant spacing. The final step is to convert automatically each polygonal section into a raster model that discriminates filled areas from void areas. All the raster sections stacked in the proper order produce a new three-dimensional volumetric model of the building, in a voxel format, useful for FEM analysis. The accuracy of the result depends on the chosen resolution of each pixel in the two-dimensional sections and each voxel in the three-dimensional model.

The semi-automatic procedure here described, called CLOUD2FEM (Figure 84), starts with a survey of a building and generates a Finite Element model. CLOUD2FEM was developed within a project involving two working group from the Department of Civil, Chemical, Environmental, and Materials Engineering (DICAM). Our working group in the geomatics area studied the algorithm that delivered a geometric voxel model starting from a raw point cloud acquired by means of TLS instrument. The structures group provided all the mechanical modeling of the created 3D voxel model in order to assess the quality of the result comparing the procedure to traditional computer-aided design (CAD) procedures. The work was published in a peer review journal (Castellazzi et al., 2015). This procedure allows a rapid processing of the three-dimensional point cloud data following a specific workflow in order to produce a voxel model. The resulting structural discretization guarantees the generation of 3D finite element meshes as well as their mechanical characterization. As a result, a large reduction in the required time in comparison to CAD-based modeling procedures is achieved. A geometrical and structural validation of the method was carried out on a masonry tower application and the findings show good reliability and effectiveness of the mesh generation approach (Castellazzi et al., 2016).

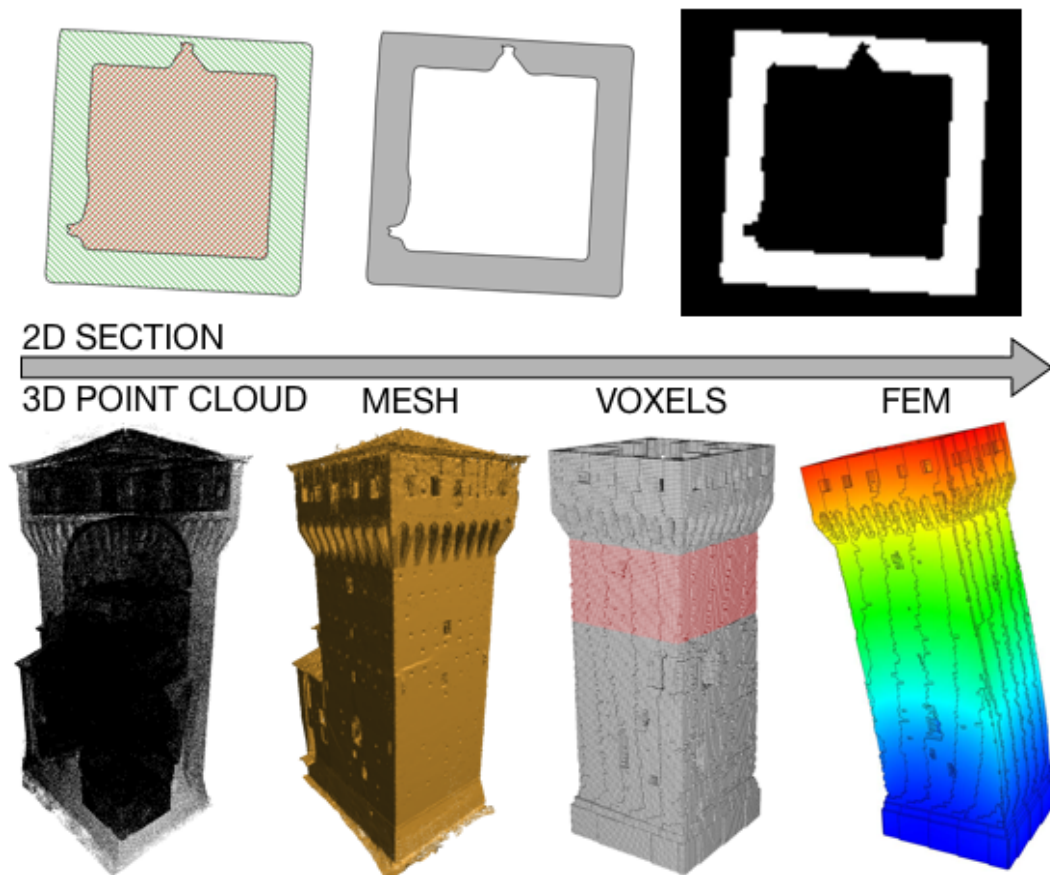


Figure 84: Concept of CLOUD2FEM procedure

4.5.2 Pipeline From Point Cloud To Voxel Model

The input data is a comprehensive three-dimensional point cloud for the whole building, both from the exterior and interior spaces. Each point of the cloud is conveniently referred to a reference system with X, Y, Z coordinates. A first operation on the data is through a sampling algorithm (in our case Poisson-disk sampling) in order to produce a new point cloud with a more regular density, starting from the original that typically presents strong variations of density related to the acquisition distance between the sensor and detected surface. A brief cleaning phase follows, with different tools but always supervised by an operator that has knowledge over the surveyed object, in order to delete all the points not useful for the subsequent analysis: neighboring structures, vegetation, terrain, and outliers. Then a first polygonal mesh is computed from the point cloud using appropriate procedures and parameters. The result is a continuous surface that represents the outer shell and interior shell of the whole structure. One of the main problems in this phase is the presence of holes in the mesh, due to data missing in the point cloud for occlusions in the line of sight between the sensor and the surface to acquire; this problem is furthermore present for

damaged buildings. At this stage we do not care to obtain a perfectly closed and topologically correct mesh since it would require a great amount of manual intervention in a three-dimensional environment by a qualified operator in relation to the complexity of the structure. Nevertheless, these holes do not allow to properly define, for a whole complex building, an accurately filled model using automatic procedures. The operator intervenes one last time at this stage resolving eventual problems found during the mesh construction phase. Then an automatic decimation procedure is performed in order to reduce the complexity of the mesh, though ensuring the correct representation the specificities of the geometry of the structure. In order to better analyze the polygonal model, our procedure aims to simplify a complex three-dimensional geometry into a series of two-dimensional closed polygons from sequential sections of the building obtained with a constant spacing. A reference plane (X, Y) is fixed in a convenient orientation: in most cases, it is efficient to consider the plane parallel to the floors of the building, but in some scenarios could be also oriented parallel to the walls. Other planes, called slices, are created parallel to the reference at a given regular distance Δ along the Z - axis. The value of Δ depends on the desired resolution for the Finite Element model. The number of slices must be sufficient to cover the whole building. The intersection between each slice and the polygonal model generates lines. A density of points are distributed along each line and a further cleaning operation is performed only on the points in order to assess eventual geometric irregularities. Then only the points belonging to the perimeter of interior surfaces and rooms of the building are selected for each slice. A concave hull model is computed around those points, representing the internal perimeter of the slice. Another concave hull model is computed around all the points in the plane, representing the external perimeter of the slice. In this phase, a couple of closed two-dimensional geometries are obtained for each slice: one for the external perimeter and one for the internal perimeter of the section. The difference between these two geometries, subtracting the internal from the external, represent a closed surface that contains the material of the building. Until now all the data processed are in vector format: points, lines, and areas. In this final step, each slice previously processed is finally converted into two-dimensional regular pixel grids at a constant resolution along X and Y axes. All the pixel grids are then gradually stacked in sequence creating a complete voxel model of the whole structure. At this stage it is also possible to assign different values to pixels in order to define the materials of different structural elements of the model (Figure 85).

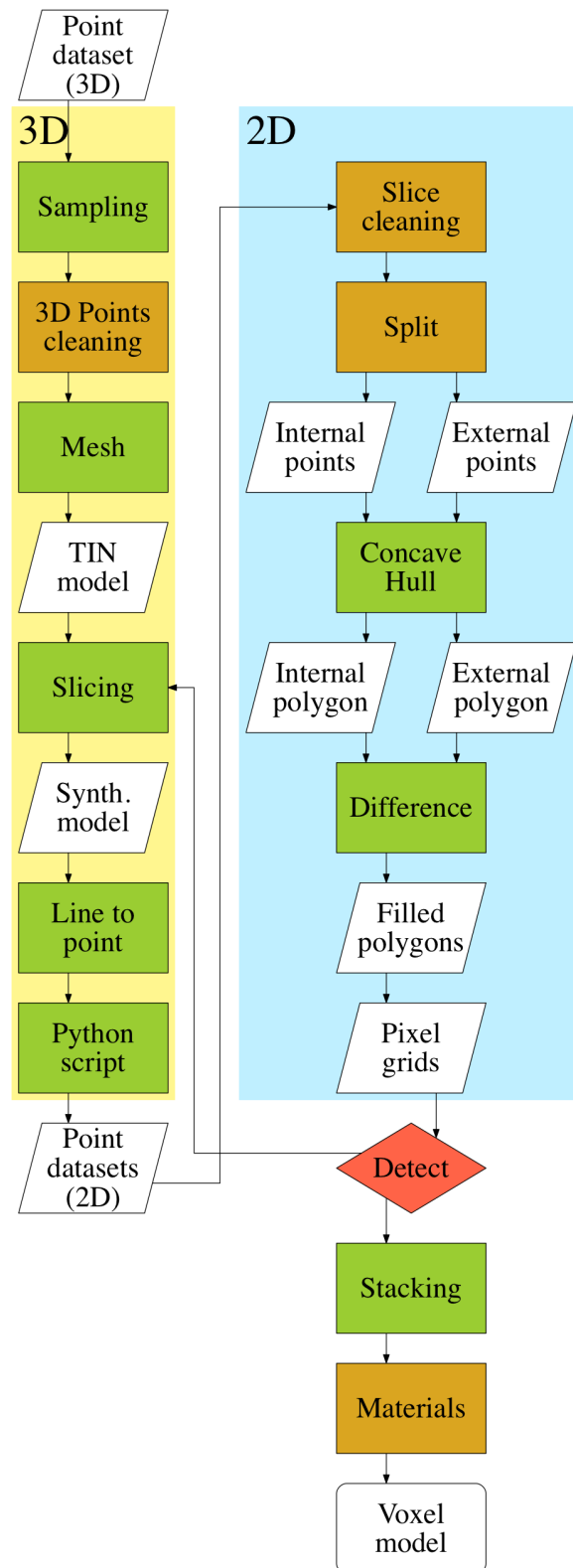


Figure 85: Workflow for the proposed method composed of completely automated procedures (green), semi-automated or manual procedures (orange) and the threshold detecting algorithm highlighted in red

4.5.3 Slicing Method

A new approach, tested in a complex case study (Bitelli et al., 2016), is here proposed in order to minimize operator intervention in the workflow previously described. The most time-consuming task, in which an operator is required to supervise the processing using specific tools, corresponds to the slice cleaning and split phases. These previously described operations are repeated for each slice in the model. Therefore, the global processing time is directly correlated to the number of slices to process. The main challenge for the approach was to lower the number of slices to process, while strictly describing the whole structure surveyed. This approach can be efficiently applied to different structures and contexts. The basic idea is to define a principal extension of the structure to process and to slice the point cloud along that direction. In order to achieve this result, the data is processed in different detail and resolution, depending on the context. Initially, the structure is sliced with a parameter 2Δ as the distance between any given slice and the following (Figure 86).

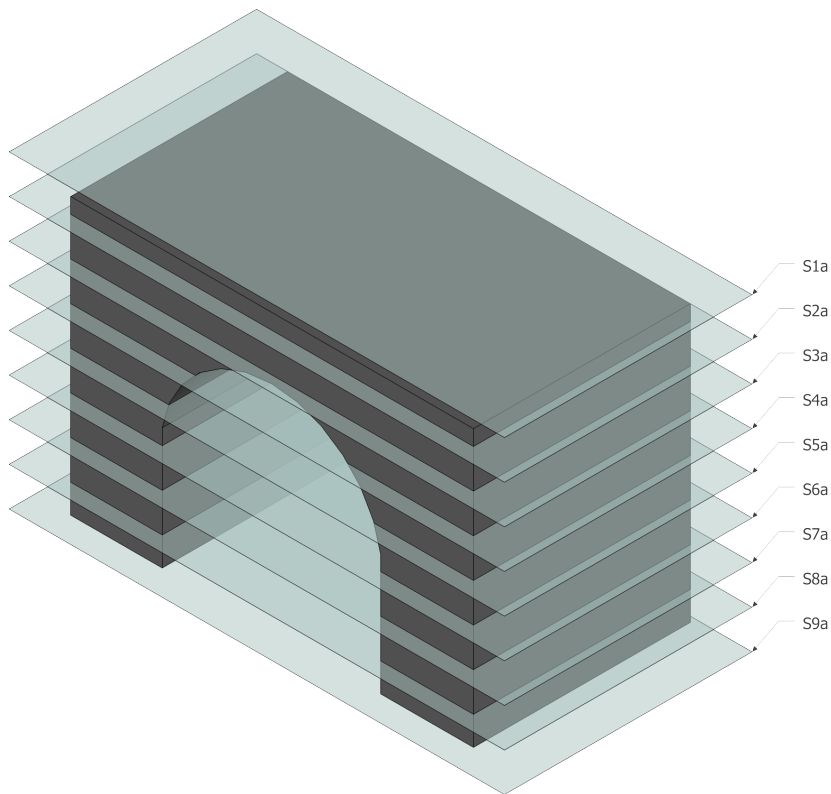


Figure 86: Visualization of the concept of slices stacking

The specific value of the parameter 2Δ is carefully chosen for the context of operations and depending on the result to achieve during the structural analysis.

An automatic script parses all the slices converted in pixel grids and compares the adjacent ones with image analysis techniques. If the difference between the two compared slices is evaluated under a certain threshold, then the algorithm proceeds to compute the following couple of adjacent slices. Only when the difference between a couple of slices is over the threshold, then the algorithm detects a significant variation in the structure between the two levels. In the example shown in figure is possible to observe how the section selected with the slice changes: from 'S1a' to 'S2a' and from 'S3a' to 'S4a' there were significant variations over the threshold. For this reason, new slices 'S1b' and 'S3b', highlighted in red, should be processed respectively (Figure 87).

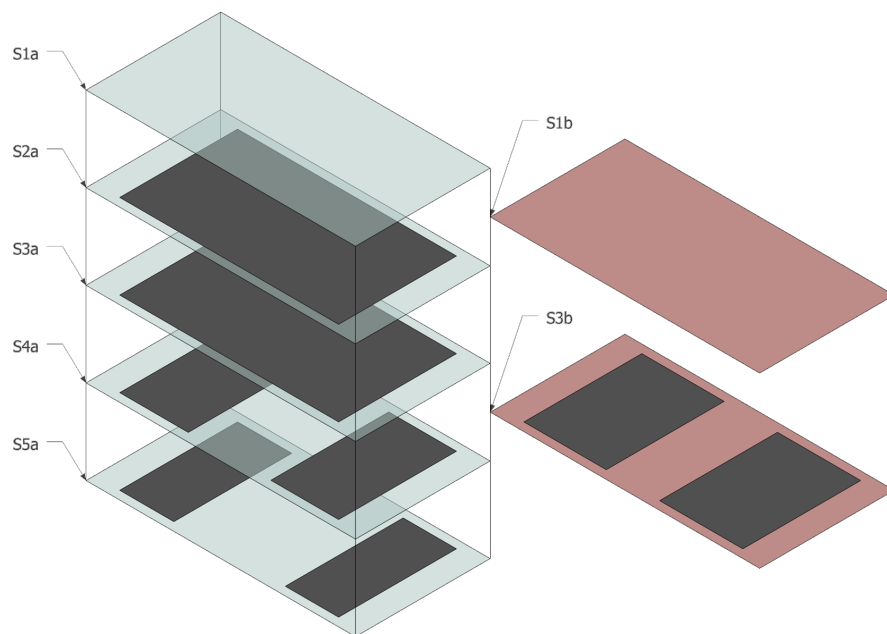


Figure 87: Visualization of the concept of slicing threshold

Therefore, in this particular case, a distance of 2Δ between the two slices is subdivided equally and another slice is added at a step of 1Δ . This procedure allows to process fewer data and reduce the time needed to analyze the simpler and regular part of the structure. At the same time, it allows describing with a higher precision all the special features of the building: curved surfaces, vaults, floors height or walls thickness. This is achieved by having a variable resolution of the analysis along the axis perpendicular to the slices (Figure 88).

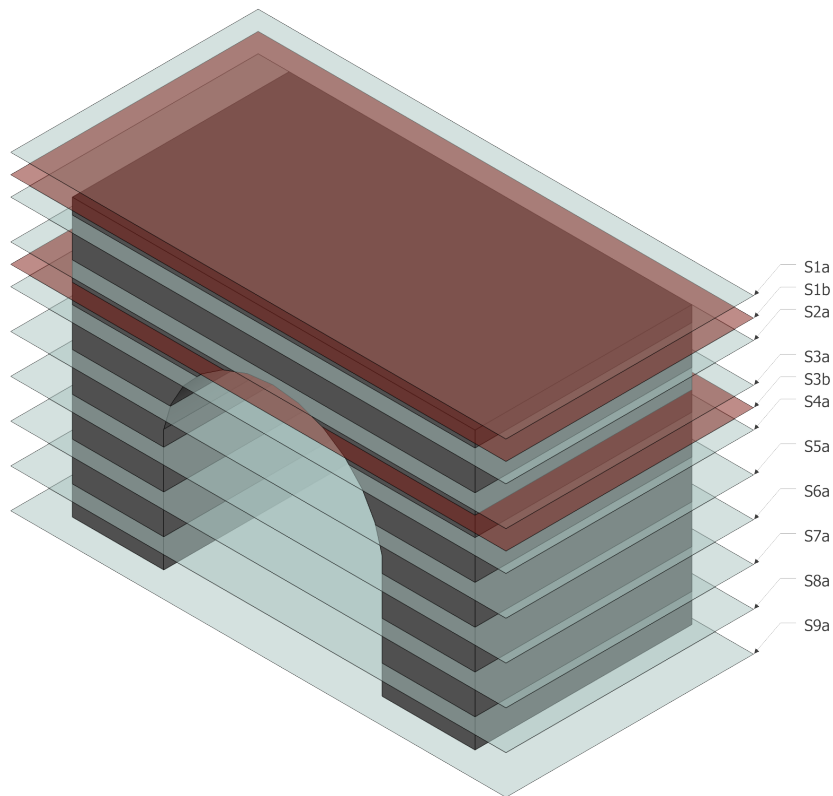


Figure 88: New displacement of slices after threshold application

4.5.4 Case Study

The described approach was applied to the San Felice sul Panaro Fortress, a monumental historical building dated back to the fourteenth and fifteenth centuries and located in San Felice sul Panaro (Modena, Italy) that was hit by an earthquake with two magnitude peaks in May 2012. The Fortress is characterized by a typical quadrilateral footprint with corner towers.

In the following image, it is possible to observe the slices computed for the North Tower, which was damaged in a greater part of its external walls, as well as the roof almost completely collapsed. The tower is composed of three floors, with inter-floors characterized by vaults. The first slices at the top left belong to the terrain level and the last slices in the bottom right part are related to the collapsed roof. In some adjacent slices couples there isn't a significant variation in the geometry and layout of the structure, such as the part close to the terrain which is repeated completely in the sequence of slices. In another part of the structure, it is possible to appreciate a significant variation between one slice and the next one. This is observable in particular in the proximity of inter-floors, as in the slice couple highlighted in red that will be explained in detail (Figure 89).

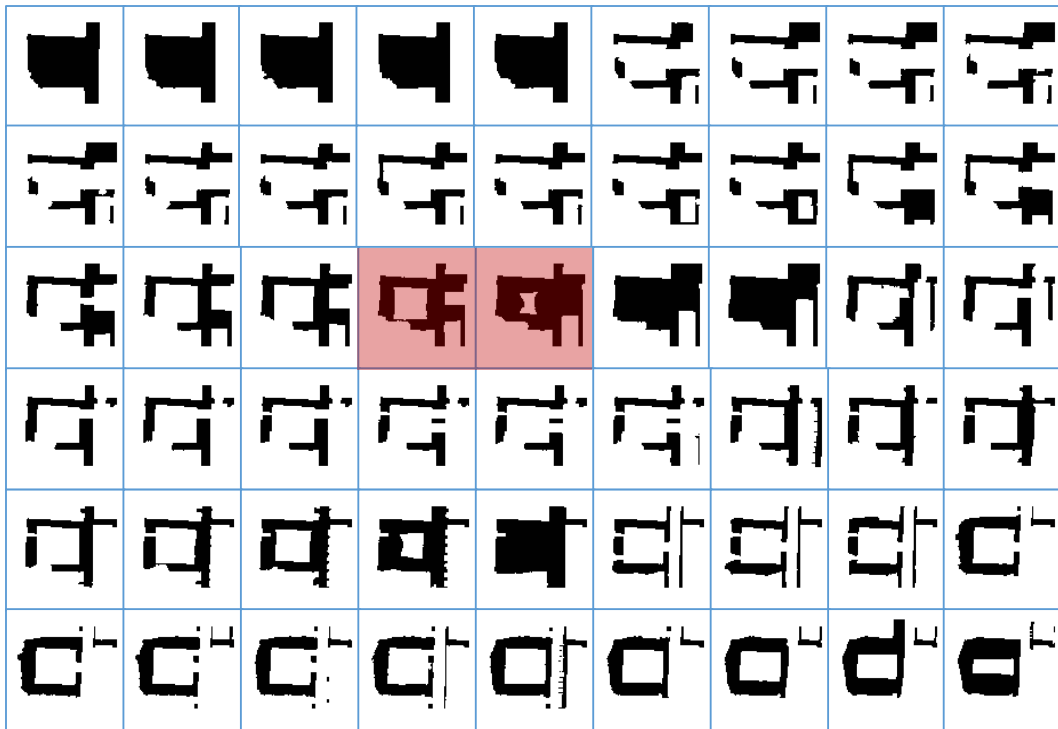


Figure 89: A selection of 54 slices from the North Tower, two of them highlighted in order to explain the algorithm processing

In the slice sequence, where there is a significant variation in the structure layout, an automatic change detection procedure is applied. There is a first step of segmentation in the original pixel grid and then a classification process that compare the two slices in analysis, in this case: Input A and Input B. Then, a change evaluation process is performed and if the change between the couple is over the determined threshold, another intermediate slice at 1Δ step is processed starting from the original dataset in order to describe with a higher precision all the particular features of the building (Figure 90).

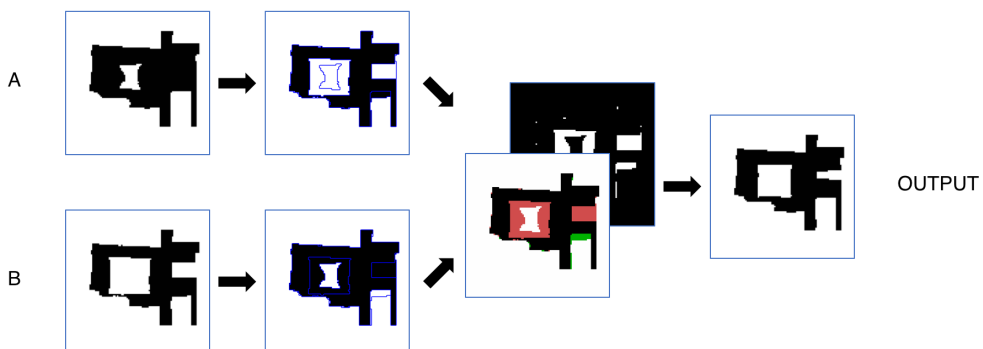


Figure 90: Automatic change detection procedure applied at the slice sequence

The described method is focused on maximizing the processing efficiency, lowering the total time needed to create a complete voxel model, in particular reducing any time-consuming step in which a human operator is involved. A complex three-dimensional problem is reduced to a series of more simple two-dimensional raster stacked (Figure 91).

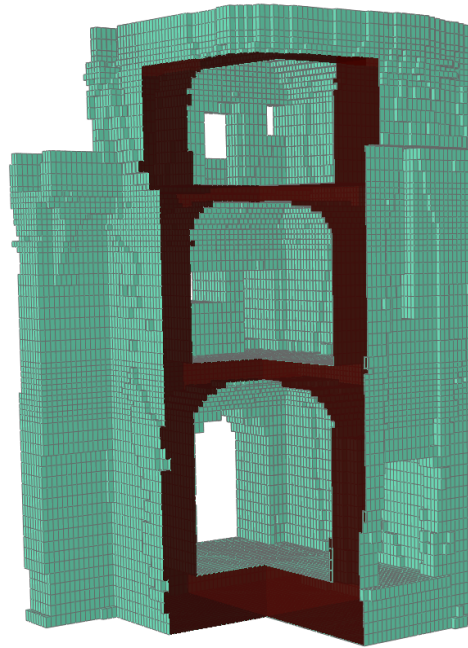


Figure 91: Final voxel model composed stacking each raster, showing floors and vaults in a section cut

Using voxel models it is possible to accurately describe a complex structure in a FEM analysis (Figure 92) with a large reduction in required time compared to CAD-based modeling procedure (Castellazzi et al., 2016).

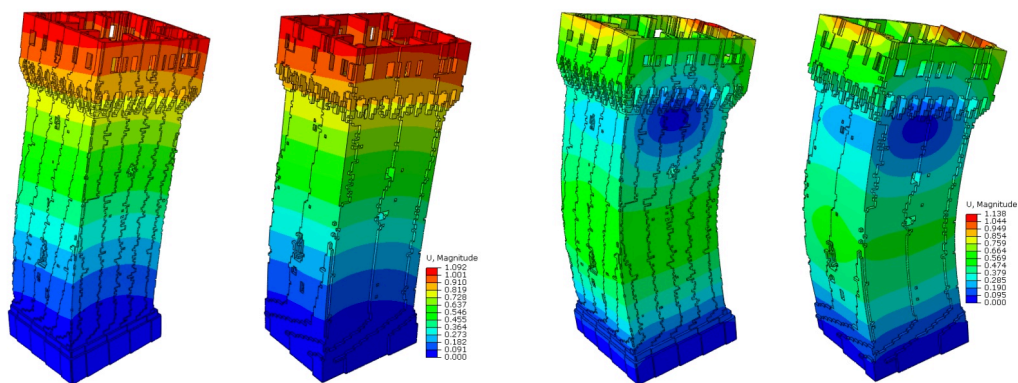


Figure 92: Different FE models with different voxel resolution (Castellazzi et al., 2016)

4.6 Rooftop Detailed Analysis

In order to take into account each element on the most complex rooftop, a LoD5 is needed modeling larger structures such as dormers and chimneys (Biljecki et al., 2014). In the example of solar panels placement, in order to assess the precise contribution in photovoltaic performance and displacement from each rooftop, a very high-density point cloud with great accuracy is needed to model and take into account for each element surveyed over the analyzed roof: chimneys, dormers, etc (Figure 93).



Figure 93: Examples of solar panels placement over complex roofs in the city of Bologna (comune.bologna.it)

This problem can be solved stressing simple GIS procedures in a specific iterative workflow in order to find any possible combination of solar panels with a certain dimension, fitting the area identified by the slope, avoiding any interference with pre-existing structures standing over the roof. Nevertheless, the source dataset must have the necessary elements to carry out the described analysis. An example is provided by the case study of Düsseldorf in which a building roof has been selected, containing numerous chimneys, dormers and other particular elements that contribute increasing the overall complexity of the slopes (Figure 94).



Figure 94: Example of a building with a roof composed of complex slopes, obtained from Google Street View over the case study of Düsseldorf

It is possible to observe that in such cases if the point cloud is not sufficiently dense, it is impossible to produce an accurate model of the increased number of slopes for the building roof (Figure 95).

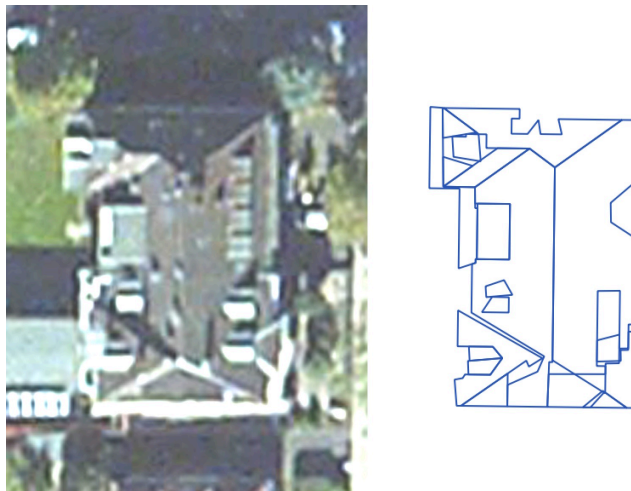


Figure 95: Results carried out over a building with a roof composed of complex slopes highlight the necessity of high density and accurate point clouds (aerial image on the left, slopes reconstructed from the point cloud on the right)

Some researches have highlighted the need for an enhanced version for certain LOD in order to explicit more details in the modeling of the roof slopes, bringing improvements in the overall accuracy of the building reconstructed. However, in order to reconstruct 3D models with such level of detail, both airborne and terrestrial surveys are needed (Biljecki et al., 2016).

The lack of information on the facades from data acquired with nadiral-mounted sensors can amplify the problem related to occlusions, that can be solved with oblique imagery or oblique LIDAR survey in order to record data in the visible

facades. In the vast majority of cases, oblique imagery may be sufficient to reconstruct information for the facades of a building (Rau and Chu, 2010), but still ,the final model can benefit from an integration of data acquired with a terrestrial survey (Figure 96).

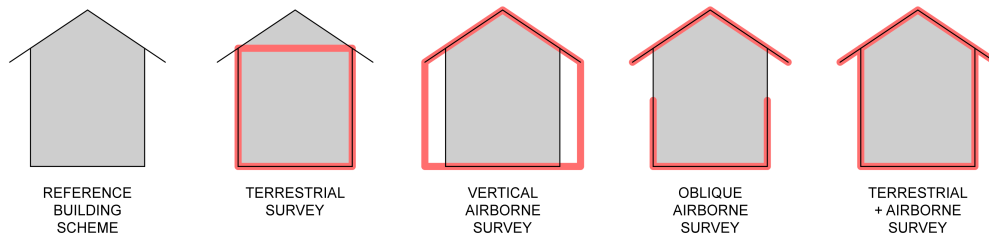


Figure 96: Explanation of building data acquired with different survey techniques

Furthermore, if there is not available a high-density dataset it is then not possible to precisely set the gutter line displacement, therefore the resulting slope will still be under-dimensioned as the 3D model will consider only the latest point acquired over the slope. The two described issues have an impact in the computation of building volumes and footprints.

Chapter 5: Final Products

Final products are intended as the result of the processing pipeline, starting from raw data acquired from a remote sensing platform, processed with specific algorithms and investigated through different methods. The final form of the data is usually a 2D thematic map in a GIS or a full 3D city model, published for the scientific community or delivered to potential stakeholders in order to assist human decisions.

As described in Biljecki et al. (2015) there are dozens of possible use cases and applications for 3D city models, such as estimation of the solar irradiation, energy demand estimation, aiding positioning, determination of the floorspace, classifying building types, geo-visualization and visualization enhancement, visibility analysis, estimation of shadows cast by urban features, estimation of the propagation of noise in an urban environment, 3D cadastre, visualization for navigation, urban planning, visualization for communication of urban information to citizenry, reconstruction of sunlight direction, understanding SAR images, facility management, automatic scaffold assembly, emergency response, lighting simulations, radio-wave propagation, computational fluid dynamics, estimating the population in an area, routing, forecasting seismic damage, flooding, change detection, volumetric density studies, forest management, and archaeology.

Some of this particular cases and implications analyzed during thesis activities will be discussed in this chapter.

5.1 3D City Model For Decision Support Systems

Abruzzo earthquake in 2009 highlighted problems, difficulties, and shortcomings in the management of emergencies derived from natural disasters. Among the tools that have been developed as a result of this experience, the analysis of the CLE (Condizione Limite per l'Emergenza), introduced with by the Italian Civil Protection in 2012, refers to the condition following a major catastrophic event in which the urban settlement still retains, as a whole, the operability of most strategic functions for the emergency, their accessibility and connection with the local context (Figure 97).

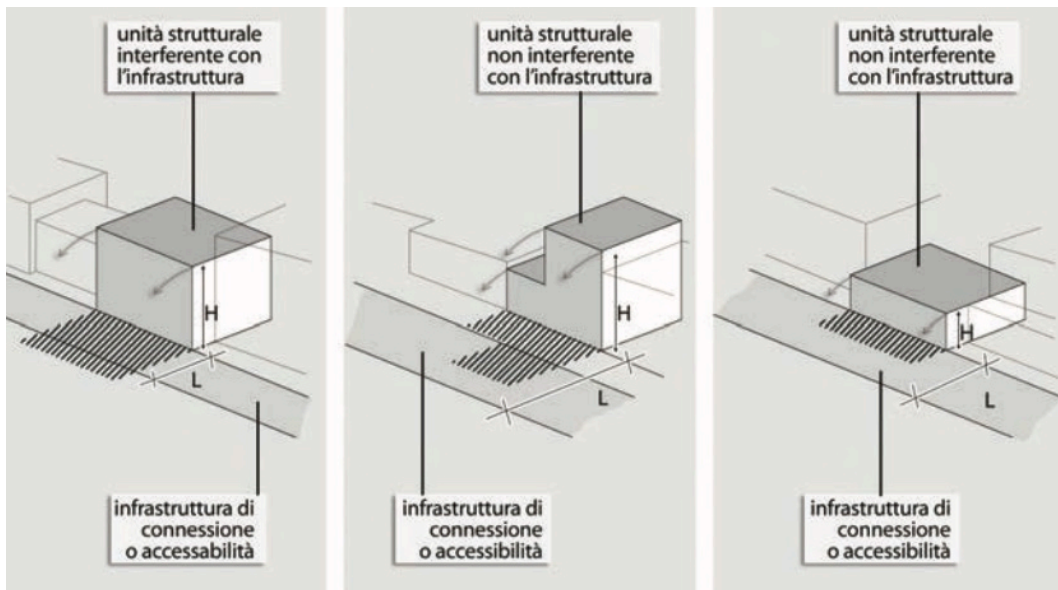


Figure 97: Interference between existing structures and infrastructures of accessibility-connection (Bramerini and Castenetto, 2014)

The results of this analysis must be included within the municipal emergency plans, in order to identify and mitigate any criticality during the emergency phase. In this case study a 3D city model is used to provide assistance to human decisions on evacuation planning and is intended to provide an automatic identification of the best routes for CLE study, with the aim of providing a useful tool to speed up the development process and provide an early, objective estimate of CLE optimal solution. GIS instruments and procedures for network analysis are used (Figure 98 and 99), creating scripts in Python language within the GRASS GIS environment (Lambertini et al., 2015).

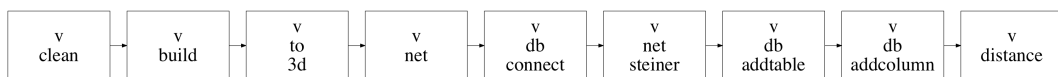


Figure 98: Workflow used to search for infrastructures of accessibility-connection

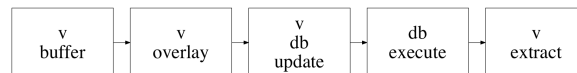


Figure 99: Workflow used to search for structural aggregates interfering with emergency areas

Through the use of the proposed method, in a GIS environment, it is possible to highlight any difference between a thematic map manually produced by a human operator following CLE guidelines and the result delivered by the algorithm (Figure 100).



Figure 100: Buildings interference with infrastructure as automatically computed with the proposed algorithm (green) and manually selected by human operators (yellow)

Among the objectives of this prototype implementation is the generalization of the procedure in order to be reproduced in other national and international territorial contexts, delivering a rich 3D city model which is a powerful tool for the city administration (Figure 101).

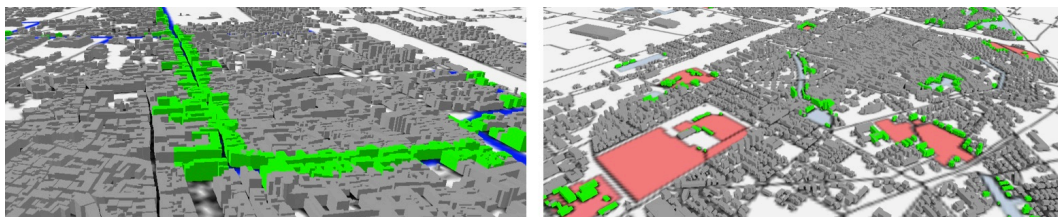


Figure 101: Buildings interference with infrastructure (left) and emergency area (right) shown in a 3D city model view

5.2 Webgis For Solar Radiation Estimation

The potential applications of three-dimensional data cover numerous fields. For example, a 3D rooftops model extracted with all the accurate information about the surface area and orientation of each slope can be useful in urban design, navigation, visual impact analysis, security and law enforcement. Within the energy sector, this applies in studies devoted to the evaluation of solar systems

installation on the rooftops (Agugiaro et al., 2012; Brito et al., 2012), or to produce surface-to-volume ratio used in energetic models. This approach can also help further validation of numerical cartography, derived from a photogrammetric database, adopted as the backbone of a municipal GIS (Africani et al., 2013). Geographic Information Systems (GIS) are powerful tools used to store, display or transform spatial data, and they are the ideal instrument to produce thematic maps to characterize the urban structure of a city.

The best results are reachable using high-density point clouds, to perform a full 3D building detection and extraction. Different algorithms and classifiers (Rottensteiner, 2012) or geometric 3D-primitives (Lafarge and Mallet, 2011) have been studied in recent years. Processing the data with specific procedures and collecting the results in a GIS environment is particularly useful in a Smart City perspective, where accurate and updated information are crucial for a great number of applications at urban scale, as described in Franci et al. (2014).

Modern cities need an increasing amount of energy for their activities. The installation of photovoltaic systems on building's roofs in urban areas is becoming more important every day and maps of the photovoltaic potential are therefore fundamental. The energy resource depends on intrinsic features such as climate conditions and geographic location (Freitas et al., 2015). These characteristics can be analyzed in depth with GIS tools (Súri and Hofierka, 2004). In each of these analyses, the accuracy is crucial and it is possible to perform a quantitative analysis with consolidated validation procedures. Furthermore, novel techniques deliver error estimate for each point of the cloud (Jalobeanu and Goncalves, 2014).

The purpose of this part of the research project is to study and develop an innovative methodology able to produce a three-dimensional model of an urban area, integrated with further information collected within a database in a GIS environment. The main idea of this research is to study the photovoltaic potential of a city and, in particular, of the rooftops of its buildings. The geometry of these rooftops can be extracted from high-density point clouds obtained with LiDAR techniques or dense image matching.

Each slope of each rooftop, after the proper processing steps, is known in its geometry with its orientation in space. All its parameters are inserted in a database in a GIS environment, collecting in particular accurate information about the surface area and orientation. These are the basis for the following evaluation of solar potential.

In this process, a crucial issue is to consider the accuracy of the models. A small error in the orientation or surface of these slopes, can deliver a wrong result in

term of solar radiation computation. The accuracy analysis of the models derived from the point cloud is possible using different statistic analysis and validation procedures.

This section of research is focused on the implementation and integration of different techniques in a workflow to produce buildings models, directly from 3D point clouds, in order to publish the result in a form understandable by potential end-users and stakeholders. Moreover an analysis on the different tools and software available was carried out providing a working scheme for a WebGIS.

5.2.1 Case Study

The processing involved several procedures with the use of different open-source software, in order to deliver a low-cost and efficient methodology for the computation of the photovoltaic potential (PV) without using data expensive to acquire, proprietary GIS or photogrammetric software. A set of aerial images from a conventional aerial platform are used in the case study: a residential district in the city of Coimbra, Portugal, composed of hundreds of buildings with various typology and dimensions (Figure 102).

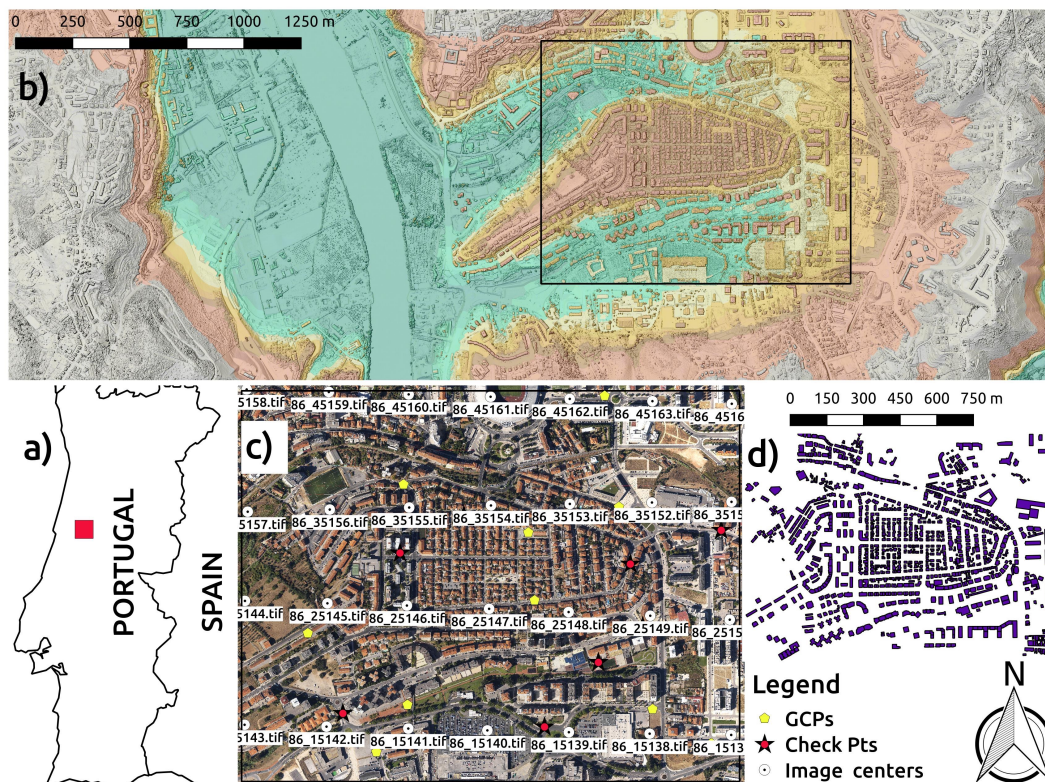


Figure 102: Localization of the study area

Those images are analyzed using the photogrammetry software library MicMac with Ground Control Points (GCPs). Therefore, using dense correlation, a Digital Surface Model (DSM) is produced from photogrammetric triangulation with self-calibration in the area covered by the images. This DSM, after a proper smoothing operation, is the dataset used for the solar radiation model and the computation of the photovoltaic potential for each building in the area, using GRASS GIS tools. An accurate parameterization of the weather for the reference period is performed with data from the PVGIS-3 database. A validation is performed using real solar radiation data from photovoltaic panels already installed on the rooftop of one of the buildings in the study area (Figure 103).

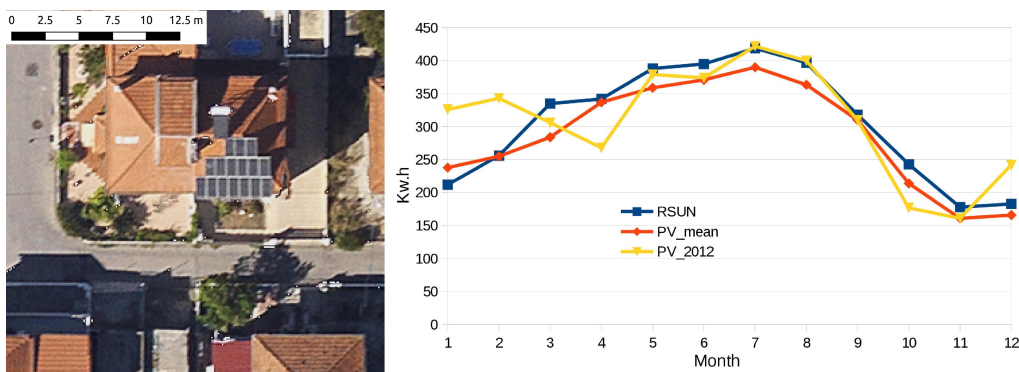


Figure 103: Validation of the results

The results show a good correlation between the real values obtained by the panels and the ones computed using the model, thus validating the presented methodology. All the results are finally presented to the public with a custom WebGIS interface giving citizens and stakeholders proper tools to understand the photovoltaic potential of the rooftops in a given area.

5.2.2 Processing With Free And Open Source Software

The experiments were performed with a critical approach to understand the easiest and most productive way to deliver geo-referenced information useful in communicating the rooftop photovoltaic potential to citizens and stakeholders. The aim is to develop a dependable and low-cost procedure that relies only on free and open source software (FOSS). The experiments assess the performances and potential of the procedures to produce photovoltaic potential maps.

Several different software solutions have been tested and studied in order to deliver to a wide audience a useful tool to analyze all the processed data. The data have to be presented in a suitable form which should be easy to explore, investigate and of course understand even for inexperienced users. The target

users of this tool can vary from an expert GIS technician to a stakeholder such as a private citizen buyer of photovoltaic panels for its rooftop.

All processed information have a geographical component and consequently, a Web-based Geographic Information Systems (WebGIS) is one appropriate tool to present the data (Figure 104).



Figure 104: Interface of the WebGIS service

WebGIS are usually composed of different pieces of software such as clients, libraries, viewers, frameworks and toolkits. These components work together in a specific workflow to allow users to view, query and interact with the requested data along with other datasets.

Many of these are free and open source software (FOSS) that have grown considerably in recent years and are now a mature and stable choice for the development of different types of applications, providing an effective low-cost solution. All this software comply to Open Geospatial Consortium (OGC), an organization that promotes the use of common standards for WebGIS specification in order to access their web services. The most common services from OGC used in a WebGIS are Web Map Service (WMS) and Web Feature Service (WFS). For all categories of GIS software required for the implementation of the WebGIS, a FOSS product is available and also several free products are able to compete with proprietary software in a number of real-world installations and their use in high-demand environments (Steiniger and Hunter, 2012).

The aim of this project was to produce a tool with high performance and independent by the platform used by the client, desktop or mobile. Different configurations of WebGIS service can be observed, based on the final requirements to provide the connection to remote sources on the Internet. In

some simple cases they are configured as client-only, but as the project grows it is more common to find configurations based on both client and server that allow more advanced capabilities.

In this project all the data is stored in a database backend, a server performs the tasks to deliver the data to the client at the user disposal. Regarding the database backend, a popular choice is PostGIS based on PostgreSQL that can provide great scalability as the project grows, meanwhile for small tests the data can be stored in a SpatiaLite file based on SQLite. On the server side, the two main choices nowadays are MapServer and GeoServer, the last of which is the one used in this project. OpenLayers is a very powerful yet simple JavaScript library with high rendering performances for displaying maps in web browsers and supports a wide variety of data sources; this has ensured it a dominant position in the web mapping libraries environment. The latest generation of client software make use of HTML5 technologies, showing improvements in interaction with vector layers and being native for Web browsers without the requirement of third party plugins to be installed by the user.

The aim of this kind of platform is to enable both the citizen and technicians to evaluate the opportunity to install solar panels in a building, estimating PV energy potential for each roof. As it is common in research, the area where the procedure was tested and validated is only a small portion of the territory. Nevertheless, such tools allow scaling the results with no additional effort to wider areas, even with national or international coverage. The use of FOSS components assures the ability to scale the project with only hardware requirements increase, without incurring in additional software costs.

5.3 Data Dissemination

5.3.1 Volunteered Geographic Information

In recent years the damage assessment based on remote sensing data has known the introduction of crowdmapping, with a group of volunteers, that immediately after a disaster, are invited to rapidly analyze portions of aerial or satellite imagery distributed through an online platform in order to identify and classify damaged regions in order of priority. This is also called Volunteered Geographic Information (VGI) and it is a growing phenomenon since the last decade (Goodchild, 2007).

However, it should be considered that the overall quality of metrical data derived from VGI is variable and not comparable to a traditional local cartography, even if containing an impressive amount of detail in certain areas. Nevertheless, this uncertainty is being studied in order to evaluate data quality and accuracy of

models reconstructed from VGI and data fused from different sources (Flanagin and Metzger, 2008). Researchers are now paying attention in assessing the explicit quality of maps derived from VGI (Senaratne et al., 2016).

On the other hand, some experiments are carried out in order to create 3D city model of a building, both outdoor and indoor, generated through methods and algorithms starting from VGI data with high level of detail (Goetz, 2013).

The largest repository of VGI is nowadays OpenStreetMap (OSM): a free map of the entire world that is constantly created and edited by millions of volunteers around the world through a process of VGI (Figure 105).

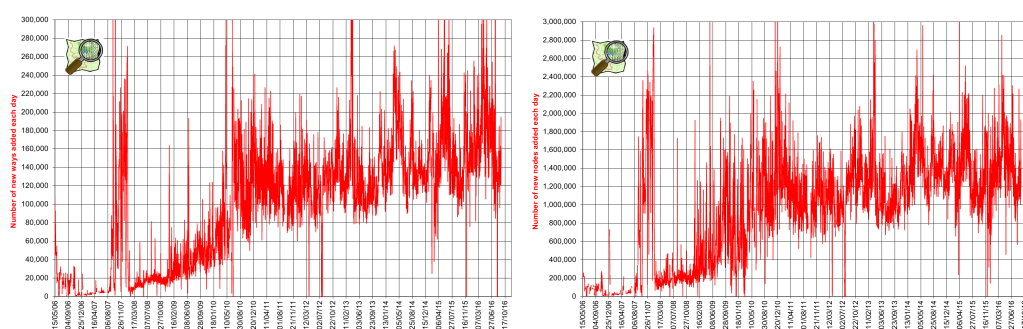


Figure 105: Openstreetmap.org database statistics for number of ways and nodes added each day

An open and editable map of the entire world allows creating custom map details based on user needs and giving awareness of surrounding environment to citizens. Furthermore, it can help providing and updating geographic data in areas of the world where a traditional cartography do not exist. In fact, cartography availability is crucial to support emergency operations in case of disasters.

Commercial operators for space imagery such as DigitalGlobe are recently embracing Open Data philosophy providing open and accurate pre and post-event high-resolution satellite imagery in a case of large-scale natural disasters. This is the purpose of Humanitarian OpenStreetMap Team (HOT): when a major event happens anywhere in the world, in case of humanitarian crisis, they provide a collaborative mapping through a huge network of volunteers with VGI methods, helping to reach the population in need of updated maps. This is a rapid intervention from a multitude of users that provide maps for areas when needed in an emergency scenario or validating data processed by an automatic algorithm in order to produce a final deliverable. HOT acts as a bridge for the OSM community, providing to humanitarian organizations deployed in the affected countries the detailed maps with updated road networks, villages, buildings, etc.

in a short time-frame in order to locate people at risk and deliver goods and services to the areas that need them most.

In the frame of the OpenStreetMap Geography Awareness Week, our working group for Geomatics area at DICAM (at University of Bologna) hosted for two years in a row a Mapathon event under the frame of CODE³, the DICAM Centre for International Cooperation and Development on the thematic areas of Engineering, Environment and Emergency, in order to bring awareness on issues that are relevant to development in emerging countries (Figure 106). These events were organized to introduce to a wide public the OSM project and assist the participants in their first steps in crowdmapping for humanitarian projects using remote sensing satellite imagery, providing training for new volunteers in order to obtain a faster intervention during a disaster.



Figure 106: OpenStreetMap Geography Awareness Week events held in 2016

A last promising research (Martin-Brualla et al., 2016) studies the contribution of gathering crowdmapped imagery acquired by users around the world for a certain scene or for a recognized object and uses computer vision techniques and Structure-from-Motion (SfM) approaches to recreate a time-series of data for the acquired scene. This has interesting impact in reconstructing data over a long period of time without any local installation of remote sensors. With the same approach, it is possible to foresee different benefits when there will be available long time-series not only for imagery but also for surveyed point clouds and recreated 3D models of cities.

5.3.2 Open Data Policies

Open data is a definition that applies to information free to access, reuse and redistribute. Releasing geographical information products, such as statistics, measurements or survey results, as Open Data can produce different direct and indirect benefits, offering the free right to access research raw data or processed products and even reuse the data for a greater efficiency in different projects and for different purposes, providing easier access to the data for other researchers.

In a political perspective, Open Data policies can demonstrate administration's transparency to their citizens that can be further involved in decisional processes like urban planning. By releasing Open Data, GIS professionals and researchers will be able to derive useful products helping to better understand the environment and create new models that are specific to different needs.

Year after year more entities are collecting three-dimensional point cloud data and sharing it: these datasets are an important piece of public spatial information. Nevertheless, data compression is necessary for storage and transmission, for navigation or visualization purposes. New approaches have been developed in order to obtain a fast compression for raw point clouds in real-time applications (Golla and Klein, 2015). These approaches can be developed in special rendering techniques in order to improve the final visual quality of point clouds (Schutz and Wimmer, 2015). These algorithms were used in FOSS WebGL viewer Potree for large point clouds. The aim was to provide a method to deliver point clouds for further analysis and experiments avoiding the time-consuming phase of reconstruction and meshing. This is of particular interest for Open Data dissemination.

Within this context, it is possible to cite the example of satellite imagery acquired by the Landsat program. Since the end of 2008 the United States Geological Survey (USGS) started delivering Landsat 7 imagery for free and from the beginning of the following year, all the Landsat archive was available for free download to the public, dropping the previous pricing policies for each image to zero. This led to an increase in downloads of several order of magnitude during the following years, providing a great direct impact on the research community and allowing a larger use of satellite imagery data in academic institutions for different purposes: environmental monitoring, agricultural monitoring, urban analysis and water management, just to cite a few.

Furthermore, remotely sensed data can provide valuable information in each phase of the disaster risk management cycle, helping to understand spatial phenomena and supporting the decision making with objective data. It can contribute to the risk management activities through the identification of hazard areas, the assessment of damaged zones in a timely manner and assisting the recovery plans. Each phase of the risk management cycle requires remotely sensed data with appropriate characteristics of spatial, spectral and temporal resolution depending on the kind of information to be obtained. In particular, in the response phase, all activities, such as evacuation, rescue, and needs assessment, must be carried out in order to save lives and minimize damages.

The European Union, for research projects funded under Horizon 2020, aims to improve access to knowledge in order to maximize the benefits of public

investment and to ensure a long-term preservation of information. As defined by European Commission Directorate-General for Research & Innovation (2017), with public access to scientific published researches and data it will be possible to: build on previous research results with an increasing quality of results, encourage collaboration and avoid duplication of effort in order to improve efficiency, speed up innovation with faster progress to market that generate faster growth, involve citizens and society with the improved transparency of the scientific process (Figure 107).

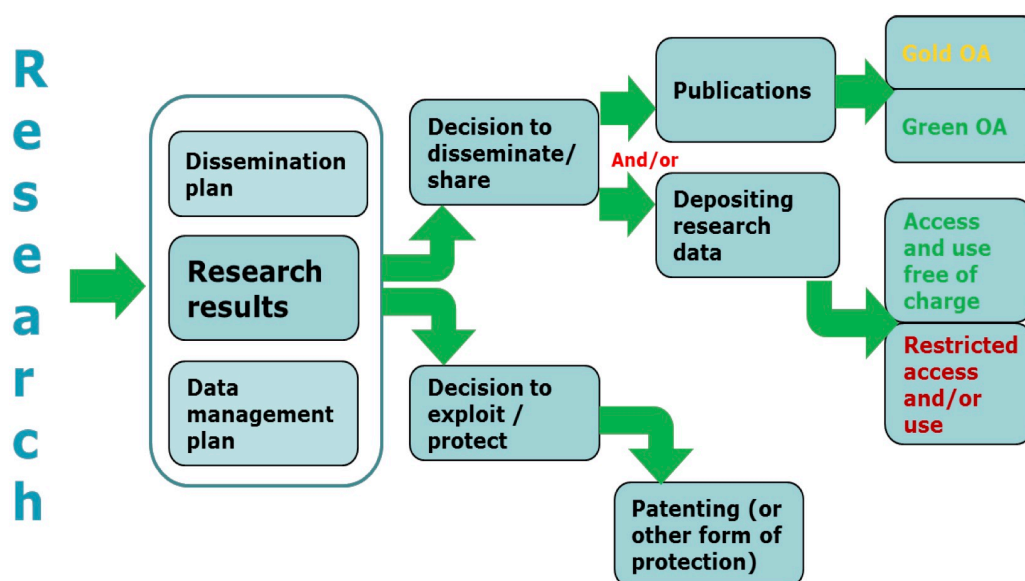


Figure 107: Open access graph to scientific publication and research data in the wider context of dissemination and exploitation (European Commission Directorate-General for Research & Innovation, 2017)

Conservation and dissemination of data and metadata has a critical importance and it is addressed under the keyword FAIR: Findable, Accessible, Interoperable and Reusable (European Commission Directorate-General for Research & Innovation, 2016)

Starting from January 2017, the Open Data Pilot is extended to any new Horizon 2020 project, that must define a Data Management Plan (DMP) in order to properly manage research data, and each partner has to identify how to store, access and disseminate data and the associated metadata. The DMP, in fact, describes any information regarding the dataset collected or generated within the project, the standard used and the relative metadata, the procedure for data sharing and Open Access, and finally specifications for storage and preservation of any data or software produced during the project. This strong requirement expressed by UE reiterates the importance of the concepts expressed in the preceding chapters of this thesis.

Conclusions

The paramount importance of remote sensed geospatial data has been highlighted through experimental results and analysis of various case studies. The research project has been focused on the use of remotely sensed data in urban areas, paying particular attention to the analysis concerning the data surveyed over buildings to propose a complete and reliable pipeline for data acquisition and processing.

In particular, the thesis begins with an examination of the available combinations of platforms and sensors used to acquire data in urban scenes, discussing the reasoning behind the choice. The following chapter describes the possibilities for an efficient data processing through the analysis of results carried out in many software environments, also discussing the critical issues related to the integration, processing, and storage of massive volumes of data, providing few examples of future research topics and directions. The subsequent chapter is devoted to various case studies at different urban scales described with some degree of detail, from 3D city models of a whole area to accurate analysis of a single building. In contexts extending beyond the topics of this thesis, these models have several critical applications such as assessment of solar radiation over an entire city or structural analysis for each building. In the end, in the final chapter, a discussion is carried out regarding the products derived from the previous phases of processing, such as 3D city models or WebGIS, and their impact on providing an improved visualization of significant information to scientific community and stakeholders. Furthermore, the concept of sharing Open Data is stressed through a series of examples.

The growing trends in data continuously acquired from a larger number of platforms and sensors lead to a significant challenge in storage and processing of the surveyed data. If we are not able to transform this vast amount of data in derived products that are meaningful providing accurate information, then we have failed the primary goal of remote sensing. Despite the efforts spent in data acquisition, the availability of high-quality models is limited by the cost and the time needed to create them. Therefore, we need to support further research in and stress the related critical issues. It has been demonstrated that it is now possible to efficiently create models of an entire city after a proper survey carried out from a remote sensing platform with the appropriate sensor. In fact, as we have seen in the state of the art review carried out through the entire thesis, a significant part of research topics concern the development of robust semi-automatic and automatic methods for 3D city models. The goal is to reduce the subjectivity of human-driven interpretation tasks, thus also reducing any time-consuming intervention that generates higher costs and delays in the delivery of

a final product. Updated city models are in some cases urgent, such as in emergency scenarios, considering that a significant number of urban centers with a population high density are located in areas prone to natural disasters. Through the use of such models, it is possible to predict and mitigate the impact of emergency events.

All the approaches described and presented in this PhD thesis can be applied to an even large number of different case studies, supporting the scientific community by defining best practices. In particular, stressing and examining some of these critical issues highlighted in the previous chapters such as point cloud density, precision, and accuracy. The urgent need for 3D city model, precise information and coherent metadata regarding building structures and their properties has been highlighted through the various chapters.

Nevertheless, some critical issues, particularly related to the production of 3D city models with a high level of detail, are still open and further research will be needed to address those topics and many procedures presented in this thesis will benefit from further improvements. However, the results presented here have proven to be promising and highlighted the clear advantages of creation and updating of a 3D city model in a Smart City perspective. Hopefully, this work will also be an inspiration for further research.

References

Websites

last accessed on 2017-03-25

- ASC www.advancedscientificconcepts.com
- Comune di Bologna www.comune.bologna.it
- DigitalGlobe www.digitalglobe.com
- DJI www.dji.com
- Drone Industry Insights www.droneii.com
- DxOMark www.dxomark.com
- European Space Agency www.esa.int
- Gartner www.gartner.com
- GoPro www.gopro.com
- GRASS GIS grass.osgeo.org
- HARRIS www.harrisgeospatial.com
- Hasselblad www.hasselblad.com
- Humanitarian OpenStreetMap Team hotosm.org
- KAARTA www.kaarta.com
- Land NRW registry.gdi-de.org/id/de.nw/DOM1L
- Leica leica-geosystems.com
- NASA www.nasa.gov
- Open Geospatial Consortium www.opengeospatial.org
- Open North Rhine-Westphalia www.open.nrw
- OpenStreetMap www.openstreetmap.org
- OSM Geography Awareness Week osmgeoweeek.org
- PHASE ONE industrial.phaseone.com
- Phoenix Lidar System www.phoenixlidar.com

- Potree potree.org
- Python Library www.python.org
- QGIS www.qgis.org
- RIEGL Laser Measurement Systems www.riegl.com
- SolarCity www.solarcity.com
- Sony www.sony.com
- The Imaging And Geospatial Information Society www.asprs.org
- Velodyne LIDAR velodynelidar.com
- YellowScan www.yellowscan.fr

Articles

- Africani, P., Bitelli, G., Lambertini, A., Minghetti, A., Paselli, E., 2013. Integration of LiDAR data into a municipal GIS to study solar radiation. *ISPRS - Int. Arch. Photogramm. Remote Sens. Spat. Inf. Sci. XL-1/W1*, 1–6. doi:10.5194/isprsarchives-XL-1-W1-1-2013
- Agugiario, G., Nex, F., Remondino, F., De Filippi, R., Droghetti, S., Furlanello, C., 2012. Solar radiation estimation on building roofs and web-based solar cadastre. *ISPRS Ann. Photogramm. Remote Sens. Spat. Inf. Sci. I-2*, 177–182. doi:10.5194/isprsannals-I-2-177-2012
- Aicardi, I., Nex, F., Gerke, M., Lingua, A.M., 2016. An Image-Based Approach for the Co-Registration of Multi-Temporal UAV Image Datasets. *Remote Sens.* 1–20. doi:10.3390/rs8090779
- Allen, C., Tsou, M.H., Aslam, A., Nagel, A., Gawron, J.M., 2016. Applying GIS and machine learning methods to twitter data for multiscale surveillance of influenza. *PLoS One* 11, 1–10. doi:10.1371/journal.pone.0157734
- Arias, P., Armesto, J., Di-Capua, D., González-Drigo, R., Lorenzo, H., Pérez-Gracia, V., 2007. Digital photogrammetry, GPR and computational analysis of structural damages in a mediaeval bridge. *Eng. Fail. Anal.* 14, 1444–1457. doi: 10.1016/j.engfailanal.2007.02.001
- Attene, M., Campen, M., Kobbelt, L., 2013. Polygon Mesh Repairing: An Application Perspective. *ACM Comput. Surv.* 45, 1–33. doi: 10.1145/2431211.2431214

- Auferbauer, D., Ganhör, R., Hilda, T., 2015. Moving Towards Crowd Tasking for Disaster Mitigation. Proc. ISCRAM 2015 Conf.
- Aull, B.F., Loomis, A.H., Young, D.J., Heinrichs, R.M., Felton, B.J., Daniels, P.J., Landers, D.J., 2002. Geiger-Mode Avalanche Photodiodes for Three-Dimensional Imaging. *Lincoln Lab. J.* 13, 335–350.
- Axelsson, P., 2000. DEM Generation from Laser Scanner Data Using adaptive TIN Models. *Int. Arch. Photogramm. Remote Sens.* 23, 110–117. doi:10.1016/j.isprsjprs.2005.10.005
- Balletti, C., Guerra, F., Tsioukas, V., Vernier, P., 2014. Calibration of Action Cameras for Photogrammetric Purposes. *Sensors* 14, 17471–17490. doi: 10.3390/s140917471
- Baltsavias, E.P., 1999. Airborne laser scanning: Basic relations and formulas. *ISPRS J. Photogramm. Remote Sens.* 54, 199–214. doi:10.1016/S0924-2716(99)00015-5
- Barazzetti, L., Banfi, F., Brumana, R., Gusmeroli, G., Oreni, D., Previtali, M., Roncoroni, F., Schiantarelli, G., 2015. BIM from Laser Clouds and Finite Element Analysis: Combining Structural Analysis and Geometric Complexity. *ISPRS - Int. Arch. Photogramm. Remote Sens. Spat. Inf. Sci. XL-5/W4*, 345–350. doi:10.5194/isprsarchives-XL-5-W4-345-2015
- Beinat, A., Sepic, F., 2008. Verifica planimetrica di rilievi LIDAR da aeromobile tramite elementi lineari: metodo e sperimentazione, in: *Atti 12a Conferenza Nazionale ASITA 2008*. pp. 323–328.
- Biljecki, F., Ledoux, H., Stoter, J., Vosselman, G., 2016. The variants of an LOD of a 3D building model and their influence on spatial analyses. *ISPRS J. Photogramm. Remote Sens.* 116, 42–54. doi:10.1016/j.isprsjprs.2016.03.003
- Biljecki, F., Ledoux, H., Stoter, J., Zhao, J., 2014. Formalisation of the level of detail in 3D city modelling. *Comput. Environ. Urban Syst.* 48, 1–15. doi: 10.1016/j.compenurbysys.2014.05.004
- Biljecki, F., Stoter, J., Ledoux, H., Zlatanova, S., Çöltekin, A., 2015. Applications of 3D City Models: State of the Art Review. *ISPRS Int. J. Geo-Information* 4, 2842–2889. doi:10.3390/ijgi4042842
- Bitelli, G., Girelli, V.A., Tini, M.A., Vittuari, L., 2004. Low-height aerial imagery and digital photogrammetrical processing for archaeological mapping. *Geo-Imagery Bridg. Cont. XXth ISPRS Congr.* 12–23.

- Bitelli, G., Camassi, R., Gusella, L., Mognol, A., 2004. Image Change Detection On Urban Area: The Earthquake Case, in: XXth ISPRS Congress. Istanbul, Turkey, p. 692.
- Bitelli, G., Conte, P., Csoknyai, T., Franci, F., Girelli, V.A., Mandanici, E., 2015. Aerial thermography for energetic modelling of cities. *Remote Sens.* 7, 2152–2170. doi:10.3390/rs70202152
- Bolognesi, M., Furini, A., Russo, V., Pellegrinelli, A., Russo, P., 2014. Accuracy of cultural heritage 3D models by RPAS and terrestrial photogrammetry. *ISPRS - Int. Arch. Photogramm. Remote Sens. Spat. Inf. Sci.* XL-5, 113–119. doi: 10.5194/isprsarchives-XL-5-113-2014
- Bramerini, F., Castenetto, S., 2014. Handbook of analysis of emergency conditions in urban scenarios (Manuale per l'analisi della Condizione Limite per l'Emergenza (CLE) dell'insediamento urbano).
- Brito, M.C., Gomes, N., Santos, T., Tenedório, J.A., 2012. Photovoltaic potential in a Lisbon suburb using LiDAR data. *Sol. Energy* 86, 283–288. doi:10.1016/j.solener.2011.09.031
- Brovelli, M.A., Longoni, U.M., Cannata, M., 2004. LIDAR data filtering and DTM interpolation within GRASS. *Trans. GIS* 8, 155–174. doi:10.1111/j.1467-9671.2004.00173.x
- Burkart, A., Aasen, H., Alonso, L., Menz, G., Bareth, G., Rascher, U., 2015. Angular dependency of hyperspectral measurements over wheat characterized by a novel UAV based goniometer. *Remote Sens.* 7, 725–746. doi:10.3390/rs70100725
- Cao, V.-H., Chu, K., Le-Khac, N.-A., Kechadi, M., Laefer, D., Truong-Hong, L., 2015. Toward a new approach for massive LiDAR data processing, in: 2015 2nd IEEE International Conference on Spatial Data Mining and Geographical Knowledge Services (ICSDM). IEEE, pp. 135–140. doi:10.1109/ICSDM.2015.7298040
- Capra, A., Dubbini, M., Bertacchini, E., Castagnetti, C., Mancini, F., 2015. 3D Reconstruction of an Underwater Archaeological Site: Comparison Between Low Cost Cameras. *ISPRS - Int. Arch. Photogramm. Remote Sens. Spat. Inf. Sci.* XL-5/W5, 67–72. doi:10.5194/isprsarchives-XL-5-W5-67-2015
- Castellazzi, G., D'Altri, A.M., De Miranda, S., Ubertini, F., Bitelli, G., Lambertini, A., Selvaggi, I., Tralli, A.M., 2016. A Mesh Generation Method for Historical Monumental Buildings: an Innovative Approach. VII Eur. Congr. Comput. Methods Appl. Sci. Eng. 1–8.

- Castellazzi, G., D'Altri, A., Bitelli, G., Selvaggi, I., Lambertini, A., 2015. From laser scanning to finite element analysis of complex buildings by using a semi-automatic procedure. *Sensors* 15, 18360–18380. doi:10.3390/s150818360
- Colomina, I., Molina, P., 2014. Unmanned aerial systems for photogrammetry and remote sensing: A review. *ISPRS J. Photogramm. Remote Sens.* 92, 79–97. doi:10.1016/j.isprsjprs.2014.02.013
- Craglia, M., de Bie, K., Jackson, D., Pesaresi, M., Remeteş-Fülöpp, G., Wang, C., Annoni, A., Bian, L., Campbell, F., Ehlers, M., van Genderen, J., Goodchild, M., Guo, H., Lewis, A., Simpson, R., Skidmore, A., Woodgate, P., 2012. Digital Earth 2020: towards the vision for the next decade. *Int. J. Digit. Earth* 5, 4–21. doi:10.1080/17538947.2011.638500
- Du, S., Zhang, Y., Qin, R., Yang, Z., Zou, Z., Tang, Y., Fan, C., 2016. Building Change Detection Using Old Aerial Images and New LiDAR Data. *Remote Sens.* 8, 1030. doi:10.3390/rs8121030
- European Commission Directorate-General for Research & Innovation, 2017. Guidelines on open access to scientific publications and research data in Horizon 2020.
- European Commission Directorate-General for Research & Innovation, 2016. Guidelines on FAIR Data Management in Horizon 2020.
- Flanagan, A.J., Metzger, M.J., 2008. The credibility of volunteered geographic information. *GeoJournal* 72, 137–148. doi:10.1007/s10708-008-9188-y
- Franci, F., Lambertini, A., Bitelli, G., 2014. Integration of different geospatial data in urban areas: a case of study, in: Hadjimitsis, D.G., Themistocleous, K., Michaelides, S., Papadavid, G. (Eds.), *Proc. SPIE 9229, Second International Conference on Remote Sensing and Geoinformation of the Environment (RSCy2014)*, 92290P (August 12, 2014). doi:10.1117/12.2066614
- Goetz, M., 2013. Towards generating highly detailed 3D CityGML models from OpenStreetMap. *Int. J. Geogr. Inf. Sci.* 27, 845–865. doi:10.1080/13658816.2012.721552
- Golla, T., Klein, R., 2015. Real-time Point Cloud Compression, in: *Proceedings of IEEE/RSJ International Conference on Intelligent Robots and Systems*. pp. 5087–5092.
- Goodchild, M.F., 2007. Citizens as sensors: The world of volunteered geography. *GeoJournal* 69, 211–221. doi:10.1007/s10708-007-9111-y

- Gore, A., 1998. The Digital Earth: Understanding our planet in the 21st Century. *Aust. Surv.* 43, 89–91. doi:10.1080/00050326.1998.10441850
- Graham, R., Read, R., 1987. *Manual of Aerial Photography*. Focal Press.
- Guarnieri, A., Milan, N., Vettore, A., 2013. Monitoring Of Complex Structure For Structural Control Using Terrestrial Laser Scanning (Tls) And Photogrammetry. *Int. J. Archit. Herit.* 7, 54–67. doi:10.1080/15583058.2011.606595
- Günay, A., Arefi, H., Hahn, M., 2002. True orthophoto production using lidar data. *Int. Soc. Photogrammetry Remote Sens.*
- Hancke, G.P., de Silva, B. de C., Hancke, G.P., 2013. The role of advanced sensing in smart cities, *Sensors (Switzerland)*. doi:10.3390/s130100393
- Hashem, I.A.T., Yaqoob, I., Anuar, N.B., Mokhtar, S., Gani, A., Ullah Khan, S., 2015. The rise of “big data” on cloud computing: Review and open research issues. *Inf. Syst.* 47, 98–115. doi:10.1016/j.is.2014.07.006
- Hinks, T., Carr, H., Truong-Hong, L., Laefer, D.F., 2013. Point Cloud Data Conversion into Solid Models via Point-Based Voxelization. *J. Surv. Eng.* 139, 72–83. doi:10.1061/(ASCE)SU.1943-5428.0000097
- Jalobeanu, A., Gonçalves, G., 2014. Robust Ground Peak Extraction With Range Error Estimation Using Full-Waveform LiDAR. *IEEE Geosci. Remote Sens. Lett.* 11, 1190–1194. doi:10.1109/LGRS.2013.2288152
- Khoshelham, K., Elberink, S.O., 2012. Accuracy and resolution of kinect depth data for indoor mapping applications. *Sensors* 12, 1437–1454. doi:10.3390/s120201437
- Kolbe, T.H., Gröger, G., Plümer, L., 2005. CityGML–Interoperable Access to 3D City Models. *Geo-Information Disaster Manag.* 883–900. doi:10.1007/3-540-27468-5_63
- Kolbe, T.H., 2009. Representing and Exchanging 3D City Models with CityGML. *3D Geo-Information Sci.* 15–31. doi:10.1007/978-3-540-87395-2_2
- Kraus, K., Pfeifer, N., 1998. Determination of terrain models in wooded areas with airborne laser scanner data. *ISPRS J. Photogramm. Remote Sens.* 53, 193–203. doi:10.1016/S0924-2716(98)00009-4
- Lambertini, A., 2011. *Tecniche e procedure innovative per l'estrazione di edifici da dati LiDAR*. University of Bologna.
- Lambertini, A., Loi, D., Bitelli, G., 2015. Sperimentazione in ambiente GIS di una metodologia per l'automatizzazione di procedure nell'analisi della

Condizione Limite per l'Emergenza (CLE), in: Atti 19a Conferenza Nazionale ASITA 2015. pp. 487–494.

- Lambertini, A., Pastorello, E., Bitelli, G., 2016. Tecniche per l'estrazione automatica di edifici da nuvole di punti con software proprietari ed open source, in: Atti 20a Conferenza Nazionale ASITA 2016. pp. 835–840.
- Lee, J.-G., Kang, M., 2015. Geospatial Big Data: Challenges and Opportunities. *Big Data Res.* 2, 74–81. doi:10.1016/j.bdr.2015.01.003
- Liu, J., Wang, Q., Li, S., Cheng, Y., Wei, J., 2009. Research on a flash imaging lidar based on a multiple-streak tube. *Laser Phys.* 19, 115–120. doi:10.1134/S1054660X09010034
- Lulla, K., Nellis, M.D., Rundquist, B., 2012. Celebrating 40 years of Landsat program's Earth observation accomplishments. *Geocarto Int.* 27, 459. doi:10.1080/10106049.2012.727604
- Mandanici, E., Conte, P., Girelli, V.A., 2016. Integration of Aerial Thermal Imagery , LiDAR Data and Ground Surveys for Surface Temperature Mapping in Urban Environments. *Remote Sens.* 8. doi:10.3390/rs8100880
- Martin-Brualla, R., Gallup, D., Seitz, S.M., 2016. 3D time-lapse reconstruction from internet photos. *Proc. IEEE Int. Conf. Comput. Vis.* 11–18–Dece, 1332–1340. doi:10.1109/ICCV.2015.157
- McLaughlin, R.A., 2006. Extracting transmission lines from airborne LIDAR data. *IEEE Geosci. Remote Sens. Lett.* 3, 222–226. doi:10.1109/LGRS.2005.863390
- Meixner, P., Leberl, F., 2011. 3-Dimensional building details from aerial photography for Internet maps. *Remote Sens.* 3, 721–751. doi:10.3390/rs3040721
- Minghetti, A., Africani, P., Paselli, E., 2011. Bologna solar city, a web application for the analysis of potential energy: from estimating solar radiation to the realization of the application, in: 17th Building Services, Mechanical and Building Industry Days - Urban Energy Conference. Debrecen, Hungary, pp. 25–30.
- Moosmann, F., Stiller, C., 2011. Velodyne SLAM. *IEEE Intell. Veh. Symp. Proc.* 393–398. doi:10.1109/IVS.2011.5940396
- Mostafa, M., Hutton, J., 2001. Airborne remote sensing without ground control, in: IGARSS 2001. Scanning the Present and Resolving the Future. Proceedings. IEEE 2001 International Geoscience and Remote Sensing

Symposium (Cat. No.01CH37217). IEEE, pp. 2961–2963. doi:10.1109/IGARSS.2001.978222

- Neteler, M., Bowman, M.H., Landa, M., Metz, M., 2012. GRASS GIS: A multi-purpose open source GIS. *Environ. Model. Softw.* 31, 124–130. doi:10.1016/j.envsoft.2011.11.014
- Nex, F., Remondino, F., 2014. UAV for 3D mapping applications: A review. *Appl. Geomatics* 6, 1–15. doi:10.1007/s12518-013-0120-x
- Niclass, C.L., Rochas, A., Besse, P.-A., Charbon, E., 2005. Design and characterization of a CMOS 3-D image sensor based on single photon avalanche diodes. *IEEE J. Solid-State Circuits* 40, 1847–1854. doi:10.1109/JSSC.2005.848173
- Núñez Andrés, M.A., Buill Pozuelo, F., 2009. Evolution of the architectural and heritage representation. *Landsc. Urban Plan.* 91, 105–112. doi:10.1016/j.landurbplan.2008.12.006
- Oreni, D., Brumana, R., Della Torre, S., Banfi, F., Barazzetti, L., Previtali, M., 2014. Survey turned into HBIM: the restoration and the work involved concerning the Basilica di Collemaggio after the earthquake (L’Aquila). *ISPRS Ann. Photogramm. Remote Sens. Spat. Inf. Sci.* II-5, 267–273. doi:10.5194/isprsannals-II-5-267-2014
- Pasquali, A., 2013. Utilizzo del dato LIDAR aviostrasportato per l’estrazione automatica del modello 3D degli edifici: potenzialità e criticità.
- Pieraccini, M., Dei, D., Betti, M., Bartoli, G., Tucci, G., Guardini, N., 2014. Dynamic identification of historic masonry towers through an expeditious and no-contact approach: Application to the “Torre del Mangia” in Siena (Italy). *J. Cult. Herit.* 15, 275–282. doi:10.1016/j.culher.2013.07.006
- Pradhan, B., 2013. A comparative study on the predictive ability of the decision tree, support vector machine and neuro-fuzzy models in landslide susceptibility mapping using GIS. *Comput. Geosci.* 51, 350–365. doi:10.1016/j.cageo.2012.08.023
- Rau, J.Y., Chu, C.Y., 2010. Photo-Realistic 3D Mapping From Aerial Oblique Imagery, in: *International Archives of the Photogrammetry, Remote Sensing and Spatial Information Sciences - ISPRS Archives.*
- Richards, J.A., 2013. *Remote Sensing Digital Image Analysis.* Springer Berlin Heidelberg, Berlin, Heidelberg. doi:10.1007/978-3-642-30062-2
- Ristevski, J., 2017. Building a Global 3D Routing Map. *GIM Int.*

- Rottensteiner, F., Briese, C., 2002. A new method for building extraction in urban areas from high-resolution LIDAR data. *Int. Arch. Photogramm. Remote Sens. Spat. Inf. Sci.* 34, 295–301.
- Rottensteiner, F., Sohn, G., Jung, J., Gerke, M., Baillard, C., Benitez, S., Breitkopf, U., 2012. The ISPRS Benchmark on Urban Object Classification and 3D Building Reconstruction. *ISPRS Ann. Photogramm. Remote Sens. Spat. Inf. Sci.* I-3, 293–298. doi:10.5194/isprsannals-I-3-293-2012
- Rottensteiner, F., Sohn, G., Gerke, M., Wegner, J.D., Breitkopf, U., Jung, J., 2014. Results of the ISPRS benchmark on urban object detection and 3D building reconstruction. *ISPRS J. Photogramm. Remote Sens.* 93, 256–271. doi:10.1016/j.isprsjprs.2013.10.004
- Sánchez-Aparicio, L., Villarino, A., García-Gago, J., González-Aguilera, D., 2016. Photogrammetric, Geometrical, and Numerical Strategies to Evaluate Initial and Current Conditions in Historical Constructions: A Test Case in the Church of San Lorenzo (Zamora, Spain). *Remote Sens.* 8, 60. doi:10.3390/rs8010060
- Schutz, M., Wimmer, M., 2015. High-quality point-based rendering using fast single-pass interpolation. *2015 Digit. Herit.* 369–372. doi:10.1109/DigitalHeritage.2015.7413904
- Senaratne, H., Mobasher, A., Ali, A.L., Capineri, C., Haklay, M. (Muki), 2016. A review of volunteered geographic information quality assessment methods. *Int. J. Geogr. Inf. Sci.* 8816, 1–29. doi:10.1080/13658816.2016.1189556
- Shan, J., Toth, C.K., 2008. *Topographic Laser Ranging and Scanning: Principles and Processing*. CRC Press.
- Siebert, S., Teizer, J., 2014. Mobile 3D mapping for surveying earthwork projects using an Unmanned Aerial Vehicle (UAV) system. *Autom. Constr.* 41, 1–14. doi:10.1016/j.autcon.2014.01.004
- Stal, C., Tack, F., De Maeyer, P., De Wulf, A., Goossens, R., 2013. Airborne photogrammetry and lidar for DSM extraction and 3D change detection over an urban area – a comparative study. *Int. J. Remote Sens.* 34, 1087–1110. doi: 10.1080/01431161.2012.717183
- Sun, M., Zhu, R., Yang, X., 2008. UAV path generation, path following and gimbal control. *Proc. 2008 IEEE Int. Conf. Networking, Sens. Control. ICNSC* 870–873. doi:10.1109/ICNSC.2008.4525338

- Swatantran, A., Tang, H., Barrett, T., DeCola, P., Dubayah, R., 2016. Rapid, High-Resolution Forest Structure and Terrain Mapping over Large Areas using Single Photon Lidar. *Nat. Publ. Gr.* 1–12. doi:10.1038/srep28277
- Tang, H., Swatantran, A., Barrett, T., DeCola, P., Dubayah, R., 2016. Voxel-Based Spatial Filtering Method for Canopy Height Retrieval from Airborne Single-Photon Lidar. *Remote Sens.* 8, 771. doi:10.3390/rs8090771
- Tang, P., Huber, D., Akinci, B., Lipman, R., Lytle, A., 2010. Automatic reconstruction of as-built building information models from laser-scanned point clouds: A review of related techniques. *Autom. Constr.* 19, 829–843. doi:10.1016/j.autcon.2010.06.007
- Tehrany, M.S., Pradhan, B., Mansor, S., Ahmad, N., 2015. Flood susceptibility assessment using GIS-based support vector machine model with different kernel types. *Catena* 125, 91–101. doi:10.1016/j.catena.2014.10.017
- Toth, C., Józków, G., 2016. Remote sensing platforms and sensors: A survey. *ISPRS J. Photogramm. Remote Sens.* 115, 22–36. doi:10.1016/j.isprsjprs.2015.10.004
- Truong-Hong, L., Laefer, D.F., Hinks, T., Carr, H., 2013. Combining an Angle Criterion with Voxelization and the Flying Voxel Method in Reconstructing Building Models from LiDAR Data. *Comput. Civ. Infrastruct. Eng.* 28, 112–129. doi:10.1111/j.1467-8667.2012.00761.x
- Urmson, C., Anhalt, J., Bagnell, D., Baker, C., Bittner, R., Clark, M.N., Dolan, J., Duggins, D., Galatali, T., Geyer, C., Gittleman, M., Harbaugh, S., Hebert, M., Howard, T.M., Kolski, S., Kelly, A., Likhachev, M., McNaughton, M., Miller, N., Peterson, K., Pilnick, B., Rajkumar, R., Rybski, P., Salesky, B., Seo, Y.-W., Singh, S., Snider, J., Stentz, A., Whittaker, W., “Red,” Wolkowicki, Z., Ziglar, J., Bae, H., Brown, T., Demitrish, D., Litkouhi, B., Nickolaou, J., Sadekar, V., Zhang, W., Struble, J., Taylor, M., Darms, M., Ferguson, D., 2008. Autonomous driving in urban environments: Boss and the Urban Challenge. *J. F. Robot.* 25, 425–466. doi:10.1002/rob.20255
- van Oosterom, P., Martinez-Rubi, O., Ivanova, M., Horhammer, M., Geringer, D., Ravada, S., Tijssen, T., Kodde, M., Gonçalves, R., 2015. Massive point cloud data management: Design, implementation and execution of a point cloud benchmark. *Comput. Graph.* 49, 92–125. doi:10.1016/j.cag.2015.01.007
- Vautherin, J., Rutishauser, S., Schneider-Zapp, K., Choi, H.F., Chovancova, V., Glass, A., Strecha, C., 2016. Photogrammetric Accuracy and Modeling of Rolling Shutter Cameras. *ISPRS Ann. Photogramm. Remote Sens. Spat. Inf. Sci.* III-3, 139–146. doi:10.5194/isprsannals-III-3-139-2016

- Vetrivel, A., Gerke, M., Kerle, N., Nex, F., Vosselman, G., 2017. Disaster damage detection through synergistic use of deep learning and 3D point cloud features derived from very high resolution oblique aerial images, and multiple-kernel-learning. *ISPRS J. Photogramm. Remote Sens.* doi:10.1016/j.isprsjprs.2017.03.001
- Vosselman, G., 2012. Automated planimetric quality control in high accuracy airborne laser scanning surveys. *ISPRS J. Photogramm. Remote Sens.* 74, 90–100. doi:10.1016/j.isprsjprs.2012.09.002
- Wagner, W., Ullrich, A., Ducic, V., Melzer, T., Studnicka, N., 2006. Gaussian decomposition and calibration of a novel small-footprint full-waveform digitising airborne laser scanner. *ISPRS J. Photogramm. Remote Sens.* 60, 100–112. doi:10.1016/j.isprsjprs.2005.12.001
- Weibel, R., Heller, M., 1991. Digital Terrain Modelling, in: Longley, P.A., Goodchild, M.F., Maguire, D.J., Rhind, D.W. (Eds.), *Geographic Information Systems*. pp. 269–297.
- Werner, M., 2001. Shuttle Radar Topography Mission (SRTM) mission overview. *Frequenz* 55, 75–79.
- Yang, Y., Tang, J., Luo, H., Law, R., 2015. Hotel location evaluation: A combination of machine learning tools and web GIS. *Int. J. Hosp. Manag.* 47, 14–24. doi:10.1016/j.ijhm.2015.02.008

Acknowledgements

I would like to express my greatest recognition to my family and especially to my partner in life, Giulia. They gave me the fundamental emotional support during my PhD research.

My professional gratitude is addressed to Prof. Gabriele Bitelli, Prof. Luca Vittuari and Prof. Gil Gonçalves. Thanks to their assistance in this study and their guidance during these years I have had the opportunity to see the edge of knowledge in many connected topics, gain experience working on different projects and obtain a broader vision.

Finally, my personal thanks to all my friends and colleagues for their precious support.